



National Library
of Canada

Bibliothèque nationale
du Canada

Canadian Theses Service

Service des thèses canadiennes

Ottawa, Canada
K1A 0N4

NOTICE

The quality of this microform is heavily dependent upon the quality of the original thesis submitted for microfilming. Every effort has been made to ensure the highest quality of reproduction possible.

If pages are missing, contact the university which granted the degree.

Some pages may have indistinct print especially if the original pages were typed with a poor typewriter ribbon or if the university sent us an inferior photocopy.

Reproduction in full or in part of this microform is governed by the Canadian Copyright Act, R.S.C. 1970, c. C-30, and subsequent amendments.

AVIS

La qualité de cette microforme dépend grandement de la qualité de la thèse soumise au microfilmage. Nous avons tout fait pour assurer une qualité supérieure de reproduction.

S'il manque des pages, veuillez communiquer avec l'université qui a conféré le grade.

La qualité d'impression de certaines pages peut laisser à désirer, surtout si les pages originales ont été dactylographiées à l'aide d'un ruban usé ou si l'université nous a fait parvenir une photocopie de qualité inférieure.

La reproduction, même partielle, de cette microforme est soumise à la Loi canadienne sur le droit d'auteur, SRC 1970, c. C-30, et ses amendements subséquents.

Thermodynamic and Spectroscopic Studies of
Alcohol/Surfactant Mixed Micelles

by

D. Gerrard Marangoni

Submitted in partial fulfillment of the requirements

for the degree of Doctor of Philosophy

at

Dalhousie University

Halifax, Nova Scotia

September 1991

© 1991, by D. Gerrard Marangoni.



National Library
of Canada

Bibliothèque nationale
du Canada

Canadian Theses Service Service des thèses canadiennes

Ottawa, Canada
K1A 0N4

The author has granted an irrevocable non-exclusive licence allowing the National Library of Canada to reproduce, loan, distribute or sell copies of his/her thesis by any means and in any form or format, making this thesis available to interested persons.

The author retains ownership of the copyright in his/her thesis. Neither the thesis nor substantial extracts from it may be printed or otherwise reproduced without his/her permission.

L'auteur a accordé une licence irrévocable et non exclusive permettant à la Bibliothèque nationale du Canada de reproduire, prêter, distribuer ou vendre des copies de sa thèse de quelque manière et sous quelque forme que ce soit pour mettre des exemplaires de cette thèse à la disposition des personnes intéressées.

L'auteur conserve la propriété du droit d'auteur qui protège sa thèse. Ni la thèse ni des extraits substantiels de celle-ci ne doivent être imprimés ou autrement reproduits sans son autorisation.

ISBN 0-315-71551-0

Canada

TABLE OF CONTENTS

Table of Contents	iv
List of Tables	vii
List of Figures	ix
List of Symbols	xii
Acknowledgements	xvii
Abstract	xviii
Chapter 1. Introduction	1
1.1 General Background and Overview	1
1.1 (a) The Hydrophobic Effect and Micelle Formation	2
1.1 (b) Micellar Parameters: CMC's, Aggregation Numbers, and Counterion Binding	5
(i) Critical Micelle Concentration	5
(ii) Aggregation Numbers and Micelle Geometry	7
(iii) Counterion Binding	9
1.2 Solubilization and Mixed Micelle Formation	11
1.3 NMR Spectroscopy of Micellar and Mixed Micellar Solutions	15
1.3 (a) Basic NMR Principles	15
(i) Interactions of Nuclei with External Magnetic Fields	15
(ii) Chemical Shift	17
(iii) Spin-Lattice and Spin-Spin Relaxation	18
(iv) Paramagnetic Relaxation	20
1.3 (b) Applications of NMR Spectroscopy in Micellar and Mixed Micellar Solutions	22
1.4 Luminescence Probing and the Determination of Aggregation Numbers in Mixed Micellar Systems	26
1.4 (a) Introduction	26
1.4 (b) Photophysical Events after Excitation	28
1.4 (c) Fluorescence Spectra	28
1.4 (d) Lifetimes of Excited Luminescent Probes; Quantum Yield	29

1.4 (e) Quenching Processes	31
1.4 (f) Excimer Formation	32
1.4 (g) Probe and Quencher Distribution among Micelles and the Static Quenching Method for determining Surfactant Aggregation Numbers	33
1.4 (h) Previous Work	37
1.5 Conclusions	38
Chapter 2. Experimental Methods and Materials	41
2.1 Materials	41
2.1 (a) Surfactants	41
2.1 (b) Alcohols	41
2.1 (c) Probe Molecules	42
2.2 Methods and Solution Preparations	42
2.2 (a) CMC Determinations	42
2.2 (b) NMR Experiments	43
2.2 (c) Luminescence Quenching Experiments	44
Chapter 3. The Application of the NMR Paramagnetic Relaxation Experiment to the Determination of Distribution Coefficients of Solubilizates in Micellar Systems	46
3.1 Introduction	46
3.2 Results and Discussion	50
3.3 Conclusions	65
Chapter 4. CMC Values and Degrees of Counterion Binding in Ionic Surfactant/Alkoxyethanol Mixed Micellar Systems	66
4.1 Introduction	66
4.1 (a) Introduction	66
4.1 (b) Experimental Determination of β : The Ratio of Slopes Method	68
4.2 Results and Discussion	73

4.2 (a) CMC Values	73
(i) Anionic Surfactant/Alkoxyethanol Mixed Micelles	73
(ii) Cationic Surfactant/Alkoxyethanol Mixed Micelles	80
4.1 (b) β Values	89
4.3 Conclusions	95
Chapter 5. NMR Studies of the Solubilization of Alkoxyethanols in Anionic and Cationic Micellar Systems	96
5.1 Introduction	96
5.2 Results and Discussion	97
5.3 Conclusions	109
Chapter 6. The Determination of the Aggregation Numbers of Surfactant and Alcohol in Ionic Surfactant/Alcohol Mixed Micelles Using the Static Fluorescence Quenching Experiment	110
6.1 Introduction	110
(a) The Static Fluorescence Quenching Experiment	110
(b) Literature Studies	121
6.2 Results and Discussion	124
(a) SDS/Alkoxyethanol Mixed Micelles	124
(b) DTAB/Alkoxyethanol Mixed Micelles	139
(c) Ionic Surfactant/Tetraethylene Glycol, Tetraethylene Glycol Dimethyl Ether Mixed Micelles	148
6.3 Conclusions	154

LIST OF TABLES

Table 3.1.	¹ H Relaxation Times and Distribution Constants (p) of 0.044 molal 1-Butanol and 0.058 molal Benzyl Alcohol in DTAB Micelles as a Function of the Concentration (mmolal) of MnCl ₂ ·6H ₂ O.	51
Table 3.2.	¹ H Relaxation Times and Distribution Constants (p) of 0.044 molal 1-Butanol in SDS Micelles as a Function of the Concentration (mmolal) of 3-Carboxylate-Proxyl.	52
Table 3.3.	¹ H Relaxation Times (Phenyl Protons) and Distribution Constants (p) of 0.058 molal Benzyl Alcohol in SDS Micelles as a Function of the Concentration of Mn[EDTA] ²⁻ and 3-carboxylate-proxyl. . .	54
Table 3.4.	Distribution Constants (p) and Transfer Free Energies of n-Alkanols in SDS Micelles	57
Table 3.5.	Distribution Constants (p) and Transfer Free Energies of n-Alkanols in SD Micelles	58
Table 3.6.	Distribution Constants (p) and Transfer Free Energies of n-Alkanols in DTAB Micelles	59
Table 3.7.	Distribution Constants (p) and Transfer Free Energies of n-Alkanols in DPC Micelles	60
Table 4.1.	CMC values (± 0.2 mmolal) for SDecS/Alkoxyethanol Mixed Micelles as a Function of the Total Concentration of Added Alcohol.	74
Table 4.2.	CMC values (± 0.2 mmolal) for SDS/Alkoxyethanol Mixed Micelles as a Function of the Total Concentration of Added Alcohol.	75
Table 4.3.	CMC values (± 0.5 mmolal, EMF measurements) for DTAB/Alkoxyethanol Mixed Micelles as a Function of the Total Concentration of Added Alcohol.	85
Table 4.4.	CMC values (± 0.5 mmolal, Conductance measurements) for DTAB/Alkoxyethanol Mixed Micelles as a Function of the Total Concentration of Added Alcohol.	86

Table 4.5.	Degrees of Counterion Binding ($\beta \pm 0.2$) for SDS/Alkoxyethanol Mixed Micelles as a Function of the Total Concentration of Added Alcohol.	90
Table 4.6.	β values (± 0.02 mmolal, Conductance measurements) for DTAB/Alkoxyethanol Mixed Micelles as a Function of the Total Concentration of Added Alcohol.	91
Table 5.1.	Distribution Coefficients and Free Energies of Transfer for Several Alcohols in SDS and SD Micellar Solutions.	98
Table 5.2.	Distribution Coefficients and Free Energies of Transfer for Several Alcohols in DTAB and DPC Micellar Solutions.	105
Table 5.3.	Distribution Coefficients and Free Energies of Transfer for TEG and TGD in SDS and DTAB Micellar Solutions.	108
Table 6.1.	Aggregation Numbers of DTAC and SDS Micelles as a Function of the Surfactant Concentration, as Determined by the Static Fluorescence Quenching Experiment.	117
Table 6.2.	Aggregation Numbers of Surfactant and Alcohol for 0.0500 molal SDS/Alkoxyethanol Mixed Micelles as a Function of the Concentration of Alcohol.	128
Table 6.3.	Aggregation Numbers of Surfactant and Alcohol for 0.0500 molal SDS/C ₆ E ₀ and SDS/C ₆ E ₂ Mixed Micelles as a Function of the Concentration of Alcohol.	129
Table 6.4.	Aggregation Numbers of Surfactant and Alcohol for 0.0750 molal DTAB/Alkoxyethanol Mixed Micelles as a Function of the Concentration of Alcohol.	140
Table 6.5.	Aggregation Numbers of Surfactant and Alcohol for 0.0750 molal DTAB/C ₆ E ₀ and DTAB/C ₆ E ₂ Mixed Micelles as a Function of the Alcohol Concentration.	141
Table 6.6.	Aggregation Numbers of Surfactant and Alcohol for 0.0500 molal SDS/TEG and SDS/TGD Mixed Micelles as a Function of the Concentration of Alcohol.	149
Table 6.7.	Aggregation Numbers of Surfactant and Alcohol for 0.0750 molal DTAB/HED and DTAB/TGD Mixed Micelles as a Function of the Alcohol Concentration.	152

LIST OF FIGURES

Figure 1.1.	Schematic diagram of an alcohol/surfactant mixed micelle	14
Figure 1.2.	The fluorescence emission spectrum of 50 mmolal SDS/0.01 mmolal pyrene	30
Figure 3.1.	Schematic diagram of a benzene molecule in equilibrium between water and the micellar phase of SDS	48
Figure 3.2.	Transfer free energies of n-alcohols from D ₂ O to the interior of SDS micelles as a function of the number of carbon atoms in the alcohol	61
Figure 3.3.	Transfer free energies of n-alcohols from D ₂ O to the interior of SD micelles as a function of the number of carbon atoms in the alcohol	62
Figure 3.4.	Transfer free energies of n-alcohols from D ₂ O to the interior of DTAB micelles as a function of the number of carbon atoms in the alcohol	63
Figure 3.5.	Transfer free energies of n-alcohols from D ₂ O to the interior of DPC micelles as a function of the number of carbon atoms in the alcohol	64
Figure 4.1.	CMC values for DTAB/H ₂ O micelles determined from plots of conductance vs. $c_{surf,t}$ and equivalent conductance vs. $c_{surf,t}^{1/2}$	72
Figure 4.2.	CMC values (\pm 0.2 mmolal, EMF measurements) for SDecS/alkoxyethanol mixed micelles as a function of c_a	76
Figure 4.3.	CMC values (\pm 0.2 mmolal, EMF measurements) for SDS/alkoxyethanol mixed micelles as a function of c_a	77
Figure 4.4.	CMC values for DTAB/H ₂ O micelles determined from plots of EMF and conductance measurements	81
Figure 4.5.	CMC values for DTAB/0.300 molal C ₄ E ₃ micelles determined from EMF and conductance measurements	83
Figure 4.6.	CMC values of DTAB/0.300 molal C ₄ E ₃ determined from plots of conductance vs. $c_{surf,t}$ and equivalent conductance vs. $c_{surf,t}^{1/2}$	84

Figure 4.7.	CMC values (± 0.5 mmolal, EMF measurements) for DTAB/alkoxyethanol mixed micelles as a function of c_a	87
Figure 4.8.	CMC values (± 0.5 mmolar, conductance measurements) for DTAB/alkoxyethanol mixed micelles as a function of c_a	88
Figure 4.9.	β values (± 0.02) of SDS/alkoxyethanol mixed micelles as a function of c_a	93
Figure 4.10.	β values of DTAB/alkoxyethanol mixed micelles (± 0.02 , conductance measurements) as a function of c_a	94
Figure 5.1.	Transfer free energies of ethoxylated alcohols from D_2O to SDS micelles	101
Figure 5.2.	Transfer free energies of ethoxylated alcohols from D_2O to SD micelles	102
Figure 5.3.	Transfer free energies of ethoxylated alcohols from D_2O to DTAB and DPC micelles	106
Figure 6.1.	Plot of calculated values of $\ln(I_0/I)$ vs. $\langle Q \rangle$ at different kinetic ratios, $k_q\tau_0$	115
Figure 6.2.	Aggregation numbers of DTAC and SDS at different surfactant concentrations	117
Figure 6.3.	Plot of $\ln(I_0/I)$ vs. $[Q]$ for the pyrene/ CP_+ probe/quencher pair in micellar solutions	125
Figure 6.4.	Surfactant aggregation numbers, N_s , for 0.0500 molal SDS/ C_4E_n mixed micelles	130
Figure 6.5.	Surfactant aggregation numbers, N_s , for 0.0500 molal SDS/ C_6E_n mixed micelles	131
Figure 6.6.	Surfactant aggregation numbers, alcohol aggregation numbers, and total aggregation numbers for 0.0500 molal SDS/ C_4E_2	132
Figure 6.7.	Plot of N_s/A vs. X_a for SDS/alkoxyethanol mixed micelles	136
Figure 6.8.	Plot of β vs. $c_{a,m}$ for SDS/alkoxyethanol mixed micelles	138
Figure 6.9.	Surfactant aggregation numbers, N_s , for 0.0750 molal DTAB/ C_4E_n mixed micelles	142

Figure 6.10. Surfactant aggregation numbers, N_s , for 0.0750 molal DTAB/ C_6E_n mixed micelles	143
Figure 6.11. Plot of N_s/A vs. X_1 for DTAB/alkoxyethanol mixed micelles . . .	146
Figure 6.12. Plot of β vs. $c_{a,m}$ for DTAB/alkoxyethanol mixed micelles	147
Figure 6.13. Surfactant aggregation numbers, N_s , for 0.0500 molal SDS/TEG and 0.0500 molal SDS/TGD mixed micelles	150
Figure 6.14. Surfactant aggregation numbers for 0.00750 molal DTAB/TEG and DTAB/TGD mixed micelles	153

LIST OF SYMBOLS

NMR	nuclear magnetic resonance
EMF	electromotive force
μ_{HC}°	chemical potential at infinite dilution of a hydrocarbon solute in a hydrocarbon solvent
μ_{aq}°	chemical potential at infinite dilution of a hydrocarbon solute in water
ΔG_t°	the free energy of transfer
a	intercept of the plot of the free energy of transfer of a homologous series of hydrocarbon solutes vs. the number of carbon atoms in the solute
b	slope of the the plot of the free energy of transfer of a homologous series of hydrocarbon solutes vs. the number of carbon atoms in the solute
n_c	number of carbon atoms in a hydrocarbon solute
ΔH_t°	the enthalpy of transfer
ΔS_t°	the entropy of transfer
CMC	critical micelle concentration
SD	sodium decanoate
SDS	sodium dodecylsulfate
SDecS	sodium decylsulfate
Cu(DS) ₂	copper dodecylsulfate
N_s	surfactant aggregation number
N_a	alcohol aggregation number
N_t	total aggregation number
a_o	optimum headgroup area

v	volume of hydrophobic chain
l_c	critical length of hydrophobic chain
P	Israelachvili packing parameter
β	degree of counterion binding
$C_{c,m}$	concentration of bound counterions
$C_{c,t}$	total counterion concentration
α	fraction of free counterions
p	fraction of solubilized alcohol
$C_{a,m}$	concentration of alcohol in the micellar phase
$C_{a,t}$	total concentration of added alcohol
p	angular momentum
\hbar	Planck's constant / 2π
I	spin quantum number
μ	magnetic dipole moment
γ	magnetogyric ratio
B_o	static magnetic field strength
ω_o	Larmor frequency
σ	shielding constant
δ	chemical shift
σ_r	reference shielding constant
σ_s	shielding constant of sample
TMS	tetramethylsilane

M_z^o	total macroscopic magnetic moment
N	total number of nuclei
k_B	Boltzmann's constant
N_{Avo}	Avogadro's number
T	absolute temperature
B_1	radio frequency magnetic field strength
M_z	z component of the macroscopic magnetic moment
T_1	spin-lattice relaxation time
R_1	spin-lattice relaxation rate
T_2	spin-spin relaxation time
$\nu_{1/2}$	line width at half-height of nmr signal
T_2^*	spin-spin relaxation rate in the presence of field inhomogeneities
R_1^p	relaxation rate of solubilizate in the presence of paramagnetic ions
$R_1(aq)$	relaxation rate of solubilizate in the aqueous phase
γ_I	Larmor frequency of spin I
γ_S	Larmor frequency of spin S
ω_I	magnetogyric ratio of spin I
ω_S	magnetogyric ratio of spin S
N_{el}	Number density of electrons
b_c	distance of closest approach of spin I and spin S
$J(\omega)$	spectral density at angular frequency ω
D_{obs}	self-diffusion coefficient of an additive distributed between the aqueous and micellar phases

D_f	self-diffusion of aqueous solubilized additive
D_b	self-diffusion coefficient of micellar solubilized species
D_m	self-diffusion coefficient of micelles
$R_{1,obs}$	relaxation rate of an additive distributed between the aqueous and the micellar phase
$R_{1,b}$	relaxation rate of micellar solubilized additive
$R_{1,f}$	relaxation rate of aqueous solubilized additive
DTAB	dodecyltrimethylammonium bromide
FT	Fourier transform
FT-PGSE	Fourier transform, pulsed-gradient spin echo
S_0	ground state of luminescent species
S_1	first excited singlet state of luminescent species
T_1	first excited triplet state of luminescent species
I_1/I_3	ratio of the intensities of the first and third peaks in the pyrene emission spectrum
k_f	rate constant of fluorescence emission
k_p	rate constant of phosphorescence emission
Φ	quantum yield
Φ_f	quantum yield of fluorescence
k_E	rate constant of excimer formation
k_{-E}	rate constant of excimer dissociation
σ_n	Poisson distribution of probes and/or quenchers
$\langle Q \rangle$	ratio of [quenchers] to [micelles]

P^*_o/P^*	ratio of fluorescing species in the presence and absence of quencher
k_q	quenching rate constant
τ_f	fluorescent lifetime
σ_o	Poisson distribution of micelles containing a fluorescent probe but no quencher
CTAB	cetyltrimethylammonium bromide
TTAB	tetradecyltrimethylammonium bromide
CP ⁺	cetylpyridinium ion
CPB	cetylpyridinium bromide
DPC	dodecylpyridinium chloride
DTAC	dodecyltrimethyl ammonium chloride
C ₂ E ₀	ethanol
C ₂ E ₁	ethylene glycol mono-n-ethyl ether
C ₂ E ₂	diethylene glycol mono-n-ethyl ether
C ₂ E ₃	triethylene glycol mono-n-ethyl ether
C ₄ E ₀	n-butanol
C ₄ E ₁	ethylene glycol mono-n-butyl ether
C ₄ E ₂	diethylene glycol mono-n-butyl ether
C ₄ E ₃	triethylene glycol mono-n-butyl ether

Acknowledgements

The author wishes to express his sincere gratitude to his supervisor, Dr. Jan C. T. Kwak, for his guidance and encouragement throughout the course of this work. It has been a lot of fun working in his lab. I would also like to thank Andrew Rodenhiser and Jill Thomas for a lot of help with the measurements during the summer of 1991. Useful discussions with the other members of the group, Andrea Anderson, John Gordon, Réjean Labonté, Sean Burns, and Dana Goski are also appreciated. In particular, I would like to thank Dr. Zhisheng Gao for his continuing interest and helpful suggestions.

Special thanks are due to Dr. Rod Wasylshen and the members of his group for useful discussions and doughnuts.

I would also like to acknowledge Dr. Ram Palepu for his support and advice throughout my academic career, and for kindling my interest in chemistry.

Dr. Don Hooper, Mr. J. B. MacDonald, and Mr. Gang Wu are acknowledged for their help with the Nicolet 360 at ARMRC.

Finally, I would like to thank my wife, Cindy, for her constant support and encouragement when the going got rough, and my family for their support during my academic career.

ABSTRACT

Critical micelle concentrations (*CMC*'s), degrees of solubilization, aggregation numbers of the surfactant and alcohol, and degrees of counterion binding have been determined for a number mixed micellar systems consisting of ionic surfactants and medium chain length alkoxyethanols, in order to investigate the role of the ethylene oxide (EO) group in the formation of these mixed micelles. In anionic surfactant/alkoxyethanol mixed micellar systems, NMR paramagnetic relaxation experiments, used to determine the degree of solubilization of the alcohol, indicate a systematic increase in the free energy of transfer of the alcohol from the aqueous to the micellar phase, as the number of EO groups in the alcohol is increased for a given alkyl chain length. At a given concentration of alcohol, *CMC*'s, surfactant aggregation numbers, and degrees of counterion binding are all found to decrease as the number of EO groups in the alcohol is increased, while the alcohol aggregation numbers are observed to increase. This suggests that the EO group imparts a small, but significant contribution to the hydrophobic interactions. However, in cationic surfactant/alkoxyethanol mixed micellar systems, the NMR results indicate that the degree of solubilization is constant for a given series of alkoxyethanols with constant hydrophobic chain length. As well, the *CMC* values, degrees of counterion binding, and the surfactant and alcohol aggregation numbers are relatively insensitive to the number of EO groups in the alcohol. These results imply that for cationic surfactant/alkoxyethanol mixed micellar systems, the alcohol EO group does not contribute to the hydrophobic interactions.

Chapter 1 Introduction

1.1 General Background and Overview

Micellar solubilization and mixed micelle formation are important facets of modern colloid science. The class of compounds known as surfactants (for surface active agents) displays a number of distinct solution properties in water. When a second surfactant is present, mixed micelles are formed, the properties of which are generally much different than the properties of the constituent micelles. Such micellar systems have found wide application in a number of important industrial processes.

Nuclear magnetic resonance (NMR) spectroscopy and luminescence probing are now well recognized as powerful tools with which the physico-chemical properties of mixed micellar systems can be investigated. The purpose of the present thesis was to completely characterize the equilibrium properties of mixed micelles composed of some typical ionic surfactants with alkoxyethanols as the cosurfactant. Chapter 1 presents an overview of the properties of micellar systems, starting with a brief discussion of the hydrophobic effect, hydrophobic interactions, and micelle and mixed micelle formation. Next, some background information dealing with NMR spectroscopy and luminescence probing will be presented, followed by a brief statement concerning the objective of the thesis. In Chapter 3, the applicability of the NMR paramagnetic relaxation experiment in alcohol/surfactant mixed micelles is discussed. Chapter 4 presents *CMC* values and degrees of counterion binding for the mixed micelles, while in Chapter 5, the fraction of alkoxyethanol in the mixed micelles is determined with the NMR paramagnetic

relaxation experiment. In Chapter 6, the surfactant and alcohol aggregation numbers are determined. The overall goal of this thesis is to completely characterize these ionic surfactant/alkoxyethanol mixed micelles, in order to determine the effect of increasing the ethylene oxide chain length of the cosurfactant on the physical properties of the aggregates.

1.1 (a) The Hydrophobic Effect and Micelle Formation

Compounds known as surface active agents, or surfactants, consist, in their most common form, of a polar or ionic headgroup (e.g., sulfate, carboxylate) and a linear or branched hydrocarbon or fluorocarbon chain. Micelle formation can be viewed as a compromise between the tendency for alkyl chains to avoid unfavourable contacts with water, and the desire for the polar parts to maintain contact with the aqueous environment. A thermodynamic description of the process of micelle formation thus includes a description of both electrostatic and hydrophobic contributions to the overall free energy of the system. Oil (e.g., dodecane) and water do not mix; the limited solubility of hydrophobic species in water can be attributed to the hydrophobic effect. The hydrophobic free energy (or the transfer free energy) can be defined as the difference between the standard chemical potential of the hydrocarbon solute in water and a hydrocarbon solvent at infinite dilution¹⁻⁴

$$\Delta G_i^o = \mu_{HC}^o - \mu_{aq}^o \quad (1.1)$$

where μ_{HC}^o and μ_{aq}^o are the chemical potentials of the hydrocarbon dissolved in the

hydrocarbon solvent and water, respectively, and ΔG_t° is the free energy for the process of transferring the hydrocarbon solute from the hydrocarbon solvent to water. In a homologous series of hydrocarbons (e.g., the n-alcohols or the n-alkanes), the value of ΔG_t° generally increases in a regular fashion

$$\Delta G_t^\circ = (a - bn_c)RT \quad (1.2)$$

where a and b are constants for a particular hydrocarbon series and n_c is the number of carbon atoms in the chain. The transfer free energy, ΔG_t° , can be divided into entropic and enthalpic contributions

$$\Delta G_t^\circ = \Delta H_t^\circ - T\Delta S_t^\circ \quad (1.3)$$

where ΔH_t° and ΔS_t° are the enthalpy and entropy of transfer, respectively. An important characteristic of the hydrophobic effect is that the entropy term is dominant, i.e., the transfer of the hydrocarbon solute from the hydrocarbon solvent to water is unfavourable (i.e., ΔG_t° is positive).⁵ The decrease in entropy is thought to be the result of the breakdown of the normal hydrogen-bonded structure of water, accompanied by the formation of "icebergs" around the hydrocarbon chain. The presence of the hydrophobic species promotes an ordering of the water molecules. To minimize the large entropy effect, the "icebergs" tend to cluster,² in order to reduce the number of water molecules involved; the "clustering" is enthalpically favoured (i.e., $\Delta H_t^\circ < 0$), but entropically unfavourable. The overall process has the tendency to force the hydrocarbon molecules together, which is known as the hydrophobic interaction. Molecular interactions, arising

from the tendency for the water molecules to maintain a tetrahedral structure, and the long-range attractive dispersion forces between hydrocarbon chains, act cooperatively to squeeze the hydrocarbon chain out of the water "icebergs", leading to an association of hydrophobic chains.

The unusual properties of aqueous surfactant solutions can be ascribed to the presence of the hydrophilic head group and the hydrophobic chain (or tail) in the molecule. The polar or ionic headgroup usually interacts strongly with its aqueous environment and is solvated via dipole-dipole or ion-dipole interactions. In fact, it is the nature of the headgroup which is used to divide surfactants into three main categories: anionic, cationic, and nonionic.

Due to the presence of the hydrophobic effect, surfactant molecules (amphiphiles) adsorb at the air-water interface, even at low surfactant concentrations. At a specific amphiphile concentration, the critical micelle concentration, or *CMC*, molecular aggregates known as micelles are formed. In fact, a large number of experimental observations can be summed up in a single statement: almost all physico-chemical properties vs. concentration plots for a given surfactant-solvent system will show an abrupt change in slope in a narrow concentration range (the *CMC*).

The most commonly held view of a surfactant micelle is not much different than that published by Hartley in 1936.^{5,6} At surfactant concentrations slightly above the *CMC*, amphiphiles tend to associate into spherical micelles, of about 50-100 monomers, with a radius similar to that of the length of an extended hydrocarbon chain. The micellar interior, being composed essentially of hydrocarbon chains, has properties closely related

to the liquid hydrocarbon.

Surfactants are widely used in industrial applications including tertiary oil recovery, emulsification, and polymerization.⁷⁻⁹ The catalytic effect of micelles on organic reactions is of considerable interest.¹⁰ In addition, micelles can serve as excellent model systems for studying colloid chemical phenomena, since they can provide a reproducible surface of high purity.^{11,12}

The techniques used to study micellar systems have become increasingly sophisticated and now include neutron scattering, luminescence probing, and NMR spectroscopy. Recent advances in theoretical modelling have led to an improved understanding of the intricate balance of electrostatic, dispersion, and hydration forces present in micellar systems. A number of reviews and conference proceedings have appeared in recent years on the properties of micellar solutions, vesicles, and microemulsions.¹³⁻²³ These have largely dealt with gaining a better understanding of the nature of the interactions which are responsible for surfactant aggregation, the development of new experimental techniques to study aggregated systems, and the application of surfactant technology to an ever expanding number of industrial processes.

1.1 (b) Micellar Parameters: CMC's, Aggregation Numbers, and Counterion Binding

(i) Critical Micelle Concentration

It is well known that the physico-chemical properties of surfactants vary markedly above and below a specific amphiphile concentration, the *CMC*.¹⁻²³ Below the *CMC*, the physico-chemical properties of the surfactant (e.g., conductivities, electromotive force

measurements) resemble those of a strong electrolyte. Above the *CMC*, these properties change dramatically, indicating a highly cooperative association process is taking place.

In terms of micellar models, the *CMC* has an exact definition in the pseudo-phase separation model, the model which treats the micelles as a separate phase. The *CMC* is defined, in terms of the pseudo-phase model, as the concentration of maximum solubility of the monomer in that particular solvent. The pseudo-phase model has a number of shortcomings; however, the concept of the *CMC*, as it is described in terms of this model, is very useful when discussing the association of surfactants into micelles. It is for this reason that the *CMC* is, perhaps, the most frequently measured and discussed micellar parameter.³

The general way of obtaining the *CMC* of a surfactant micelle is to plot the physico-chemical property of interest versus the surfactant concentration and observe the break in the plot. It should be noted that different experimental techniques may give slightly different values for the *CMC*. However, Mukerjee and Mysels,²⁴ in their vast compilation of *CMC*'s, have noted that the majority of values for a single surfactant (e.g., sodium dodecyl sulfate, or SDS, in the absence of additives) are in good agreement and the outlying values are easily accounted for.

CMC's show little variation with regards to the nature of the charged head group. The main influence comes from the charge of the hydrophilic head group. For example, the *CMC* of dodecyltrimethylammonium chloride (DTAC) is 20 mmolal, while for a 12 carbon nonionic surfactant, hexaethylene glycol mono-n-dodecyl ether ($C_{12}E_6$), the *CMC* is 0.087 mmolal;^{3,5,24} the *CMC* for potassium dodecanoate is 24.0 mmolal, while the

CMC for $C_{10}CH(COOK)_2$ is 130 mmolal. In addition to the relative insensitivity of the *CMC* of the surfactant to the nature of the charged head group, *CMC*'s show little dependence on the nature of the counterion. It is mainly the valence number of the counterion that affects the *CMC*. For example, the *CMC* for $Cu(DS)_2$ is about 1.2 mmolal, while the *CMC* for SDS is about 8 mmolal.^{24,25}

CMC's exhibit a weak dependence on both temperature²⁶⁻²⁸ and pressure.^{29,30} The effect of added substances on the *CMC* are complicated and interesting, and depends greatly on whether the additive is solubilized in the micelle, or in the intermicellar solution. The addition of electrolytes to ionic surfactant solutions results in a well established linear dependence of $\log(CMC)$ on the concentration of added salt.³¹⁻³⁵ For nonionic micelles, electrolyte addition has little effect on *CMC*'s. When non-electrolytes are added to the micellar solution, the effects are dependent on the nature of the additive. For polar additives (e.g., n-alcohols), the *CMC* decreases with increasing concentration of alcohol, while the addition of urea to micellar solutions tends to increase the *CMC*, and may even inhibit micelle formation.^{36,37} Nonpolar additives tend to have little effect on the *CMC*.³⁸

(ii) Aggregation Numbers and Micelle Geometry

The surfactant aggregation number, N_s , is defined as the average number of monomers in the micelle. Unlike what was detailed above for the dependence of the *CMC* on various properties, aggregation numbers are quite dependent on the nature of the head group,³⁹ the temperature,^{39,40} and the nature of the counterion.^{39,41} The

aggregation number appears to decrease slightly with an increase in the external pressure.^{30,42}

The dependence of N_s on the presence of additives is complex.⁴² Addition of electrolyte tends to increase the surfactant aggregation number. The addition of nonpolar additives, such as n-octane to SDS micelles, has a similar effect. The addition of short to medium chain alcohols tends to decrease the aggregation number, the rate of decrease being proportional to the length of the alcohol chain. While the addition of long chain alcohols has the same initial effect, the aggregation number tends to increase as the alcohol concentration is increased. Specific examples of the dependence of the aggregation number on the addition of alcohols and other solubilizers will be presented in detail in a later section.

The type of geometry which surfactants adopt on aggregation depends on two factors: the length of the hydrophobic surfactant chain and the electrostatic properties of the head group. An optimal head group area, a_o , can be defined as the head group area with which the electrostatic head group repulsions balance the packing constraints imposed by the alkyl chain.^{1,43,44} It should be clear that a_o is dependent on temperature, surfactant concentration, and the nature and concentration of additives. To discuss the ways that monomers pack into aggregated structures, Israelachvili has introduced the dimensionless packing parameter, P , equal to $v/(a_o l_c)$, where v is the volume of the hydrocarbon chain and l_c is the critical length of the hydrocarbon chain. In general, Israelachvili^{1,43} predicts that for $P < 1/3$, spherical micelles would be formed. For surfactants with $1/3 < P < 1/2$, rod-like micelles are predicted, while for $1/2 < P < 2/3$, bilayer type structures are

predicted. As P increases still further, inverted structures (e.g., reversed micelles) are predicted. In spite of the overall utility of the packing parameter, only general trends can be predicted using this approach.⁴⁴ The final constraint on the system is the entropy dominated free energy, i.e., the desire for the monomers to eliminate the unfavourable hydrocarbon-water contacts is balanced by the fact that monomers wish to pack into micelles with as small an aggregation number as possible, within the geometrical constraints imposed by the packing parameter, since the packing of monomers into micelles (or other types of aggregated structures) is entropically unfavourable.

(iii) Counterion Binding

Aggregation of ionic amphiphiles is opposed by the electrostatic repulsions between neighbouring head groups. These repulsions are balanced by the adsorption of counterions at the micellar surface. It is generally believed that "site-binding" of counterions does not take place and that counterion attachment is generally described in terms of a continuous radial distribution function.^{3,45} The concentration of counterions "localized" at the surface is high; thus, a simple distinction between bound and free counterions does not exist.

The degree of counterion binding, β , is defined as follows

$$\beta = \frac{C_{c,m}}{C_{c,t}} \quad (1.4)$$

where $C_{c,m}$ is the concentration of counterions "bound" to the micellar surface, and $C_{c,t}$ is the total counterion concentration. The parameter β is not an experimentally well

defined quantity since the distinction between "bound" and "free" counterions is, in itself, not well defined.

The experiments used to determine β are generally grouped into three broad categories: thermodynamic, kinetic, and spectroscopic. Thermodynamic methods are best exemplified by counterion activity measurements.⁴⁷ Spectroscopic methods, such as NMR relaxation rates,⁴⁸ monitor ions whose spectroscopic behaviour is altered by the micelle. Kinetic methods, best exemplified by self-diffusion, monitor the counterions that move with the micelle.⁴⁹

Counterion association is one of the more frequently determined micellar parameters, perhaps in part due to the number of available experimental techniques. By examining the available literature, Lindman and Wennerström made the following generalizations for the case of ionic micelles of a single surfactant.³

- 1) β is usually found to be in the range 0.5-0.8.
- 2) Different experiments can be classed into one of the three categories listed above, but they generally tend to give a similar picture of counterion association.
- 3) Among counterions of the same charge, ion specificity is usually small. Ionic effects may be important for micelle size and shape and for phase equilibria.
- 4) β is fairly independent of amphiphile concentration, chain length and temperature.
- 5) As the shape of the micelle is changed, the degree of counterion binding also changes.
- 6) β is relatively independent of added electrolyte.

Many of the above generalizations also apply in mixed micellar systems. In these

micelles, the fraction of bound counterions is of interest because it gives an indication of the surface charge density. In binary mixtures of surfactants where the charges on the head groups are the same, β varies monotonically between the values for the pure surfactant components as the composition of the micelle is varied.^{50,51} In an ionic surfactant/alcohol/water system or an ionic/nonionic mixed micelle, the degree of association decreases as the fraction of nonionic surfactant or alcohol in the mixed system is increased.⁵¹⁻⁵⁵ Since alcohols and nonionic amphiphiles are incorporated in the micelle with the nonionic hydrophilic groups in the palisade layer (or headgroup region), the surface potential of the micelle will decrease. This reduces the surface charge density of the micellar system, decreasing β .

Among the many procedures used to determine the degree of counterion binding EMF measurements,⁵⁶⁻⁵⁹ NMR self-diffusion and relaxation rates,^{46,48} variation of the *CMC* with added salt,⁶⁰⁻⁶⁵ and conductivities⁶⁶⁻⁷⁰ are perhaps the most widely used. Conductance determinations of β will be discussed briefly in Chapter 4.

1.2 Solubilization and Mixed Micelle Formation

In practical applications, the surfactants used are almost always composed of mixtures of different homologs of surface-active agents. In fact, in addition to being more expensive to manufacture, pure surfactants generally have little advantage in performance over the less expensive mixtures. Mixed micelles composed of different types of surfactants (i.e., an anionic and a nonionic surfactant) often exhibit synergism. The synergistic properties of mixed micellar systems have attracted a great deal of

interest in recent years.⁷¹

The physical and chemical properties of the micellar interior are generally believed to resemble those of a liquid hydrocarbon.⁵ A solute, originally sparingly soluble in the aqueous environment, may preferentially solubilize in the micellar interior. If this compound is an alcohol, or another hydrophobic molecule, this facilitates micellization due to mixed micelle formation.

Mixed micelles composed of surfactant, alcohol, and water have been studied extensively over the past few years.^{7,8,17,42,72} The properties of aqueous alcohol solutions, and the effect they have on surfactant aggregation are gaining increasing attention, since alcohols are an important component in microemulsion systems.⁷³ The degree of solubilization of the alcohol in the micelle is of paramount importance, since the addition of alcohols to ionic surfactant solutions has been found to decrease the concentration of the monomer in equilibrium with the micelles, i.e., to lower the *CMC*.⁷⁴⁻⁸¹ This decrease can best be explained by the incorporation of the alcohol in the micelle, since the addition of the alcohol and similar substances to water should diminish the hydrophobic effect. Therefore, the solubility of the monomer in the solvent phase should be increased, and an increase in the *CMC* might be expected. However, the opposite has been observed consistently at low alcohol concentrations.⁷⁵⁻⁸¹

A number of investigations indicate that the role of alcohols in micelle formation may be explained in the following manner.

- (1) Modification of water structure.^{81,82}
- (2) Partitioning of alcohol between aqueous and micellar phases.⁸³⁻⁸⁶

- (3) Shift in monomer-micelle equilibria due to a decrease of the hydrophobic effect at very high alcohol concentrations.⁷²

The critical micelle concentration is not the only micellar parameter affected by alcohol solubilization. Mean activities of the surfactant,⁸⁷⁻⁸⁹ counterion binding,⁹⁰ aggregation numbers,⁹¹⁻⁹⁴ and the micellar surface charge density⁹⁵ are also affected when alcohol is incorporated in the micelles.

There has been a good deal of discussion about where the alcohol is solubilized in the micelle.^{93,94} Some authors suggest "alcohol swollen" micelles⁹³ composed of an alcohol core to explain the apparent large degrees of solubilization at moderate to high alcohol mole fractions. This view is consistent with the observed high solubility of alcohols in hydrocarbon solvents. However, the commonly held view is that the alcohol is solubilized with the hydrocarbon tail in the micellar interior and the hydroxyl group in the headgroup region as shown in Figure 1.1.⁷³ The location of alcohols in the micelle is still being debated.⁹⁶

The fraction of the total concentration of alcohol that is distributed in the mixed micelles is expressed as the *p*-value of the solubilizate

$$p = \frac{C_{a,m}}{C_{a,t}} \quad (1.5)$$

where $C_{a,m}$ is the concentration of alcohol solubilized in the micelles, and $C_{a,t}$ is the total alcohol concentration. A number of experiments have been used for determining the micellar bound fraction (or *p*-value) of the solubilizate in the micellar phase. These experiments include vapour pressure measurements,⁹⁷⁻⁹⁹ NMR experiments,⁸⁴⁻⁸⁷ the total

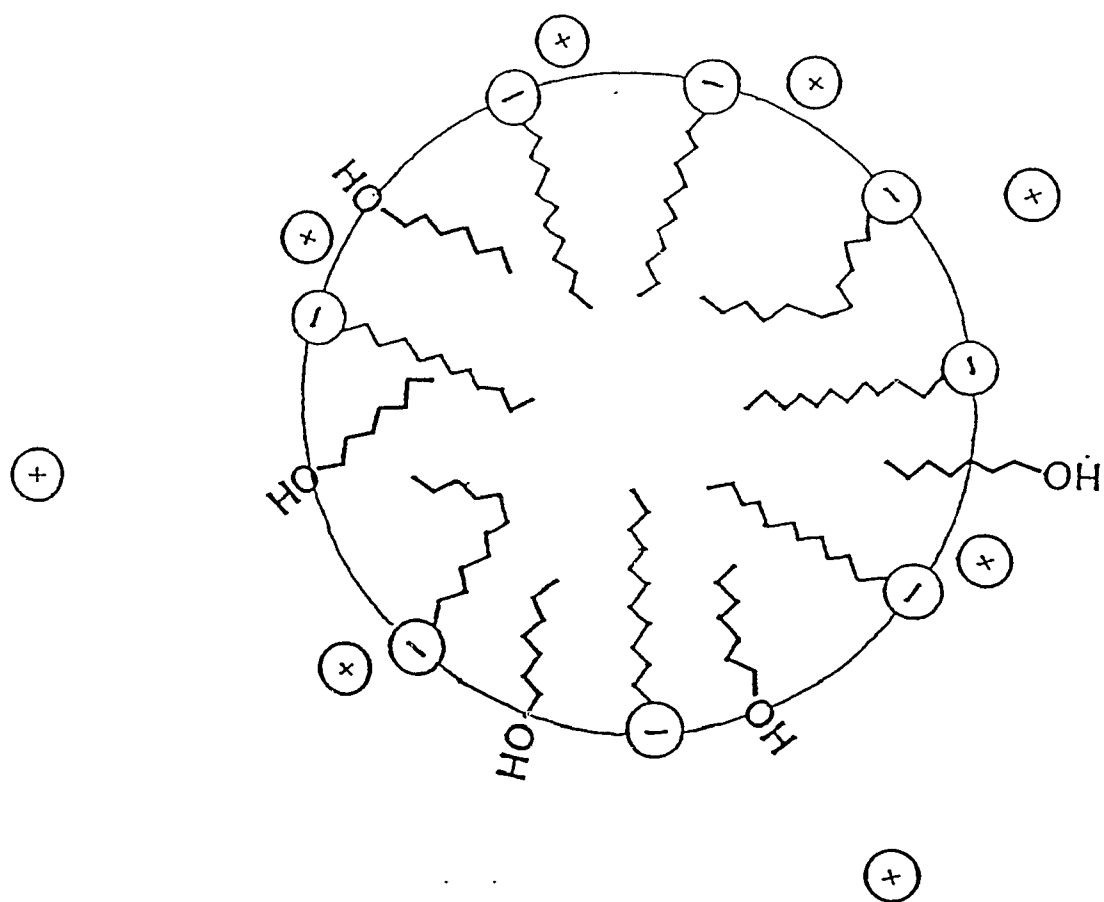


Figure 1.1. Schematic Diagram of an alcohol/surfactant mixed micelle.

solubility method,¹⁰⁰⁻¹⁰⁸ and luminescence probing.¹⁰⁹ NMR experiments for studying solubilization equilibria will be discussed in future sections.

1.3 NMR Spectroscopy of Micellar and Mixed Micellar Solutions

1.3 (a) Basic NMR Principles¹¹³⁻¹²⁰

(i) Interactions of Nuclei with External Magnetic Fields

Nuclear magnetic resonance is a phenomenon found in nuclei possessing a nuclear magnetic moment and, hence, a spin angular momentum. Transitions between the nuclear spin levels give rise to the observables in a nuclear magnetic resonance experiment. The angular momentum, p , of the nuclear spin is quantized in units of \hbar ($\hbar = h/2\pi$)

$$p = I \hbar \quad (1.6)$$

where I is a constant for a particular nuclear spin called the nuclear spin quantum number. For certain nuclei, those with an even mass number and an even charge number (e.g., ^{12}C and ^{32}S), I is equal to zero. Those nuclei that have both an odd mass and an odd charge number, have half-integral values of the nuclear spin quantum number, while those having an even mass number and an odd charge number have integral values of I . The class of nuclei for which $I \neq \frac{1}{2}$ are called quadrupolar nuclei, since the charge distribution at the nucleus is non-spherically symmetrical. All nuclear spins for which $I \neq 0$ have an associated nuclear magnetic moment, μ

$$\mu = \gamma p \quad (1.7)$$

where the proportionality constant, γ , is called the magnetogyric ratio, which is specific for each individual nucleus. The interaction of the magnetic moment, μ , with the applied field, B_o , generates a torque and tends to tip the magnetic moment towards B_o , tracing out a cone at an angle θ about the vector defining the applied field.

In terms of classical theory, the torque is the rate of change of the angular momentum

$$L = \mu \times B_o = \frac{dp}{dt} \quad (1.8)$$

From eq. 1.8, the change of the magnetic moment vector with time can be calculated

$$\frac{d\mu}{dt} = \gamma \frac{dp}{dt} \quad (1.9)$$

The precession of the vector μ about B_o is expressed by

$$\frac{d\mu}{dt} = \omega \times \mu \quad (1.10)$$

where ω_o is the Larmor frequency, the magnitude of which is given by

$$|\omega_o| = -\gamma |B_o| \quad (1.11)$$

The nuclear spin precesses about B_o at a frequency given by

$$\nu_o = \frac{|\omega_o|}{2\pi} = \frac{\gamma}{2\pi} |B_o| \quad (1.12)$$

(ii) Chemical Shift

When a sample is placed in a static magnetic field, nuclei with the same value of γ in different chemical environments experience different magnetic shieldings produced by the electronic environment surrounding the nucleus. In the presence of a strong applied magnetic field, the electrons in the atom are induced to circulate about the nucleus. A local magnetic field is produced by the electron circulation in an opposite direction to the static field. The magnetic field experienced by the nucleus is diminished by an amount proportional to the local field created by the electrons

$$B = B_o(1 - \sigma) \quad (1.13)$$

where σ is called the shielding constant. The resonance frequencies of the nuclei are given by

$$\nu_i = \left(\frac{\gamma}{2\pi}\right) B_o(1 - \sigma_i) \quad (1.14)$$

Individual shielding constants are difficult to determine. Therefore, the resonance frequencies of nuclei are generally determined with respect to a reference compound. The chemical shift scale is a dimensionless scale which expresses the resonance frequencies as chemical shifts, δ 's, with respect to the resonance frequency of the

reference

$$\delta = 10^6 \frac{(\nu_s - \nu_r)}{\nu_r} \approx 10^6(\sigma_r - \sigma_s) \quad (1.15)$$

where σ_r and σ_s are the shielding constants for the reference and sample, respectively.

For protons and ^{13}C , the reference generally used is tetramethylsilane, or TMS.

(iii) Spin-Lattice and Spin-Spin Relaxation

A macroscopic sample is a collection of nuclear spins. When placed in the external field, B_o , the energy of the spin system is divided into $2I + 1$ energy levels, with the individual nuclei distributed among these levels. At equilibrium, the populations of the energy levels are given by the Boltzmann distribution, and the net magnetization in the z direction, M_z^o is given by

$$M_z^o = \frac{N(\gamma\hbar)^2(I(I+1)) B_o}{3kT} ; M_x^o = M_y^o = 0 \quad (1.16)$$

where N is the number of spins, k is the Boltzmann constant (R/N_{Av}), and T is the absolute temperature. The expression for M_z^o is known as the Curie Law.

If the spin system is perturbed from its equilibrium state, it will attempt to reestablish the Boltzmann distribution. Experimentally, this perturbation takes the form of a small field, B_1 , which rotates at the Larmor frequency in the x-y plane. The theory of Bloch¹⁴ predicts that the rate at which the spin system will proceed towards the equilibrium is given by

$$\frac{dM_z}{dt} = \frac{(M_z - M_z^o)}{T_1} \quad (1.17)$$

where M_z is the magnetization along the z axis at time t and T_1 is the time constant that fully characterizes the first order process. Integrating equation 1.17 yields

$$\ln(M_z^o - M_z) = -\frac{t}{T_1} + \ln C \quad (1.18)$$

The rate at which the spin system proceeds toward the equilibrium distribution, $R_1 = 1/T_1$, depends on the ease with which the spin system can transfer energy to the surroundings (i.e., the "lattice"). Hence, R_1 is referred to as the spin-lattice relaxation rate. A number of mechanisms are available to the spin system for transferring the spin energy to the lattice, including dipole-dipole, spin rotation, scalar relaxation, interaction with unpaired electrons, and for nuclei with $I > 1/2$, an additional mechanism, quadrupolar relaxation, is available. The enhancement of the rate of relaxation of the spin system due to its interaction with unpaired electrons will be discussed in some detail below.

It was stated above that the net macroscopic magnetization in the x - y plane is zero. Application of a $90^\circ B_1$ pulse rotates the macroscopic magnetization into the x - y plane along an axis defined by the direction of the B_1 pulse. In a perfectly homogeneous magnetic field, the decay of the x - y magnetization is governed by T_2 , the spin-spin relaxation time

$$\frac{dM_x}{dt} = -\frac{M_x}{T_2}; \quad \frac{dM_y}{dt} = -\frac{M_y}{T_2} \quad (1.19)$$

The spin-spin relaxation time is related to the line width at half-height for an NMR signal, $\nu_{1/2}$

$$\nu_{1/2} = \frac{1}{\pi T_2} = \frac{R_2}{\pi} \quad (1.20)$$

Since the magnetic field is not perfectly homogeneous, the line width is actually the sum of the "natural" line width and the line width due to the inhomogeneity in B_0

$$\nu_{1/2}(obs) = \nu_{1/2}(nat) + \nu_{1/2}(inhomo) \quad (1.21)$$

The inverse of the observed line width is related to an "effective" spin-spin relaxation time, T_2^*

$$\nu_{1/2}(obs) = \frac{1}{\pi T_2^*} \quad (1.22)$$

Relaxation mechanisms that contribute to T_1 also contribute to T_2 so that, in general, $T_2 \leq T_1$.

(iv) Paramagnetic Relaxation

Paramagnetic ions or molecules can contribute to the relaxation of a nuclear spin system in one of two ways: dipole-dipole relaxation by the electron magnetic moment, or by the transfer of some unpaired electron spin density to the relaxing nucleus itself.

The basic equations describing the relaxation of nuclei involved in complexation with paramagnetic complexes were derived by Solomon, Bloembergen, and Morgan.^{121,122} However, in the event that the nuclei and paramagnetic ions do not form stable complexes, paramagnetic relaxation enhancement is due to the dipole-dipole relaxation between the nucleus of interest and the electron magnetic moment. In this case, the paramagnetic contribution to the spin lattice relaxation rate of the nuclei is given by¹²³⁻¹²⁶

$$\begin{aligned} \Delta R_1 &= R_1^p(aq) - R_1(aq) \\ &= \left(\frac{8\pi}{15}\right) \left(\frac{\mu_o}{4\pi}\right)^2 (\gamma_I \gamma_S \hbar)^2 S(S+1) \left(\frac{N_{el} \tau}{b^3}\right) [3J(\omega_I) + 7J(\omega_S)] \end{aligned} \quad (1.23)$$

where $R_1^p(aq)$ and $R_1(aq)$ are the spin lattice relaxation rates in the presence and absence of paramagnetic ions, respectively, S is the total electron spin, γ_I and γ_S are the magnetogyric ratios of the nuclei and the electron, respectively, and ω_I and ω_S are the Larmor frequencies of the nucleus and electron, respectively. N_{el} is the number density of the electrons, b is the distance of closest approach of the paramagnetic agent to the nucleus, τ is the translational correlation time (defined as $b^2/(D_I + D_S)$ where D_I and D_S are the translational diffusion coefficients of spin I and spin S), and $J(\omega)$ is the spectral density function. The nature of the paramagnetic enhancement of the spin-lattice relaxation rate can be deduced by measuring the relaxation rate as a function of the nuclei containing solute, in the presence of a fixed quantity of the paramagnetic species. If the rate enhancement is intramolecular, the relaxation rate will be dependent on the solute concentration, and the rate enhancement will be described by the Solomon-Bloembergen-Morgan relationships,¹²¹⁻¹²² if there is no dependence of the relaxation rate

on the solute concentration, the paramagnetic relaxation enhancement is intermolecular, and is described by equation 1.23. The utility of paramagnetic relaxation enhancement for determining the concentration of micellar bound solubilizates will be further explored in the next section.

1.3 (b) Applications of NMR Spectroscopy in Micellar and Mixed Micellar Solutions

NMR spectroscopy is now widely recognized as a powerful tool for the investigation of many physico-chemical phenomena. It is an inherently useful technique for studying micellar solutions, since the transfer of a monomer from the bulk solution to the micellar phase is generally accompanied by changes in a large number of NMR parameters (e.g., chemical shifts and relaxation rates). Since the advent of the pulsed Fourier transform NMR spectrometer, studies can be made on a wide number of nuclei with good resolution. NMR studies of surfactant solutions include:

- 1) Solubilization of insoluble compounds using the relaxation rates of ^1H and ^{13}C .^{108,127-129}
- 2) Counterion binding using counterion relaxation rates, e.g., ^{23}Na and ^{35}Cl .^{48,130,131}
- 3) Solubilization, counterion binding, phase diagrams, and aggregation numbers using the Fourier-transform, pulsed-gradient spin echo (FT-PGSE) method.^{84-86, 132-138}
- 4) The study of micellar structure and the determination of the p -value of solubilizates using ^1H and/or ^{13}C paramagnetic relaxation experiments.¹³⁹
- 5) Reorientation and segmental motions of amphiphiles in lamellar or other ordered

phases using ^{13}C , ^{31}P , ^2H , and ^{14}N relaxation experiments.¹⁴⁰⁻¹⁴⁵

The strength of the NMR technique, in general, lies in its multi-nuclear, multiparameter approach. NMR experiments have been shown to provide important insight into the nature of the solubilization process, and, hence, mixed micelle formation.³ Many of these studies have taken the form of determining the p -value (eq. 1.5) of a cosurfactant in the micellar phase.^{84-86,132-138} Some work has also dealt with the location of the solubilizates in the micellar phase, and the relationship between the interactions of the individual surfactants in the micellar phase and their chemical structures and mole fractions.¹⁴⁶⁻¹⁴⁹ Two excellent reviews have been published recently on the application of NMR spectroscopy to the investigation of micellar and mixed micellar systems.^{138,150}

Two NMR experiments for determining p are the NMR self-diffusion experiment, and a recently developed NMR paramagnetic relaxation experiment.¹³⁹

The NMR self-diffusion experiment is a well established method for measuring solubilization equilibria,^{150,151} which has contributed greatly to our understanding of many simple and complex surfactant systems. The micellization process is known to affect a number of parameters, including self-diffusion. Under conditions of fast exchange of the solubilizate between the aqueous and micellar phases, the observed self-diffusion coefficient for the solubilized species is a weighted average of the self-diffusion coefficients of the solubilizate residing in the bulk solution and the micelles. This is described as follows

$$D_{obs} = (1-p)D_f + pD_b \quad (1.24)$$

where D_{obs} is the experimentally determined self-diffusion coefficient, and D_f and D_b are the diffusion coefficients of the solubilize in the aqueous and micellar phases, respectively. Rearranging equation 1.24 yields

$$D_{obs} = D_f + p(D_b - D_f) \quad (1.25)$$

Therefore, if the self-diffusion coefficients of the free and bound species are known, p can be determined. D_f is measured in the absence of surfactant, in a separate experiment, by monitoring the self-diffusion of the solubilize in aqueous solution. However, determining D_b is not straightforward. If the diffusion of solubilized species within the micellar interior can be considered unimportant, D_b can then be taken as the diffusion coefficient of the solubilize which moves with the micelle.^{150,152} Equality of the micellar diffusion coefficient, D_m , with D_b is assumed, and D_m is determined as the self-diffusion coefficient of a very hydrophobic solute (usually TMS).¹⁵⁰

Another NMR experiment for measuring the p -value has been developed recently by Gao et al.^{139,153} This method is based on the difference in the relaxation rates of the solubilize, in aqueous and micellar solutions, in the presence and absence of a very small concentration of paramagnetic ion. If the paramagnetic ion and the surfactant headgroup have the same charge, the paramagnetic ion should reside exclusively in the aqueous phase, away from the micellar headgroup. Assuming that the paramagnetic ion does not influence the relaxation of micellar bound species, a solubilize (e.g., an

alcohol) which is distributed between the aqueous and micellar phases, will be affected by the paramagnetic ion in one of two ways. If the solubilize distribution favours the aqueous phase, its relaxation rate will be enhanced significantly by the paramagnetic ion. Conversely, if the distribution favours the micellar phase, relaxation enhancement will not be significant.

Under conditions of fast exchange, the observed relaxation rate for the solubilize is a weighted average of the rates for the solubilize in the aqueous and the micellar phase. When there are no paramagnetic species in the solution, the observed rate of spin-lattice relaxation is described by the following equation

$$R_{1,obs} = R_{1,f} + p(R_{1,b} - R_{1,f}) \quad (1.26)$$

where $R_{1,obs}$ is the observed spin-lattice relaxation rate of the solubilized species, $R_{1,b}$ is its relaxation rate in the micellar phase, and $R_{1,f}$ is its rate of relaxation in the water phase. When paramagnetic ions are present, the observed rate is written

$$R_{1,obs}^p = R_{1,f}^p + p(R_{1,b} - R_{1,f}^p) \quad (1.27)$$

Since the paramagnetic ion is assumed not to have an influence on the micellar bound solubilize (i.e, $R_{1,b}$ is unaltered), subtracting equation 1.27 from equation 1.26 and rearranging allows the fraction of the solubilize in the micellar phase to be calculated

$$p = 1 - \frac{R_{1,obs}^p - R_{1,obs}}{R_{1,f}^p - R_{1,f}} \quad (1.28)$$

Gao et al. have determined the p -values of a number of solubilizes in anionic SDS

and cationic DTAB micellar systems, using the paramagnetic relaxation experiment.¹³⁹ These authors compared their results for the p -values of a number of organic solubilizates, to those determined by Stilbs for the same solubilizates, using the NMR self-diffusion experiment.^{84,85} Generally, the results obtained with the paramagnetic relaxation method were in good agreement with those of Stilbs.^{139,153}

The paramagnetic relaxation experiment has the advantage of being applicable to systems where the NMR self-diffusion experiment is difficult to use.^{139,153} Such systems include polymer-surfactant solutions, where polymer diffusion is slow and difficult to measure.¹⁵⁰ The NMR paramagnetic relaxation enhancement experiment has been used in these systems.¹⁵³ It also has the advantage that it can be done on any FT-spectrometer, whereas special probes and hardware modifications are necessary for the FT-PGSE experiment.¹⁵⁰ The precision of the distribution coefficients measured by the NMR paramagnetic relaxation experiment are at least equal to those of the FT-PGSE experiment. The FT-PGSE experiment has been applied successfully in microemulsion systems;¹⁵⁴⁻¹⁵⁷ the application of the NMR paramagnetic relaxation experiment in microemulsion systems is currently being investigated.¹⁵⁸ Nuclei which relax quickly (²³Na for example) are difficult to study by either method.

1.4 Luminescence Probing and the Determination of Aggregation Numbers in Mixed Micellar Systems

1.4 (a) Introduction

Luminescence probing involves the use of probe molecules, or ions, which emit

photons when excited by light of the proper wavelength. In the past 10-15 years, luminescent probing has been used extensively to investigate a wide variety of aggregated systems, ranging from simple micelles to vesicles and biological membranes.

Historically, the first use of luminescent probing in micellar systems involved the change in spectral intensity of an organic dye molecule after the onset of micellization, in order to determine the *CMC* of the micellar system.^{5,159} The use of luminescence probing to investigate the microviscosity and micropolarity of biological membranes and micelles has been reviewed.¹⁶⁰ In micellar solutions, luminescence probing allows a facile determination of the surfactant aggregation number.¹⁶¹⁻¹⁷⁴ Recently, depth dependent fluorescent quenching of 9-(anthroyloxy)stearic acids by water has been used to investigate water penetration in cationic, anionic, and nonionic micelles.¹⁷⁵ The reviews by Zana⁴² and Blatt et al.¹⁶⁰ are excellent overviews of the development and application of luminescence probing in a number of aggregated systems.

The determination of surfactant aggregation numbers by the static quenching of the fluorescence of a micelle solubilized probe was proposed originally by Turro and Yekta.¹⁷⁰ In spite of some shortcomings of this method (to be discussed later), the static quenching experiment allows a quick, reliable, and convenient way of determining N_s , the surfactant aggregation number. Lianos and Zana,¹⁷⁶ and later Almgren and Swarup,¹⁷⁷ have applied the static quenching method to alcohol surfactant mixed micelles, determining both the surfactant and alcohol aggregation number, N_a . The application of time-resolved fluorescence quenching methods to micelles and microemulsions has also been reviewed recently.¹⁷⁸

1.4 (b) *Photophysical Events after Excitation*¹⁷⁹⁻¹⁸¹

When a luminescent probe is excited by light of a proper wavelength (either from a pulsed or continuous source), photons are absorbed and electronic excitation of the probe results. The absorption processes promote an electron from the ground state (S_0) to various upper excited states (S_1, S_2, \dots, S_n), with the retention of electron spin. Following the excitation process, the excited state electron is brought back to lower energy electronic states by a number of processes. Two of these (vibrational relaxation and internal conversion) are fast. A third process, involving a change of spin of the excited electron, can be much slower. Internal conversion, occurring on the order of 10^{-12} s, brings the electron from a higher to lower electronic state, but a higher vibrational level. Since internal conversion, intersystem crossing, and vibrational relaxation do not result in the emission of photons, they are termed non-radiative processes.

Fluorescence and phosphorescence are radiative processes in which the excited state electron decays to S_0 from the first singlet excited state (S_1) and the first excited triplet state, respectively, with the emission of a photon. The time scale for fluorescence is on the order of nanoseconds, while intersystem crossing ($S_1 \rightarrow T_1$) can occur as quickly as 10^{-8} seconds, thus competing with the emission of photons by fluorescence. Generally, emission of photons by phosphorescence is slow (10^{-5} to several seconds).

1.4 (c) *Fluorescence Spectra*

The fluorescence emission spectrum is the change of the emission intensity of the

luminescent probe with wavelength, at a constant exciting wavelength and intensity. It can be easily seen from the emission spectrum of pyrene in SDS micellar solution (Fig. 1.2) that emission spectra may show fine structure reflecting the vibrational levels of the ground state. For pyrene, that ratio of the intensity of the first and third vibronic peaks (I_1/I_3) has been shown to be sensitive to the polarity immediately surrounding the probe. In water, at a concentration of 10^{-7} molal, the I_1/I_3 ratio is about 1.8, while in n-hexane and cyclohexane, the pyrene I_1/I_3 ratio is about 0.6.^{181,182} It can be seen from Fig. 1.2, the ratio in SDS is about 1.2, indicating that the pyrene senses a polarity approximately midway between water and oil.

1.4 (d) Lifetimes of Excited Luminescent Probes; Quantum Yield

The decay of excited luminescent probes from the first triplet or singlet excited states to the ground state, S_0 , can be represented as follows



where k_f and k_p are the rate constants for fluorescent and phosphorescent decay, respectively. The fluorescent and phosphorescent lifetimes are simply the reciprocals of the radiative rate constants

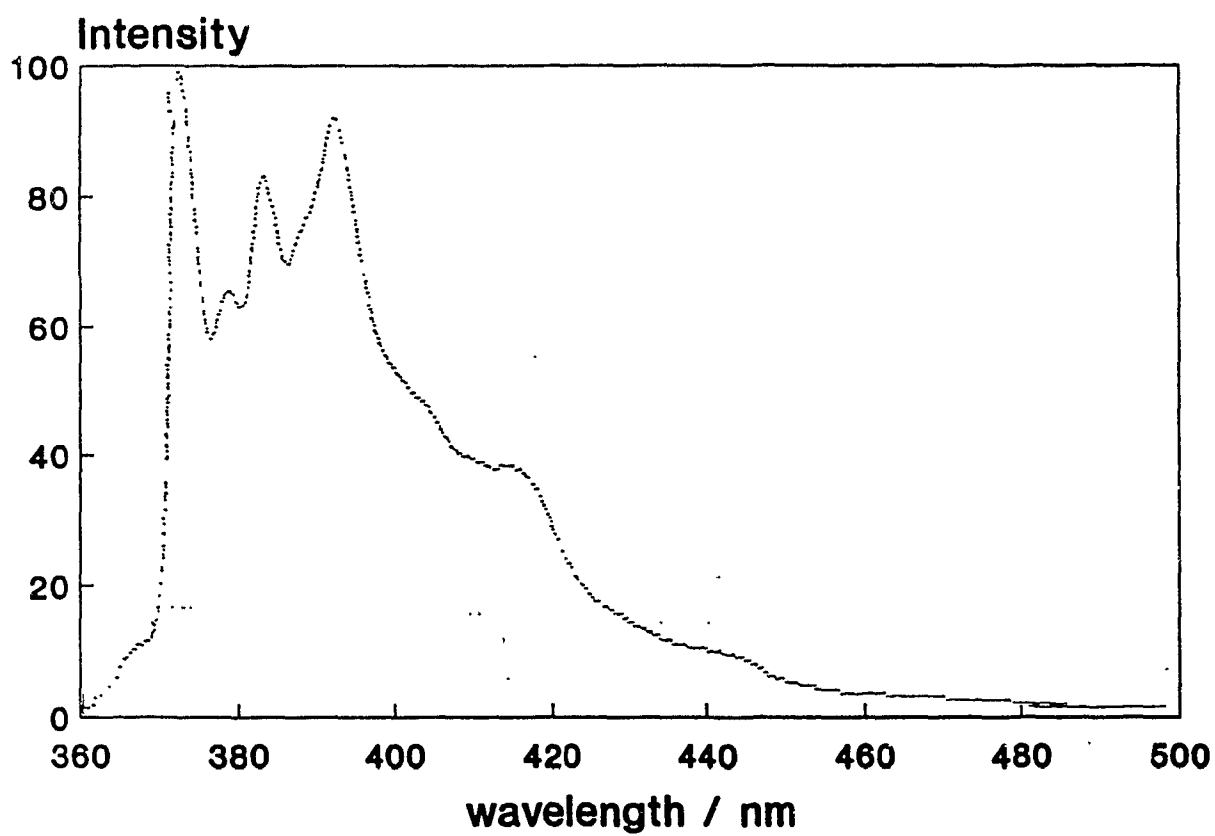


Figure 1.2. The fluorescence emission spectrum of 50 mmolal SDS/0.01 mmolal pyrene.

$$\tau_f^r = \frac{1}{k_f} \quad ; \quad \tau_p^r = \frac{1}{k_p} \quad (1.31)$$

In practice, however, the non-radiative processes contribute to the deactivation of the excited luminescent probe. This leads to experimental lifetimes that are shorter than the "true" radiative lifetimes

$$\tau_f = (k_f + \sum k_d)^{-1} = k^{-1} \quad (1.32)$$

The quantum yield, denoted Φ , is defined as the ratio of the number of emitted photons to the number of absorbed photons. In the case of fluorescence, the quantum yield of fluorescence, Φ_f is written

$$\phi_f = \frac{k_f}{k_f + k_d} \quad (1.33)$$

1.4 (e) Quenching Processes

In the presence of a quencher, q , an additional process is available for the excited luminescent probe to decay to the ground state, S_0 . Most quenching processes are generally pseudo first-order. For the quencher to be effective, quenching should occur near the diffusion limit in fluid media.

Quenching can occur by energy transfer, electron transfer, or by excimer formation. In electron transfer, the luminescent probe is either oxidized or reduced, forming a radical cation/anion pair with the quencher, while retaining, or not retaining its excitation energy. Depending on the dielectric constant of the medium, the radical cation/anion

pair may dissociate.¹⁷⁹ In micellar systems, due to the low value of the dielectric constant in the micellar interior, the radical ion pair cannot break apart and back electron transfer occurs, thereby deactivating the luminescent probe.

In energy transfer mechanisms, the excited probe passes off its excitation energy to an acceptor molecule during the lifetime of the excited state. Deactivation of the probe may occur by collisional mechanisms, which involve simultaneous transfer of the excited electron to the quencher and return transfer of a ground state electron from the quencher, or by a photon transfer mechanism, whereby the luminescent probe emits a photon of the proper excitation wavelength to excite the quencher molecule.

1.4 (f) *Excimer Formation*

Excimers are molecular dimer aggregates formed when an excited state luminescent probe complexes a ground state probe



where k_E and k_{-E} are the rate constants for excimer formation and dissociation, respectively. Excimer formation produces a broad emission at a longer wavelength than the singlet emission, and generally occurs in concentrated solutions and in the solid state. Excimer formation has been used extensively to probe the microviscosities of vesicles and biological membranes.¹⁶⁰

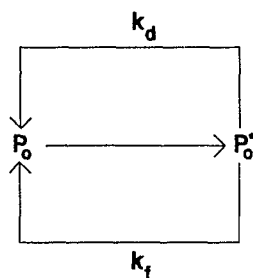
1.4 (g) Probe and Quencher Distribution among Micelles and the Static Quenching Method for determining Surfactant Aggregation Numbers

Pyrene is a fluorescent probe having a lifetime of 330 ns in SDS micellar solutions.¹⁸¹ The pyrene emission spectrum (Fig. 1.2) of 10^{-5} molal pyrene in 0.0500 molal SDS micellar solution is typical of emission of monomeric pyrene. It is well known that pyrene excimers are formed at concentrations as low as 6×10^{-5} molal in SDS solutions slightly above the *CMC*, or at a [pyrene]/[micelle] ratio of 0.3.^{42,183} This indicates double occupancy of the micelle by pyrene is occurring, which can be accounted for by a number of different statistical distributions of probes among the micelles. It is generally agreed upon in the literature that the distribution of probes (and quenchers) in micelle solutions follows Poisson statistics;¹⁸⁴⁻¹⁸⁹ the probability of finding n probes (or quenchers) is given by

$$\sigma_n = \frac{\langle Q \rangle^n}{n!} \exp(-\langle Q \rangle) \quad (1.35)$$

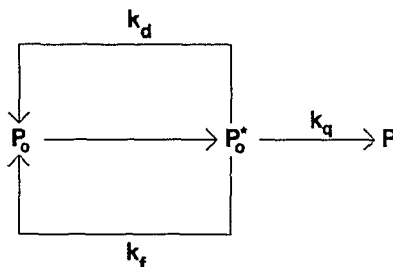
where σ_n is the probability of finding n probes (or quenchers) in a given micelle and $\langle Q \rangle$ is the average occupancy number of the micelle, and is equal to ratio of probe (or quencher) molecules to the number of micelles.

Consider a very immobile, hydrophobic probe dissolved in a micellar solution. In the absence of micellar bound quenchers, the steady state concentration of fluorescing species can be obtained from the series of reactions shown below



$$P_0^* = \frac{F}{k_d + k_f} \quad (1.36)$$

where F is the formation rate of excited probe molecules and k_d is the sum of the rate constants of all other nonradiative deactivation processes. With the addition of quencher to the micellar solution, the distribution of which is given by Poisson statistics,¹⁸⁵⁻¹⁸⁹ the concentration of fluorescing species in the presence of quencher, P^* , is obtained as shown below



$$P^* = \frac{\sigma_n F}{k_d + k_f + k_q} \quad (1.37)$$

The ratio P_0^*/P^* can be obtained from equations 1.36 and 1.37

$$\frac{P_0^*}{P^*} = \frac{I_0}{I} = \frac{F(k_f + k_d + nk_q)}{\sigma_n F(k_f + k_d)} \quad (1.38)$$

$$\frac{I_0}{I} = \frac{(1 + nk_q \tau_f)}{\sigma_n} \quad (1.39)$$

If the quencher is chosen such that $k_q \tau_f \gg 1$, then fluorescence will be observed only from micelles containing a probe and no quencher (i.e., static quenching). Therefore,

the probability of observing fluorescence is proportional to σ_o

$$\frac{I_o}{I} = \sigma_o^{-1} = \exp(\langle Q \rangle) = \exp\left(\frac{[Q]}{[M]}\right) \quad (1.40)$$

$$\ln \frac{I_o}{I} = \frac{[Q]}{[M]} \quad (1.41)$$

It should be obvious from the above derivation that experimental conditions should be carefully chosen in order to comply with the assumptions of the steady-state method. Micelles are dynamic structures; therefore, the micelle size must remain constant and the quencher and probe must stay solubilized in the micelle on the time scale of the fluorescent lifetime. Pyrene has a τ_f of 330 ns in SDS micellar solution, and 175 ns in DTAB micelles,^{42,190} with a residence time in the micelles on the order of 10^{-4} seconds.^{180,182} The residence time of the quencher, in this case cetylpyridinium ion (CP⁺), has been shown to be above 50 μ s.^{191,192} Since cetylpyridinium ion is a long chain cationic surfactant, it binds to SDS micelles both hydrophobically and electrostatically, while it forms mixed micelles with DTAB.

Quenching must occur at a rate sufficiently fast enough that the fluorescence will occur from micelles containing a probe and no quencher. This assumption is generally good for small spherical micelles with an aggregation number less than 80,^{42,193} while in larger micelles, diffusion over the micellar surface may not be fast enough to allow a fast quenching rate. The rate constants for the quenching of pyrene fluorescence by cetylpyridinium ion in SDS and CTAB micelles have been reported to be 5×10^{-7} ¹⁹⁴ and 1×10^{-7} ¹⁹⁵ s⁻¹, respectively. Thus, the rate of fluorescence quenching is slightly better

than an order of magnitude faster than the rate of fluorescence decay. It is also assumed that the micellar size and shape are unaltered with the introduction of the probe and quencher into solution. Although this has been a source of lively debate in the literature for a number of years,^{193,196} it is generally, but incorrectly stated that the micelles are not affected when the pyrene concentration is ≈ 1 pyrene per 100 micelles. It is instructive to reiterate the underlying principle of the static quenching method; fluorescence is observed only from micelles containing a solubilized probe and no quencher, in effect, counting the number of micelles with solubilized probes. The argument above, correctly stated, is that the *solubilization of very hydrophobic probes (and quenchers), like pyrene, does not affect the number of micelles in solution.* It is for this reason also that the quencher concentrations are also kept low (on average, less than 1 per micelle).

The static quenching method is, therefore, a convenient and useful method for determining the surfactant aggregation number. It is more versatile than the classical methods for determining surfactant aggregation numbers, in that the static quenching method determines the actual concentration of micelles, $[M]$, at a specific concentration of surfactant. Classical methods, such as light scattering, determine the surfactant aggregation at the *CMC*.¹⁹⁷ Recently, small angle neutron scattering has also been shown to provide reliable estimates of the surfactant aggregation number.^{42,198} However, a disadvantage is the requirement for deuterated solvents and access to specialized equipment,¹⁹⁸ while the static fluorescence quenching method can be routinely performed on a simple fluorescence spectrophotometer. It is, however, limited by several assumptions which must be verified. The probe/quencher pairs pyrene/cetylpyridinium

ion and $\text{Ru}(\text{BPy})_3^{2+}$ /9-methylanthracene have been shown to satisfy the assumptions of the steady state method.^{42,194,199}

1.4 (h) Previous Work

Although a number of authors have used the steady-state or the time-resolved fluorescence quenching experiment to probe the aggregation state of a wide variety of aggregated species,^{42, 160-183} relatively few investigators have examined the effects of alcohols on the aggregation number of ionic surfactants. Lianos and Zana^{177,200,201} reported on the effects of the addition of 1-butanol and 1-pentanol to CTAB and TTAB micelles. These authors were the first to calculate the alcohol aggregation number from the micellar concentration, obtained from the time-resolved fluorescence quenching experiment, and the distribution coefficient of the alcohol between the aqueous and micellar phases. Almgren and Swarup^{176,202,203} reported on the effects of the addition of a number of organic solubilizates on the aggregation number of SDS, as a function of both the concentration of surfactant and added solubilizate, determining both the surfactant aggregation number and the aggregation number of the additive. These authors reported a slight increase in the aggregation number of SDS as the surfactant concentration was increased, in the absence of solubilizate. At a specific concentration of surfactant, the addition of polar solubilizates, e.g., n-alcohols, was generally observed to decrease the surfactant aggregation number, while the alcohol aggregation number increased sharply. The total aggregation number, $N_s + N_a$, was found to increase slightly, as the concentration of polar solubilizate was increased. Somewhat surprising

was the observation by both groups^{176,177,200-203} that at high concentrations of alcohol as cosurfactant, the micelles are composed essentially of alcohol molecules (i.e., N_a is large); the surfactant molecules appear to act as a "glue", stabilizing the micelles.

1.5 Conclusions

As described in sections 1.2, 1.3, and 1.4, it can be seen that mixed micelles of alcohol and surfactant are of considerable interest and have been studied widely. A thorough understanding of the effects of alcohols on ionic surfactant solutions is an essential step in clarifying the role of alcohols as cosurfactants in microemulsions, and may help understand the interaction between some neutral polymers and ionic surfactants. NMR and luminescence probing have been shown to be useful tools in investigations of these systems.^{3,42,138,150,179-181}

In sections 1.2, 1.3, and 1.4, a brief discussion of previous investigations on alcohol/surfactant mixed micelles has been presented. It is interesting to note that much of this work has been done on the n-alcohols and some of their branched isomers. Few investigations have been carried out on other families of alcohols, such as the alkoxyethanols. Although 2-butoxyethanol (BE) has been a much investigated cosurfactant in the literature, there are only a few studies on mixed micelles of BE with various surfactants.²⁰⁴⁻²⁰⁷ Apparently, only one study has appeared dealing with the effects of the addition of alkoxyethanols on the *CMC* of an ionic surfactant, SDS.²⁰⁴ As well, relatively little work has been done on the interaction of ethoxylated alcohols with cationic surfactants. Because of the importance of BE as a cosurfactant in microemulsion

studies, it was decided to extend previous work in our laboratory⁸⁷⁻⁸⁹ on sodium decanoate/alcohol mixed micellar systems to other ionic surfactant/alkoxyethanol systems. Specifically, the interactions of alkoxyethanols with some typical anionic and cationic micelles, and the subsequent formation of alcohol/surfactant mixed micelles, have been investigated by a number of techniques, in order to obtain as complete a picture as possible with regards to the influence of the ethylene oxide (EO) group on the formation of mixed micelles. In Chapter 3, the applicability of the NMR paramagnetic relaxation experiment to the determination of the distribution constants of alcohols in micellar systems is discussed. In Chapter 4, the *CMC*'s and the degrees of counterion binding of some ionic surfactant/alkoxyethanol mixed micelles are determined for a typical anionic surfactant (SDS) and a typical cationic surfactant (DTAB), using EMF and conductivity measurements. The results are discussed in terms of the contribution of the EO group to the free energy of mixed micelle formation. In Chapter 5, the distribution constants and the transfer free energies of alkoxyethanols from heavy water to the micellar phase of anionic SDS and sodium decanoate (SD), and cationic DTAB and dodecylpyridinium chloride (DPC) micelles have been determined. In Chapter 6, the aggregation numbers of the surfactant of anionic SDS/alkoxyethanol and cationic DTAB/alkoxyethanol mixed micelles are determined by the static fluorescence quenching technique, using the recommended probe/quencher pair pyrene/cetylpyridinium ion. Employing the distribution constants determined with the paramagnetic relaxation experiment in Chapter 5 and the concentration of micelles determined from the static quenching experiment, the aggregation numbers of the cosurfactant in these mixed

micelles have been obtained. As well, the micropolarity of the environment surrounding the luminescent probe (pyrene) has been evaluated in all the mixed micellar systems, using the I_1/I_3 ratios of the pyrene emission spectrum. All these results are discussed in terms of the influence of the EO group on the formation of mixed micelles, as well as some possible reasons why alkoxyethanols interact differently with anionic than with cationic micelles. Chapter 7 presents a summary and a number of proposals for future work.

Chapter 2

Experimental Methods and Materials

2.1 Materials

2.1 (a) Surfactants

Sodium decylsulfate (Kodak Chemical) and sodium dodecylsulfate (Sigma) were purified by repeated recrystallizations from ethanol. Sodium decanoate (SD) was prepared by dissolving the decanoic acid (Aldrich Gold Label) in ethanol and adding an equimolar amount of NaOH (Fisher Chemical Co.), which was dissolved in a water/ethanol mixture. After freeze-drying, the purified SD was redissolved in water to a final aqueous solution pH of 9.2.⁸⁷⁻⁸⁹ Dodecyltrimethylammonium bromide (DTAB), dodecylpyridinium chloride (DPC), and cetylpyridinium bromide (CPB) were obtained from Sigma and purified by repeated recrystallizations from an acetone/ethanol mixture. In the case of DPC and CPB, the final recrystallizations were preceded by stirring with decolourizing charcoal. Water was purified by passing it through Millipore R/Q ion exchange system. The deionized water had a resistivity of $1.5-2.5 \times 10^6$ ohm \cdot cm.

2.1 (b) Alcohols

Ethanol (C_2E_0), 1-propanol (C_3E_0), 1-butanol (C_4E_0), 1-pentanol (C_5E_0), 1-hexanol (C_6E_0), 1-octanol (C_8E_0), and ethylene glycol mono-n-butyl ether (C_4E_1) were reagent grade solvents from the Fisher Chemical Company; they were purified by two distillations and stored over molecular sieves. Ethylene glycol mono-n-ethyl ether

(C₂E₁), diethylene glycol mono-n-ethyl ether (C₂E₂), diethylene glycol mono-n-butyl ether (C₄E₂), and diethylene glycol mono-n-hexyl ether (C₆E₂) were spectroscopic grade solvents (Aldrich) and were used as received. Triethylene glycol mono-n-ethyl ether (C₂E₃) and triethylene glycol mono-n-butyl ether (C₄E₃) were obtained from Tokyo Kasei and used without further purification. Tetraethylene glycol (TEG) and tetraethylene glycol dimethyl ether (TGD) were obtained from the Aldrich Chemical Company (> 98 % purity) and were used as received.

2.1 (c) *Probe Molecules*

Highly purified pyrene was a kind gift from Dr. K. Hayakawa, Kagoshima, Japan. Manganese chloride was an analytical grade reagent from the MacArthur Chemical Company. Mn(EDTA)²⁻ was prepared in D₂O from manganese chloride and a slight excess of Na₂H₂EDTA. The sodium salt of 3-carboxy-proxyl was prepared by neutralizing the acid form (Sigma) with a slight excess of NaOD.

2.2 *Methods and Solution Preparations*

2.2 (a) *CMC Determinations*

Mixed solvent systems were prepared on a molality basis by mixing the appropriate quantities of alcohol and deionized water. For *CMC* determinations from EMF measurements, surfactant concentrations are expressed in molality units, *m*, where *m* is defined as the number of moles of surfactant/kilogram of H₂O, D₂O, or kilogram of the mixed solvent. The *CMC* values of SDecS/alcohol mixed micellar systems were obtained

from Na^+ activity determinations, using a sodium responsive glass electrode (Fisher) and a double junction calomel reference electrode with NH_4NO_3 as the external filling solution. This was done to eliminate the precipitation of KDecS in the salt bridge. The *CMC* values in DTAB/alcohol mixed micellar systems were determined from EMF titrations using a PVC membrane electrode responsive to the cationic amphiphile, in combination with a calomel reference electrode. The EMF titrations were carried out on an automatic titration system consisting of a Dosimat automatic buret (Metrohm) and a Keithley high impedance electrometer (model A614), controlled by an IBM PC. *CMC* values of SDS/alkoxyethanol and DTAB/alkoxyethanol mixed micellar systems were determined on a molarity basis, M (where M is defined as the number of moles of surfactant/liter of solution), from the measurement of solution conductances, using an Industrial Instruments conductance bridge (operating at a frequency of 1000 Hz) and a Fisher conductance cell ($K_{\text{cell}} = 1.0 \text{ cm}^{-1}$). The temperature of the conductance cell was controlled to within $\pm 0.05 \text{ }^\circ\text{C}$ with a Cole Parmer Polytemp water bath.

2.2 (b) NMR Experiments

All proton spin-lattice relaxation times (T_1 's) were measured on freshly prepared solutions. Solutions of paramagnetic salts, i.e., the sodium salt of 3-carboxypropyl for anionic surfactant solutions and $\text{MnCl}_2 \cdot 6\text{H}_2\text{O}$ for cationic micelles, were prepared in D_2O (99.9% Aldrich, Norell, or Stohler Isotope). Stock surfactant solutions were prepared on a molality basis in either D_2O or in the paramagnetic ion solution. Portions of the stock surfactant solutions, corresponding to 1 g of solvent, were transferred to

small sample vials. The solubilizates (alcohols) were added to the sample vials with a Hamilton syringe. The measurements reported here are in mixtures of relatively low alcohol concentration, not exceeding 0.05 molal (m). The contents of the glass vials were transferred directly to NMR tubes. The concentrations of surfactant used in the present work were 50 mg DTAB/g solvent (0.162 m), 50 mg DPC/g solvent (0.166 m), 70 mg SDS/g solvent (0.243 m), and 90 mg SD/g solvent (0.463 m).

Proton NMR spectra were recorded at 361.008 MHz ($B_0 = 8.48$ T) on a Nicolet 360 NB spectrometer. Spin-lattice relaxation times (T_1 's) were measured using the inversion recovery pulse sequence available on the Nicolet computer system, in which alternate $\pi/2$ pulses are phase shifted by 180° , and a composite π pulse is used to account for pulse imperfections. The T_1 's were calculated from the peak heights obtained at twelve or more variable delays, using a three parameter, non-linear least squares fitting procedure.¹¹⁸ The experiments were carried out at 25 ± 1 °C for SDS and SD; at 35 ± 1 °C for DPC and DTAB.

2.2 (c) *Luminescence Quenching Experiments*

All solutions were prepared by mass; the concentrations are reported in molality units, corresponding to the number of moles of surfactant per kilogram of the solvent system (either water or a water/alcohol mixture). Solution preparation for the luminescence quenching experiments was carried out as follows. A small amount of a 0.0500 molal pyrene/ethanol solution was placed in a fleaker and the solvent allowed to evaporate, usually overnight, depositing the pyrene as a thin film on the bottom of the

vessel. A stock solution of the surfactant/mixed solvent system was prepared directly in the fleaker containing the pyrene, and stirred for at least four hours to ensure complete dissolution of the pyrene in the surfactant solution. This method of solution preparation was found previously^{42,179-181} to be a very effective means of dissolving hydrophobic fluorescent probes (i.e., pyrene) into a surfactant solution. As an example of an alternative preparation, Almgren and Löfroth¹⁶⁴ mixed small volumes of their stock solutions of quencher (9-methylanthracene) in benzene, injected the desired amount into the surfactant solutions, and then evaporated the benzene from the solutions by bubbling with nitrogen. It has been found since that the preparation is simplified if the solvent medium for the probe (or quencher) is allowed to evaporate before addition of the surfactant solution.⁴² The stock quencher solutions were prepared from one-half of the stock surfactant/probe solutions by adding the desired amount of quencher (cetylpyridinium ion, or CP⁺) to the solution, and stirring for 1-2 hours. Solutions at different quencher concentrations were prepared by weighing \approx 0, 2, 4, 6, 8, and 10 g of the stock quencher solution and adding enough of the blank surfactant/probe solution to make a 10 g sample. Steady-state pyrene fluorescence emission spectra were recorded at room temperature (\approx 23°C) on a Perkin-Elmer MPF-66 spectrophotometer, using an excitation wavelength of 338 nm and scanning the emission from 350 to 500 nm. The slits were adjusted so that the intensity of the solution containing pyrene and no quencher was about 80 - 90% of the maximum. I_1/I_0 ratios were measured directly from the spectra. The intensity of the emission at 373 nm was used in the plots of $\ln(I_0/I)$ versus the quencher concentration.

Chapter 3. The Application of the NMR Paramagnetic Relaxation

Experiment to the Determination of Distribution

Coefficients of Solubilizates in Micellar Systems

3.1 Introduction

In a number of practical applications, surfactants are often used in solutions containing additional surface active agents (i.e., co-surfactants) such as alcohols or polymers. It was discussed in the introduction of this thesis that the properties of these mixed systems can be very different from those of solutions of the individual components. Generally, these surfactants and co-surfactants form mixed micellar solutions;^{3,7-19,71} in the presence of polymers, polymer-surfactant complexes may be formed.^{208,209} Studies of the interactions between surfactants and alcohols or polymers are of great interest in many industrial applications of surfactants,⁶⁻⁸ such as detergency, mineral processing, oil recovery, and emulsion polymerization. The determination of the micelle-water distribution coefficients of alcohols and polymers in micellar solutions has been the focus of a number of investigators.^{25,91-107} In the past decade, a number of experimental techniques have been proposed to measure the distribution coefficients of solubilizates in micellar systems, including vapour pressure,^{25,97-99} total solubility,¹⁰³⁻¹⁰⁴ adsorption and fluorescence spectrophotometry,¹⁰⁹⁻¹¹¹ thermodynamic measurements,^{206,207} and NMR self-diffusion measurements.¹⁵⁰ However, each of the above methods suffers from experimental limitations. For example, the vapour pressure method is suitable only for volatile solubilizates, while thermodynamic measurements are suitable only for

surfactants with high *CMC*'s. None of these methods can be applied easily to determine the distribution coefficients of large solubilizates, e.g., water soluble polymers, in micellar solutions.

The Fourier Transform Pulsed-Gradient Spin Echo (FT-PGSE) is a very powerful method for determining the distribution equilibria of solubilizates in micellar solutions. However, the major drawback of the FT-PGSE experiment is the need for specialized probes and hardware for generating the pulsed-gradients necessary for the experiment.¹⁵⁰ Recently, a new NMR technique to measure the distribution coefficients of solubilizates in micellar solution, based on NMR paramagnetic relaxation, has been developed by Gao et al.^{139,153} The fundamentals of the paramagnetic relaxation experiment are relatively straightforward. In Figure 3.1, a benzene molecule distributed between SDS micelles and aqueous phases is shown; a two-site model for the solubilization of benzene and rapid exchange of the solubilizate between the water and the micelles is implicitly assumed. The observed relaxation time, $R_{1,obs} = 1/T_{1,obs}$, is a weighted average of the observed relaxation times of the benzene in water, $R_1(aq)$, and in the SDS micelles, $R_{1,mic}$

$$R_{1,obs} = pR_{1,mic} + (1-p)R_1(aq) \quad (3.1)$$

where p is the fraction of the total number of moles solubilizate located in the micelles. If we add a paramagnetic ion to the solution (a co-ion of the surfactant), this ion will be repelled from the micellar surface; only the fraction of solubilizate contained in the aqueous phase will be affected by the added paramagnetic ion. Equation 3.1 is rewritten to include the contribution of the paramagnetic ion to the solubilizate relaxation rate

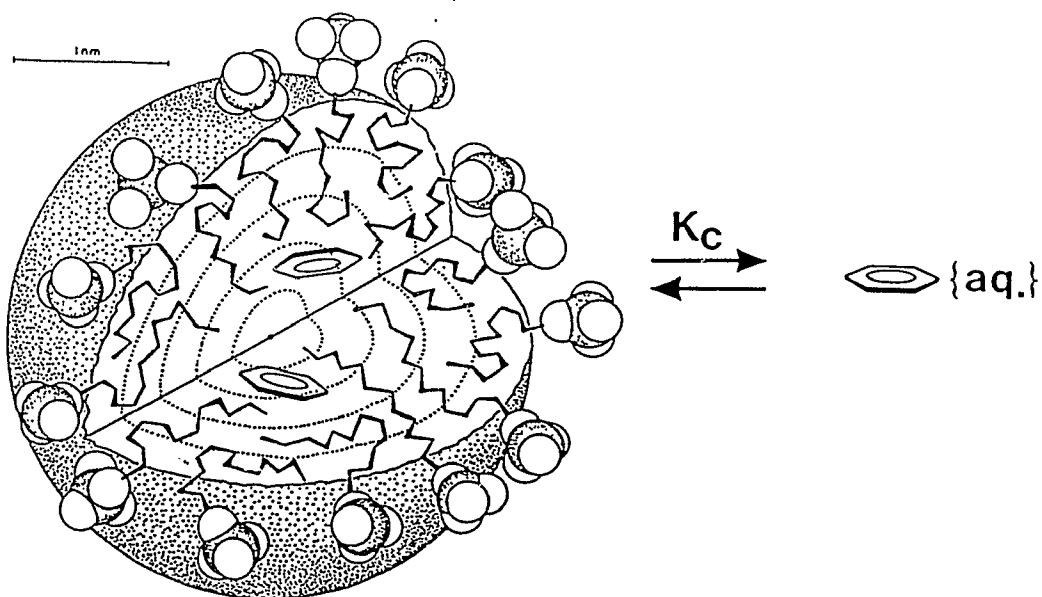


Figure 3.1. Schematic diagram of a benzene molecule in equilibrium between water and the micellar phase of SDS (modified from ref. 43).

$$R_{1,obs}^p = pR_{1,mic} + (1-p)R_1^p(aq) \quad (3.2)$$

where the superscript "p" indicates the relaxation time is affected by the presence of the paramagnetic ion. Subtracting equation 3.2 from equation 3.1 yields the expression for the calculation of the p -value from NMR relaxation measurements

$$p = 1 - \left(\frac{R_{1,obs}^p - R_{1,obs}}{R_1^p(aq) - R_1(aq)} \right) \quad (3.3)$$

In principle, the NMR paramagnetic relaxation experiment can be applied to study solubilization in a variety of aggregated systems, including vesicles and microemulsions. It is useful here to reiterate the assumptions of the paramagnetic relaxation experiment stated previously in the Introduction of this thesis:

- (i) *fast exchange of solubilize between the micellar phase and the aqueous phase (lifetime in the micellar phase is in the order of 10^6 - 10^3 s),*
- (ii) *the addition of paramagnetic ions to the aqueous phase has no effect on the spin-lattice relaxation rate of the solubilize located in the micellar phase, and*
- (iii) *the paramagnetic ions do not form stable complexes with the solubilize.*

Therefore, in applying the paramagnetic relaxation method to study solubilization equilibria, care should be taken to choose a paramagnetic species which does not form a complex with the solubilize. If the solubilize and paramagnetic species form stable complexes, the solubilization equilibrium may be perturbed. Also in this case, $R_1^p(aq)$ in equations 3.2 and 3.3 will be dependent on the solubilize concentration in the

aqueous phase and, thus, cannot be easily measured.

In this chapter, the utility of the NMR paramagnetic relaxation method to study the solubilization equilibria of n-alcohols in SDS, SD, DTAB, and DPC micelles is demonstrated. Of particular interest here is the verification of the three assumptions listed above. $\text{Mn}(\text{D}_2\text{O})_6^{2+}$ was used as the paramagnetic probe in DTAB and DPC micelles, while $\text{Mn}(\text{EDTA})^{2-}$ and 3-carboxylate-proxyl (charge: -1) were used as the paramagnetic probes in the anionic SDS and SDS micelles. The dependence of the spin-lattice relaxation rates of the solubilizates as a function of concentration was examined to determine the nature of the interaction of the paramagnetic ions with the solubilizate (i.e., intermolecular or intramolecular). The utility of the paramagnetic relaxation experiment for estimating the transfer free energy of a homologous series of compounds is also examined and compared with the FT-PGSE experiment.

3.2 Results and Discussion

In Table 3.1, the measured ^1H spin-lattice relaxation times of the $\alpha\text{-CH}_2$ group of 0.044 m 1-butanol, and of the phenyl protons of 0.058 molal benzyl alcohol, and the degrees of solubilization of the alcohols in 50 mg surfactant/g D_2O (0.162 m) DTAB micellar solution at 35°C (calculated from equation 3.3), using different concentrations of $\text{Mn}(\text{D}_2\text{O})_6^{2+}$, are presented. In Table 3.2, the measured ^1H spin-lattice relaxation times and the distribution constants (p) of the same concentration of 1-butanol in 70 mg surfactant/g D_2O (0.243 m) SDS micelles at 25°C, as a function of the concentration of 3-carboxylate-proxyl, are presented. The reported error limits in the relaxation times,

Table 3.1. ^1H Relaxation Times and Distribution Constants (p) of 0.044 molal 1-Butanol and 0.058 molal Benzyl Alcohol in DTAB Micelles¹ as a Function of the Concentration¹ (mmolal) of $\text{MnCl}_2 \cdot 6\text{H}_2\text{O}$.

$C(\text{MnCl}_2)$	$T_1(aq)/s$	$T_1^p(aq)/s$	$T_{1,obs}^p/s$	$T_{1,obs}^p/s$	p
1-Butanol					
0.00	4.77 ± 0.19		3.72 ± 0.15		
0.20		2.12 ± 0.08		2.17 ± 0.08	0.27 ± 0.11
0.40		1.16 ± 0.05		1.51 ± 0.06	0.39 ± 0.06
0.60		0.93 ± 0.04		1.17 ± 0.05	0.32 ± 0.06
0.80		0.76 ± 0.03		0.96 ± 0.04	0.30 ± 0.05
1.00		0.63 ± 0.03		0.79 ± 0.03	0.28 ± 0.05
2.00		0.32 ± 0.02		0.45 ± 0.02	0.32 ± 0.04
Benzyl Alcohol (Phenyl Protons)					
0.00	11.6 ± 0.46		3.56 ± 0.14		
0.40		1.83 ± 0.08		2.23 ± 0.09	0.64 ± 0.06
0.80		1.21 ± 0.05		1.72 ± 0.07	0.59 ± 0.04
1.00		0.97 ± 0.04		1.55 ± 0.06	0.61 ± 0.03
2.00		0.50 ± 0.03		1.00 ± 0.04	0.62 ± 0.03

1. $c_{\text{DTAB}} = 0.162$ molal; $T = 308$ K.

Table 3.2. ^1H Relaxation Times and Distribution Constants (p) of 0.044 molal 1-Butanol in SDS Micelles¹ as a Function of the Concentration (mmolal) of 3-Carboxylate-Proxyl.

C(Proxyl)	$T_1(aq)/s$	$T_1^p(aq)/s$	$T_{1,obs}^p/s$	$T_{1,obs}^p/s$	p
0.0	3.38 ± 0.12		2.43 ± 0.10		
2.0		1.47 ± 0.06		1.54 ± 0.06	0.38 ± 0.09
5.0		0.88 ± 0.04		1.14 ± 0.05	0.45 ± 0.06
7.5		0.59 ± 0.02		0.81 ± 0.03	0.42 ± 0.05
10.0		0.43 ± 0.02		0.64 ± 0.03	0.43 ± 0.03
15.0		0.31 ± 0.01		0.50 ± 0.02	0.46 ± 0.04
20.0		0.23 ± 0.01		0.36 ± 0.02	0.42 ± 0.04

1. $c_{\text{SDS}} = 0.243$ molal; $T = 298$ K.

T_1 's (approximately 4%), reflect the reproducibility of the relaxation time data in a separate series of measurements. It should be noted here that these error limits are much larger than the estimated error in T_1 obtained from the least squares fitting procedure, which are generally less than 1%. The estimated error in p (dp) is calculated from the following equation

$$dp = \left(\frac{(dR_{1,m}^p)^2 + (dR_{1,m})^2}{R_1^p(aq) - R_1(aq)} + \frac{(R_{1,m}^p - R_{1,m})^2}{(R_1^p(aq) - R_1(aq))^4} ((dR_1^p(aq))^2 + (dR_1(aq))^2) \right)^{\frac{1}{2}} \quad (3.4)$$

The p -values obtained at different paramagnetic ion concentrations, (3-carboxylate-proxyl in SDS micelles and $\text{Mn}(\text{D}_2\text{O})_6^{2+}$ in DTAB micelles) are equal within experimental error, and are independent of the concentration of paramagnetic ion. The results in Tables 3.1 and 3.2 also indicate that the error in p (dp) decreases as the paramagnetic ion concentration increases. Optimum results are obtained for DTAB micelles when the $\text{Mn}(\text{D}_2\text{O})_6^{2+}$ concentration exceeds 0.60 mmolal, and for SDS micelles when the concentration of 3-carboxylate-proxyl exceeds 10 mmolal.

In Table 3.3, the results for the ^1H T_1 's and the distribution constants (p) of 0.058 molal benzyl alcohol in 70 mg/g D_2O (0.243 m) SDS micellar solution have been measured, using 3-carboxylate-proxyl and $\text{Mn}(\text{EDTA})^{2-}$ as the paramagnetic probes. The p -values obtained using 3-carboxylate-proxyl and $\text{Mn}(\text{EDTA})^{2-}$ are comparable, although the values obtained with $\text{Mn}(\text{EDTA})^{2-}$ appear slightly higher. The average of the p -values obtained with 3-carboxylate-proxyl (0.67) agrees very well with the distribution constant determined by Stilbs ($p = 0.67$),⁸⁴ using the FT-PGSE self-diffusion method.

Table 3.3. ^1H Relaxation Times (Phenyl Protons) and Distribution Constants (p) of 0.058 molal Benzyl Alcohol in SDS Micelles¹ as a Function of the Concentration of $\text{Mn}[\text{EDTA}]^{2-}$ and 3-carboxylate-proxyl.

C_p/mmolal	$T_1(\text{aq})/\text{s}$	T_1^p/s	$T_{1,\text{obs}}/\text{s}$	$T_{1,\text{obs}}^p/\text{s}$	p
[$\text{Mn}(\text{EDTA})^{2-}$]					
0.0	9.10 ± 0.36		2.92 ± 0.12		
1.0		0.47 ± 0.02		1.16 ± 0.05	0.74 ± 0.03
2.0		0.24 ± 0.01		0.71 ± 0.03	0.73 ± 0.02
5.0		0.11 ± 0.04		0.34 ± 0.03	0.73 ± 0.02
[3-carboxylate-proxyl]					
0.0	9.10 ± 0.36		2.92 ± 0.12		
2.0		1.91 ± 0.08		2.17 ± 0.08	0.71 ± 0.06
10.0		0.46 ± 0.02		0.91 ± 0.04	0.63 ± 0.03
15.0		0.29 ± 0.01		0.65 ± 0.03	0.64 ± 0.02
20.0		0.22 ± 0.01		0.58 ± 0.02	0.69 ± 0.02

1. $c_{\text{SDS}} = 0.243$ molal; $T = 298$ K.

Finally, the p -values of benzyl alcohol in SDS, measured using the NMR paramagnetic relaxation experiment, are independent of the paramagnetic ion concentration; again, the error in p decreases as the paramagnetic ion concentration increases. It should be noted that a much higher concentration of 3-carboxylate-proxyl is required to obtain a similar enhancement of spin-lattice relaxation rate compared to $\text{Mn}(\text{D}_2\text{O})_6^{2+}$ or $\text{Mn}(\text{EDTA})^{2-}$. The optimum concentration of 3-carboxylate-proxyl was again found to be around 10 - 20 mmolal.

The degrees of solubilization, p , and the apparent distribution coefficients, K_x , of some n-alcohols in DTAB, DPC, SDS, and SD micellar solutions, obtained using the paramagnetic relaxation technique, are given in Tables 3.4 - 3.7. The apparent distribution coefficient, K_x , was calculated using the following equation

$$K_x = \frac{X_{mic}}{X_{aq}} \quad (3.5)$$

where X_{aq} and X_{mic} are the mole fractions of the solubilize in the aqueous phase and micellar phase, respectively, and are calculated as follows

$$X_{mic} = \frac{pn_{a,t}}{pn_{a,t} + n_{surf,mic}} \quad (3.6)$$

and

$$X_{aq} = \frac{(1-p)n_{a,t}}{n_{D_2O}} \quad (3.7)$$

From the apparent distribution coefficient, the free energy of transfer of the alcohol from the aqueous phase to the micellar phase can be calculated from the following

$$\Delta G_i^\circ = -RT \ln K_x \quad (3.8)$$

These values are also presented in Tables 3.4 - 3.7. The free energies of transfer of *n*-alcohols from D₂O to SDS and SD micelles are plotted in Figures 3.2 and 3.3, while the values for DTAB and DPC micelles are presented in Figures 3.4 and 3.5, as a function of the total number of carbon atoms in the alcohols. The results in Figures 3.2 - 3.5 indicate that ΔG_i° increases linearly with an increase in the number of carbons in the alcohol. The slopes of these linear plots each represent an estimate of the free energy of transferring a methylene group in the alcohol from the aqueous phase to the micellar phase. From Figures 3.2 and 3.3, the free energy of transfer of an alcohol CH₂ group from the aqueous phase to the interior of DTAB and DPC micelles was estimated to be -2.67 ± 0.21 kJ/mol and -2.57 ± 0.38 kJ/mol, respectively. In anionic SDS and SD micelles, the transfer free energies per alcohol CH₂ group were estimated to be -2.53 ± 0.53 kJ/mol and -2.33 ± 0.47 kJ/mol, respectively. The transfer free energy for the alcohol methylene group obtained for the SDS micellar system is in excellent agreement with the value obtained by Stilbs (-2.55 kJ/mol), estimated from the *p* values obtained using the NMR FT-PGSE self-diffusion method.⁸⁴ This agreement once again illustrates the general applicability of the paramagnetic relaxation method to obtain *p* values in a variety of micellar systems.

Table 3.4. Distribution Constants (p) and Transfer Free Energies of n-Alcohols in SDS Micelles¹.

Alcohol	p	K_x	$-\Delta G_i^0/\text{kJ mol}^{-1}$
Ethanol	0.06 ± 0.06	13 ± 13	2.43 ± 2.5
1-Propanol	0.27 ± 0.05	70 ± 16	10.5 ± 0.6
1-Butanol	0.44 ± 0.04	146 ± 22	12.4 ± 0.4
1-Pentanol	0.68 ± 0.03	378 ± 50	14.7 ± 0.3
1-Hexanol	0.82 ± 0.02	806 ± 106	16.6 ± 0.3
1-Octanol	0.98 ± 0.01	8743 ± 4450	22.5 ± 1.3

1. $c_{\text{SDS}} = 0.243$ molal; $T = 298$ K; $c(\text{proxyl}) = 10$ mmolal; $c_a \approx 0.050$ molal.

Table 3.5. Distribution Constants (p) and Transfer Free Energies of n-Alcohols in SD Micelles¹.

Alcohol	p	K_x	$-\Delta G_i^0/\text{kJ mol}^{-1}$
Ethanol	0.06 ± 0.06	7 ± 7	4.8 ± 2.5
1-Propanol	0.17 ± 0.06	22 ± 9	7.7 ± 1.0
1-Butanol	0.34 ± 0.05	55 ± 12	9.9 ± 0.5
1-Pentanol	0.59 ± 0.05	146 ± 30	12.4 ± 0.5
1-Hexanol	0.72 ± 0.04	258 ± 50	13.8 ± 0.5
1-Octanol	0.92 ± 0.03	1154 ± 468	17.5 ± 1.2

1. $c_{\text{SD}} = 0.463$ molal; $T = 298$ K; $c(\text{proxyl}) = 15$ mmolal; $c_a \approx 0.050$ molal.

Table 3.6. Distribution Constants (p) and Transfer Free Energies of n-Alcohols in DTAB Micelles¹.

Alcohol	p	K_x	$-\Delta G_i^\circ/\text{kJ mol}^{-1}$
1-Propanol	0.13 ± 0.05	46 ± 25	9.8 ± 1.4
1-Butanol	0.32 ± 0.05	144 ± 32	12.7 ± 0.6
1-Pentanol	0.57 ± 0.04	401 ± 53	15.4 ± 0.3
1-Hexanol	0.77 ± 0.03	1007 ± 206	17.7 ± 0.5
1-Octanol	0.94 ± 0.03	3957 ± 2082	21.2 ± 1.3

1. $c_{\text{DTAB}} = 0.162$ molal; $T = 308$ K; $c(\text{MnCl}_2) = 1.0$ mmolal; $c_a \approx 0.050$ molal.

Table 3.7. Distribution Constants (p) and Transfer Free Energies of n-Alcohols in DPC Micelles¹.

Alcohol	p	K_x	$-\Delta G_i^\circ/\text{kJ mol}^{-1}$
1-Propanol	0.13 ± 0.06	45 ± 25	9.8 ± 1.4
1-Butanol	0.36 ± 0.05	168 ± 36	13.1 ± 0.5
1-Pentanol	0.65 ± 0.03	549 ± 72	16.2 ± 0.3
1-Hexanol	0.83 ± 0.03	1437 ± 304	18.6 ± 0.5
1-Octanol	0.96 ± 0.04	7033 ± 5000	22.7 ± 1.8

1. $c_{\text{DPC}} = 0.166$ molal; $T = 308$ K; $c(\text{MnCl}_2) = 1.0$ mmolal; $c_a \approx 0.050$ molal.

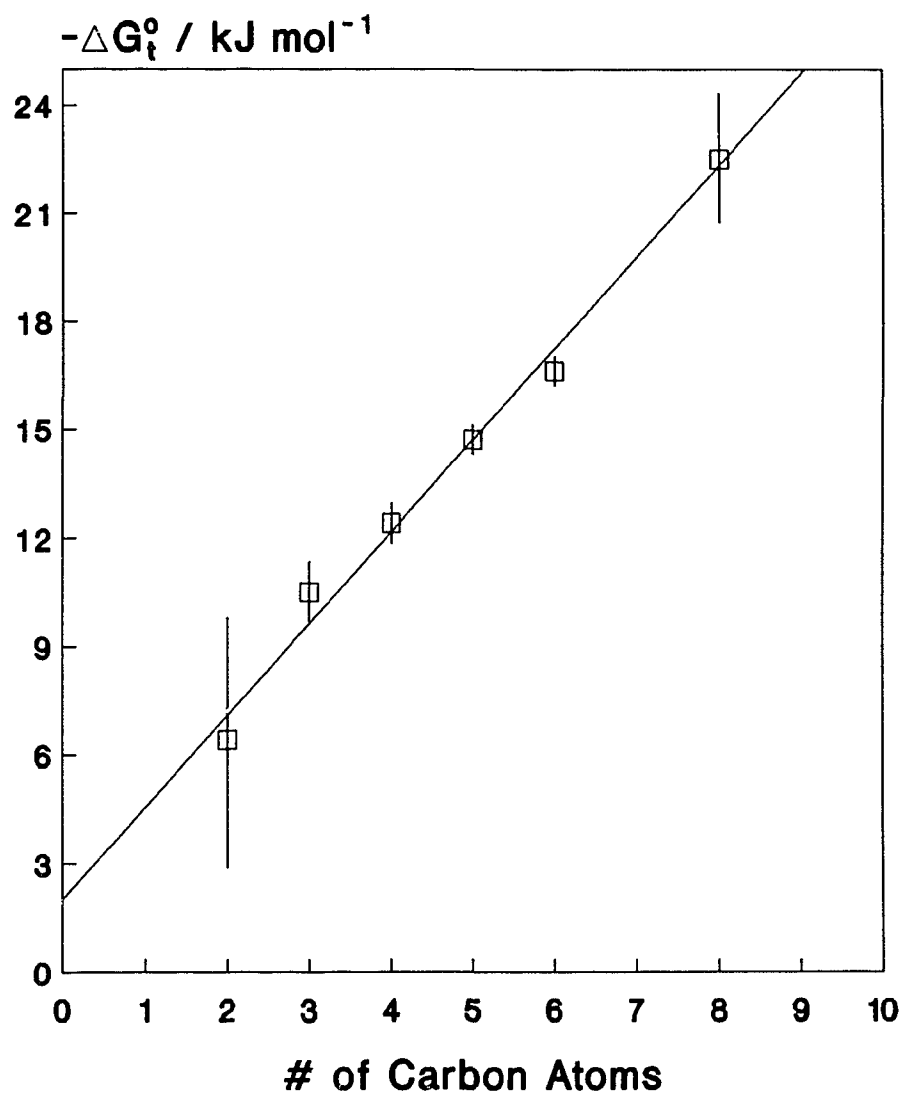


Figure 3.2. Transfer Free Energies of n-Alcohols from D_2O to the interior of SDS Micelles as a function of the number of carbon atoms in the alcohol.

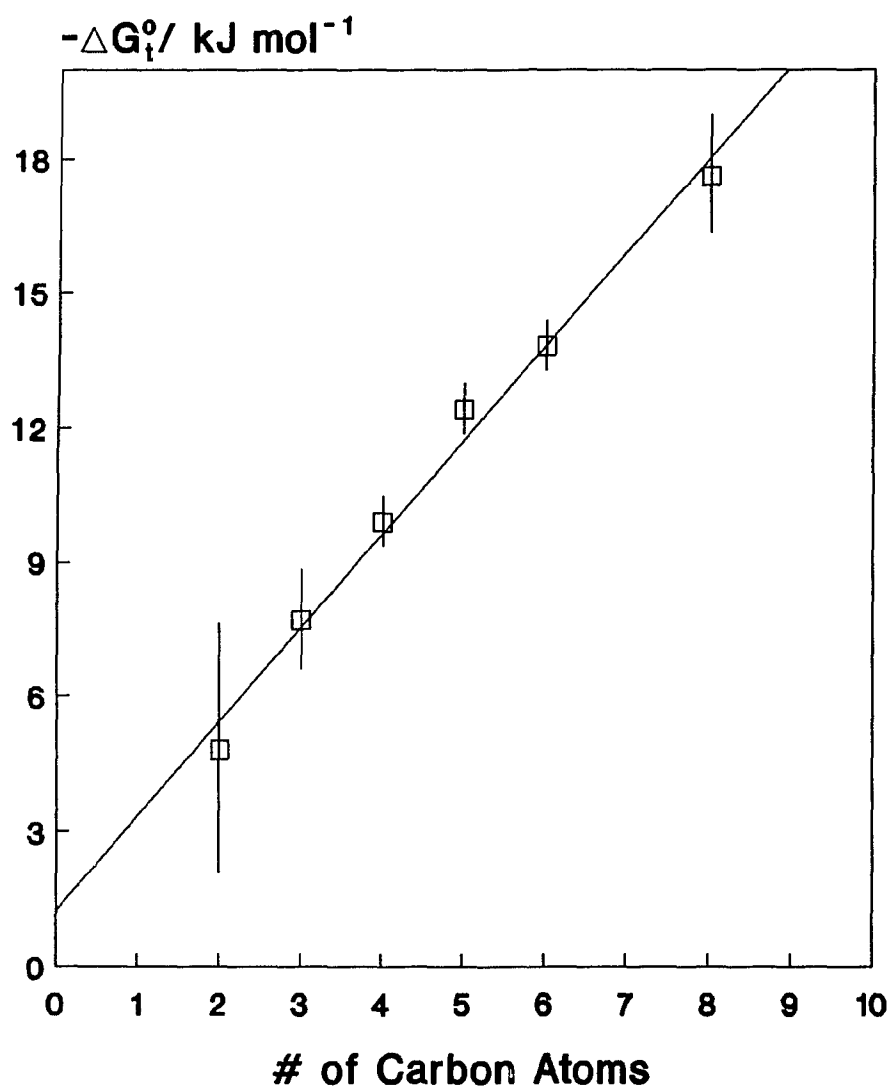


Figure 3.3. Transfer Free Energies of n-Alcohols from D_2O to the interior of SD Micelles as a function of the number of carbon atoms in the alcohol.

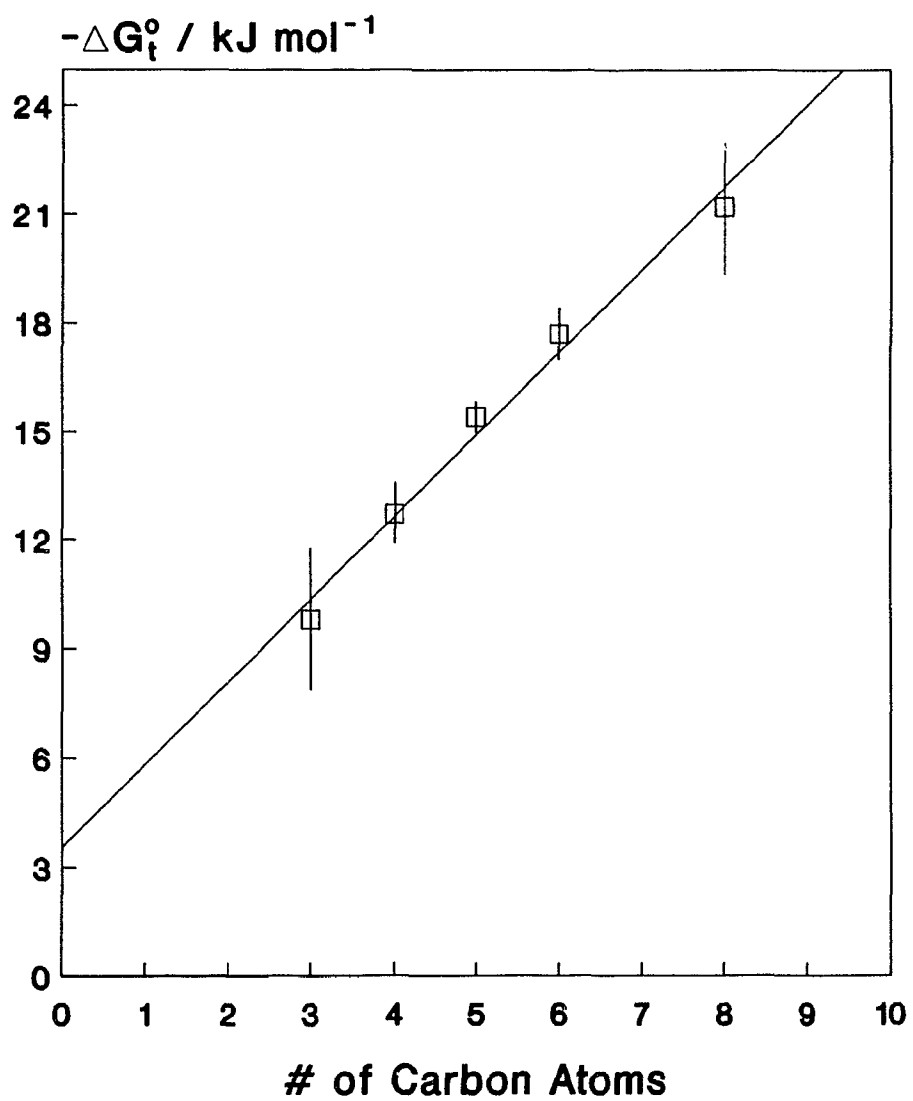


Figure 3.4. Transfer Free Energies of n-Alcohols from D_2O to the interior of DTAB Micelles as a function of the number of carbon atoms in the alcohol.

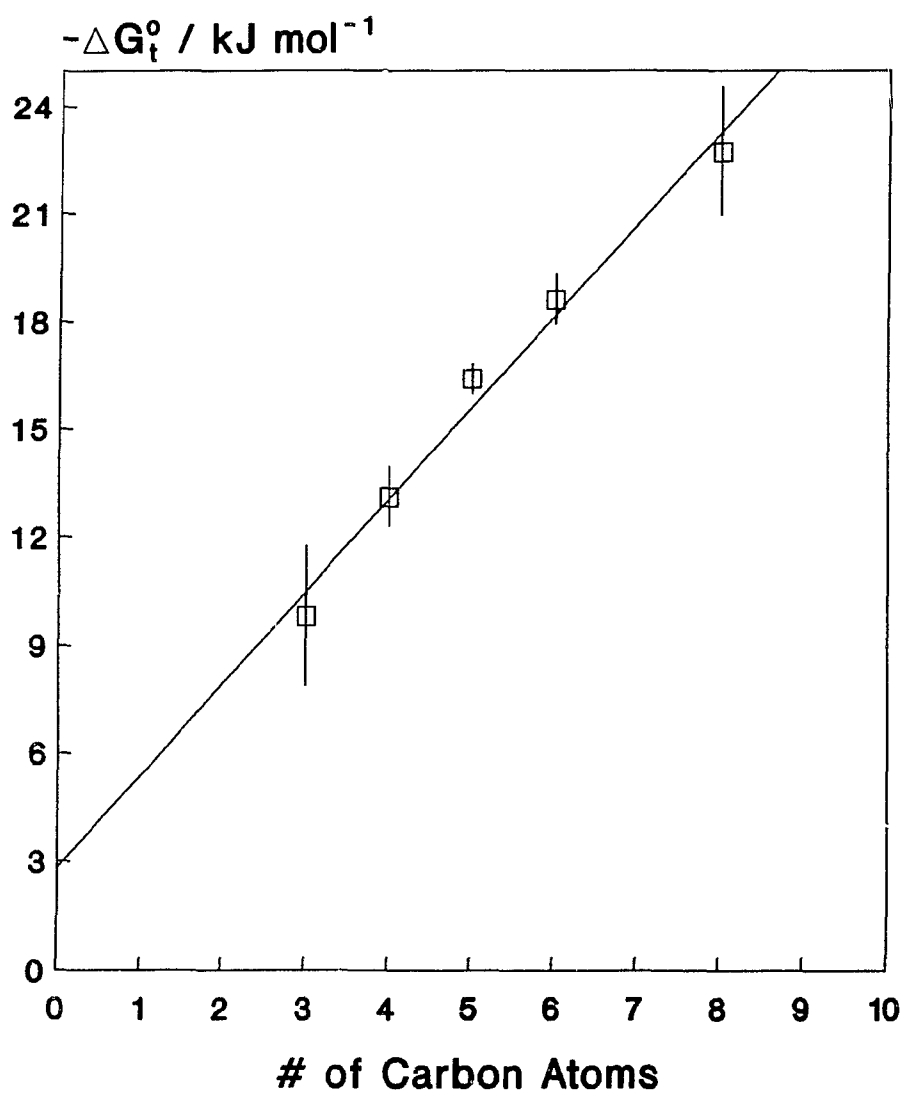


Figure 3.5. Transfer Free Energies of n-Alcohols from D_2O to the interior of DPC Micelles as a function of the number of carbon atoms in the alcohol.

3.3 Conclusions

The NMR paramagnetic relaxation technique can be used to study the solubilization equilibria of alcohols in cationic and anionic micellar systems. In ionic micellar solutions, paramagnetic ions of the same charge as the micellar surface are used in order to eliminate the effect of paramagnetic ions on the $^1\text{H } T_1$ of the solubilize located in the micellar phase. The degrees of solubilization of alcohols determined in cationic and anionic micellar solutions do not depend on the paramagnetic ion concentration, but the error in p decreases with increasing paramagnetic ion concentration. For SDS micellar solutions, the degree of solubilization obtained using 3-carboxylate-proxyl is slightly lower than the value obtained using $\text{Mn}(\text{EDTA})^{2-}$ as the paramagnetic probe.

The free energies of transfer of *n*-alcohols from the aqueous phase to the DTAB and SDS micellar phase relate linearly to the total number of carbons in the alcohols. From the slopes of these plots, the free energy of transfer of an alcohol methylene group from the aqueous phase to the micellar phase was determined to be -2.67 ± 0.23 kJ/mol and -2.57 ± 0.27 kJ/mol in DTAB and DPC micelles, respectively, -2.57 ± 0.53 kJ/mol in SDS, and -2.33 ± 0.47 kJ/mol in SD micelles. The transfer free energy of the CH_2 micelles is in excellent agreement with the results of Stilbs,^{84,85} based on the p -values determined with the NMR PGSE self-diffusion method.

Chapter 4

CMC Values and Degrees of Counterion Binding in Ionic Surfactant/Alkoxyethanol Mixed Micellar Systems

4.1 (a) Introduction

The early work of Shinoda⁷⁸ and Herzfeld et al.¹⁵⁹ presented the first systematic studies on the effects of added solutes, particularly n-alcohols, on the *CMC* values of ionic surfactants. Since that time, a vast literature has developed on the interaction of organic solubilizates with ionic and nonionic surfactant micelles, the focus of which has generally been to examine the effect of the solubilizate on a single, specific property of the surfactant micelle (e.g., aggregation number, micelle shape, thermodynamics of micelle formation, and the degree of counterion binding).^{3,12-17,42,60,87-89,94,206,207} However, much of the work in the literature has dealt with the interaction of n-alcohols (and some branched isomers) and hydrocarbons with ionic and nonionic micellar solutions. Recently, some interest has been shown in examining the interaction of other novel families of alcohols, e.g., α,ω -alkanediols,^{38,103,204} with micellar solutions. Although ethoxylated alcohols or alkoxyethanols (in particular, 2-butoxyethanol) are widely used cosurfactants in a number of different systems,²⁰⁴⁻²⁰⁷ including microemulsions, very little information has been found in the literature on the interaction of alcohol ethoxylates with ionic micelles.²⁰⁴⁻²⁰⁶

Interactions between small solubilizate molecules and micelles have been studied by many different techniques.⁷¹ Determining the change in the *CMC* as a function of added

solubilize concentration, as referred to above, is used to estimate the change in the free energy of micellization. When the *CMC* is measured by electromotive force (EMF) measurements to monitor the activity of the counterion, the ionic amphiphile, or both, data on the degree of counterion binding can be obtained as well, if the EMF measurements are extended into the micellar region.⁵⁵⁻⁵⁹ As an example, Vikingstad and Kvammen⁹⁰ studied the effects of methanol, ethanol, 1- and 2-propanol on the *CMC* of sodium decanoate (SD) micelles, using density and ultrasound measurements, and EMF activity measurements of the counterion. These authors reported a decrease in both the free energy of micellization (the *CMC* values) and the degree of counterion binding, β , of the mixed micelles as the concentration and the chain length of the alcohol were increased, in agreement with earlier work by Larsen and Tepley⁷⁹ and Lawrence and Pearson.⁷⁵ Yamashita et al.^{88,89} have determined the mean activities of SD in a number of alcohol solutions, using a sodium responsive glass electrode and the silver/silver decanoate electrode developed by Vikingstad.^{210,211} These authors also observed a decrease in the *CMC* values with both the chain length and the concentration of alcohol. Of particular interest was the observation that the *CMC* values of SD/2-butoxyethanol mixed micelles are lower than those of SD/1-butanol mixed micelles at the same concentration of alcohol. Manabe et al.²⁰⁴ have studied the effect of the addition of a homologous series of alkoxyethanols on the *CMC* values of sodium dodecyl sulfate (SDS) as a function of the number of ethylene oxide (EO) groups in the alcohol, at a constant alkyl chain length. These authors also observed a decrease in the *CMC* values of the SDS/alkoxyethanol mixed micelles as the number of EO groups in the alcohol was

increased.

2-Butoxyethanol, or ethylene glycol mono-n-butyl ether, can be considered as a lower member of the group of nonionic surfactants, C_iE_j , where i is the number of CH_2 groups in the alkyl chain and j is the number of ethylene oxide groups in the headgroup region. In this notation, 2-butoxyethanol is C_4E_1 . For nonionic surfactants, an increase in the number of ethylene oxide groups in the amphiphile, for a constant alkyl chain length, results in an increase in the *CMC* of the surfactant.^{212,213} Surfactant aggregation numbers are found to decrease when the number of EO groups is increased for a given alkyl chain length.²¹⁴ These trends can be easily understood if the EO chain is considered to be the hydrophilic part of the surfactant. However, Schwuger²¹⁵ pointed out that in the case of alkyl polyoxyethylene sulphates, a number of observations indicate a different role for the EO group in this class of surfactants. The first of these observations is that the *CMC* values of alkyl polyoxyethylene sulphates decrease with an increase in the number of EO groups.²¹⁶⁻²²⁰ As well, the surface activity of alkyl ether sulphates increases with an increase in the number of EO groups. Aggregation numbers for alkyl ether sulphates increase as a function of the number of EO groups in the presence and absence of salt. According to Schwuger,²¹⁵ these results are consistent with a contribution of the EO group to the hydrophobicity of the amphiphile ion.

4.1 (b) Experimental Determination of β : The Ratio of Slopes Method

A number of methods are available in the literature for calculating the degrees of counterion binding, β . Among the most common are conductivities,⁶⁶⁻⁷⁰ EMF

measurements,⁵⁶⁻⁵⁹ and NMR self-diffusion experiments.^{49,136,148,149,152} The ratio of slopes method for calculating β is outlined below. This simple method of calculating β involves an analysis of the slopes of the conductance vs. $c_{surf,t}$ curves above and below the *CMC*. Below the *CMC*, the surfactant is observed to behave as a strong electrolyte

$$\begin{aligned}\kappa &= c_c \lambda_c + c_{mon} \lambda_{mon} \\ &= S_1 c_{surf,t}\end{aligned}\quad (4.1)$$

where λ_c and λ_{mon} are the molar conductivities of the counterion and surfactant monomer, respectively, and S_1 is the slope of the conductance vs. $c_{surf,t}$ below the *CMC*, respectively. Above the *CMC*, the formation of micelles is described using the pseudo-phase model; the specific conductivity of a surfactant solution is then written as follows

$$\kappa = CMC(\lambda_c + \lambda_{mon}) + (c_{surf,t} - CMC) \left[\frac{N_s - m_c}{N_s} \lambda_c + \frac{\lambda_{mic}}{N_s} \right] \quad (4.2)$$

where λ_{mic} is the molar conductivity of the micelles, N_s is the surfactant aggregation number, m_c is the number of bound counterions, and the fraction of free counterions is $(1 - \beta) = (N_s - m_c)/N_s$. Therefore, β can be calculated with a knowledge of λ_{mic} . A simple way of estimating λ_{mic} is to assume the molar conductivity of the micelle is directly proportional to the number of charged surfactant ions in the micelle, i.e., $\lambda_{mic} = (N_s - m_c) \lambda_{mon}$. Equation 4.2 can be rewritten as follows

$$\kappa = CMC(\lambda_c + \lambda_{mon}) + [c_{surf,t} - CMC] (1 - \beta)(\lambda_c + \lambda_{mon}) \quad (4.3)$$

Applying the *CMC* condition

$$\lambda_c + \lambda_{mon} = \frac{\kappa_{CMC}}{CMC} \quad (4.4)$$

equation 4.3 becomes

$$\begin{aligned} \kappa &= \kappa_{CMC} + (1 - \beta)[c_{surf,t} - CMC](\lambda_c + \lambda_{mon}) \\ &= \kappa_{CMC} + (1 - \beta)S_1[c_{surf,t} - CMC] \end{aligned} \quad (4.5)$$

$$\begin{aligned} \frac{\kappa - \kappa_{CMC}}{c_{surf,t} - CMC} &= S_2 = [1 - \beta](\lambda_c - \lambda_{mon}) \\ &= (1 - \beta)S_1 \end{aligned} \quad (4.6)$$

where S_2 is the slope of the conductance vs. $c_{surf,t}$ above the CMC . Thus, β is determined simply from the ratio of the slopes of the conductance curve, S_2/S_1 .

It is useful here to reiterate the assumptions in the simple ratio of slopes method for calculating degrees of counterion binding. The first of these is that the ratio of slopes method requires the assumption of the pseudo-phase model of micelle formation. As well, it is necessary to account for the fraction of charge carried by the micelles. A number of authors incorrectly state that the simple ratio of slopes method neglects the fraction of the total charge transported by the micelles, since the mobility of the micelles is small compared with the counterions and free monomer.^{61,90,200} In fact, the ratio of slopes method does account for the molar conductivity of the micelles, although the estimation of λ_{mic} is extremely crude. For this reason, the degrees of counterion binding determined using the ratio of slopes method, as well as most other methods available in the literature for determining β , really measure an "apparent" β . For convenience, the

β values determined in this thesis are simply referred to as degrees of counterion binding.

If the plot of κ vs. $c_{surf,t}$ is used to obtain an estimate of the *CMC* value for the micellar system of interest, the uncertainty in numerical value of λ_{mic} may also lead to an error in the determination of the *CMC* values from conductance measurements. If, for example, either β is small, λ_{mic} is significant, or both occur, the break point in the κ vs. $c_{surf,t}$ plot would be small (or, possibly, non-existent), and curvature about the break point would be apparent. This would lead to difficulties in assigning a precise value for the *CMC* for the micellar system being investigated. In their extensive compilation of *CMC* values for a wide variety of surfactant systems, Mukerjee and Mysels²⁴ noted that *CMC* values obtained by different methods are slightly different, depending on the choice of physico-chemical property used to probe the onset of micellization. Somewhat surprising is the fact that different ways of representing the same data may lead to a different estimate of the *CMC* value.²⁴ In Figure 4.1, two representations of the conductance data for a DTAB/H₂O micellar solution are presented: the first is a plot of the conductance (L) vs. $c_{surf,t}$, while the second is a plot of the equivalent conductance against $c_{surf,t}^{1/2}$. The estimated *CMC* values are 16.3 mmolar and 15.9 mmolar, respectively. Such differences in the *CMC* values will be explored further in the Results and Discussion section.

In this chapter, previous investigations by Yamashita et al.^{88,89} on anionic SD/alkoxyethanol mixed micelles have been extended to include a number of other ionic surfactant/alkoxyethanol mixed micellar systems. In particular, the *CMC* values of mixed micelles formed by two anionic surfactants (sodium decylsulfate, or SDecS, and

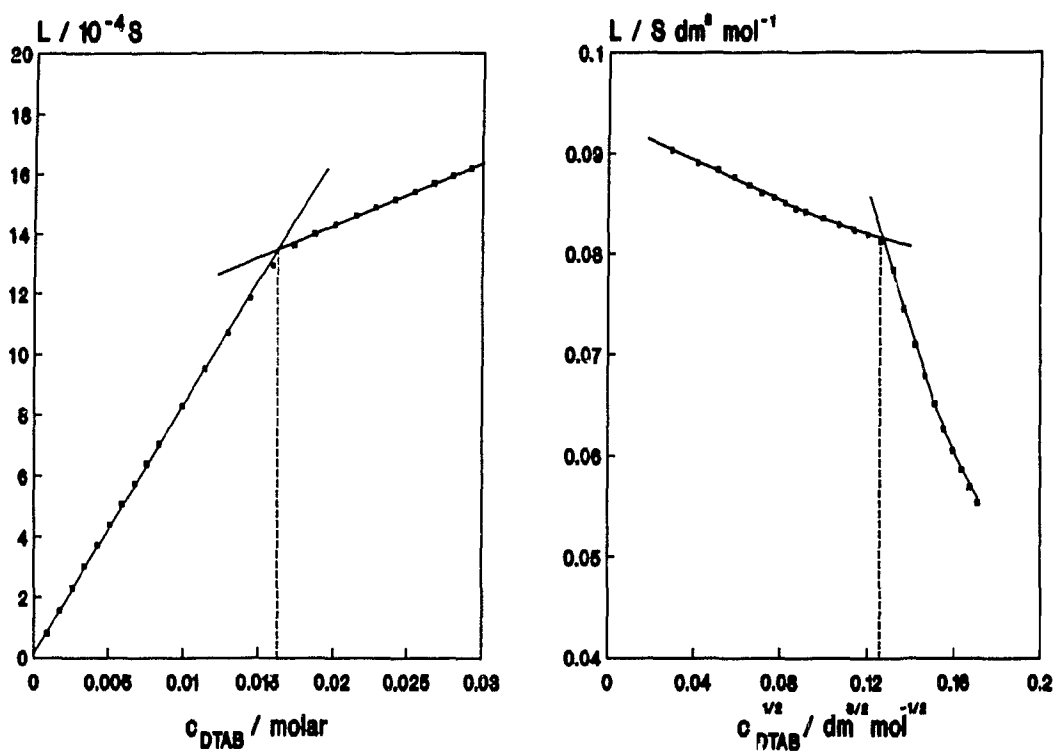


Figure 4.1. CMC values for DTAB/H₂O micelles determined from plots of conductance vs. $c_{\text{surf},t}$ and equivalent conductance vs. $c_{\text{surf},t}^{1/2}$.

SDS) and a cationic surfactant (DTAB), with a number of medium chain length alkoxyethanols, have been determined as a function of the concentration of alcohol and its EO chain length. In addition, degrees of counterion binding (β 's) have been determined using the ratio of slopes method for SDS/alkoxyethanol and DTAB/alkoxyethanol mixed micellar systems. The rate of decrease of the *CMC* with an increase in the alcohol concentration is compared with the corresponding surfactant/n-alcohol systems, in order to investigate the role of the ethylene oxide (EO) group in the formation of mixed micelles. All these results will be discussed in terms of the change in the free energy of transfer from H_2O to the micellar phase when an EO group is added to the alcohol, and the significant differences between the interactions of ethoxylated alcohols with anionic and cationic micelles.

4.2 Results and Discussion

a) *CMC Values*

i) Anionic Surfactant/Alkoxyethanol Mixed Micelles

CMC values for SDecS/alkoxyethanol mixed micelles, obtained from the breaks in the EMF_{Na^+} vs. $\log c_{surf,t}$ plots, are presented in Table 4.1 and plotted in Fig. 4.2 as a function of the total concentration of alcohol. In Table 4.2, the *CMC* values of SDS/alkoxyethanol mixed micelles, determined from the break in the conductance vs. $c_{surf,t}$ curves, are presented; these values are also plotted in Figure 4.3. A number of trends are apparent in Figures 4.2 and 4.3. The first of these is, of course, the expected

Table 4.1. CMC values (± 0.2 mmolal, EMF Measurements) for SDecS/Alkoxyethanol Mixed Micelles as a Function of the Total Concentration of Added Alcohol.

c_t /molal	C_4E_0	C_4E_1	C_4E_2	C_4E_3
0.000	30.1	30.1	30.1	30.1
0.010	----	----	27.9	27.3
0.020	----	----	26.3	24.5
0.025	27.8	26.9	24.6	----
0.030	----	----	23.9	22.5
0.040	----	----	22.6	19.7
0.050	25.9	22.7	20.5	17.3
0.075	24.1	19.9	----	
0.100	22.1	17.1		

Table 4.2. CMC values (± 0.2 mmolar, Conductance Measurements) for SDS/Alkoxyethanol Mixed Micelles as a Function of the Total Concentration of Added Alcohol.

c_a /molal	C_4E_0	C_4E_1	C_4E_2	C_4E_3
0.0000	8.10	8.10	8.10	8.10
0.0025	---	---	---	7.82
0.0050	---	---	---	7.55
0.0075	---	---	---	7.34
0.0100	---	---	7.54	7.08
0.0150	---	---	---	---
0.0200	---	---	6.85	
0.0250	7.58	7.06	---	
0.0300	---	---	6.24	
0.0500	7.18	6.21		
0.0750	6.64	5.09		
0.1000	6.02	4.56		

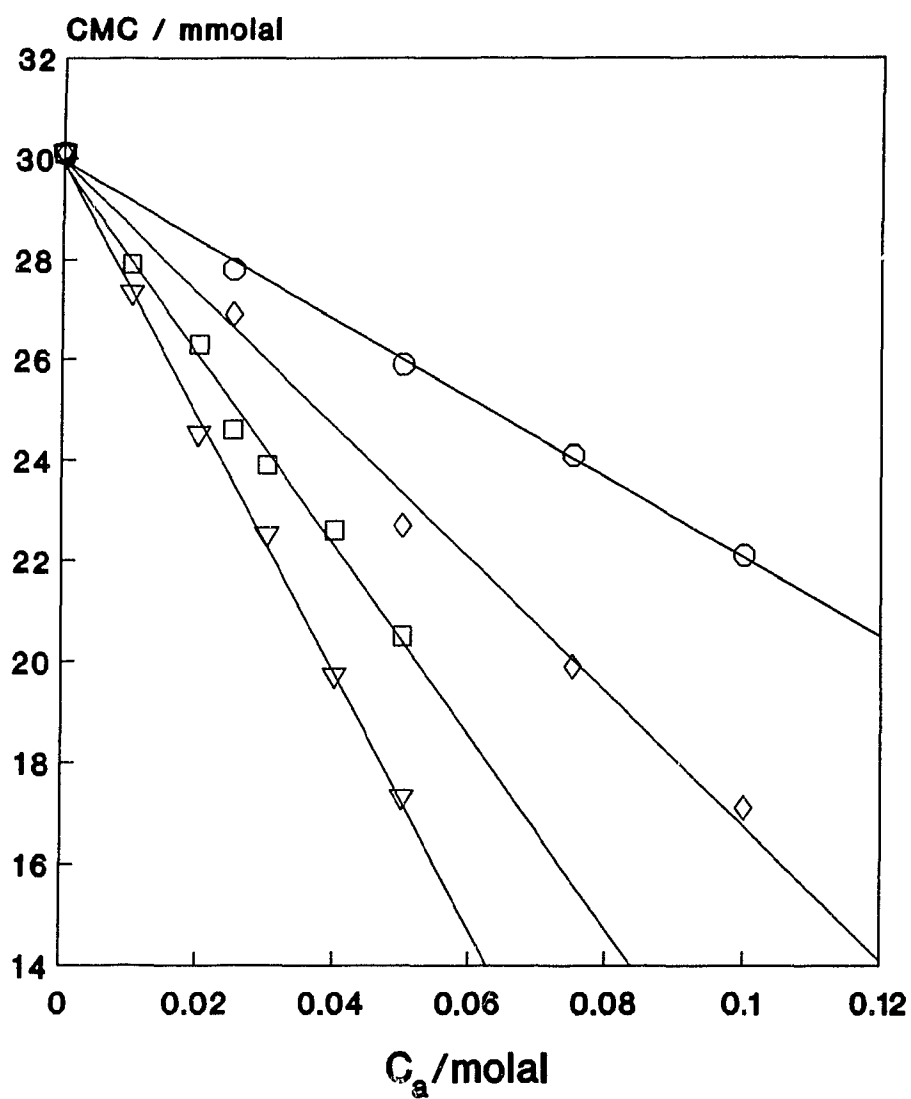


Figure 4.2. CMC values (± 0.2 mmolal, EMF Measurements) for SDecS/alkoxyethanol mixed micelles as a function of c_a . \circ C_4E_0 ; \diamond C_4E_1 ; \square C_4E_2 ; ∇ C_4E_3 .

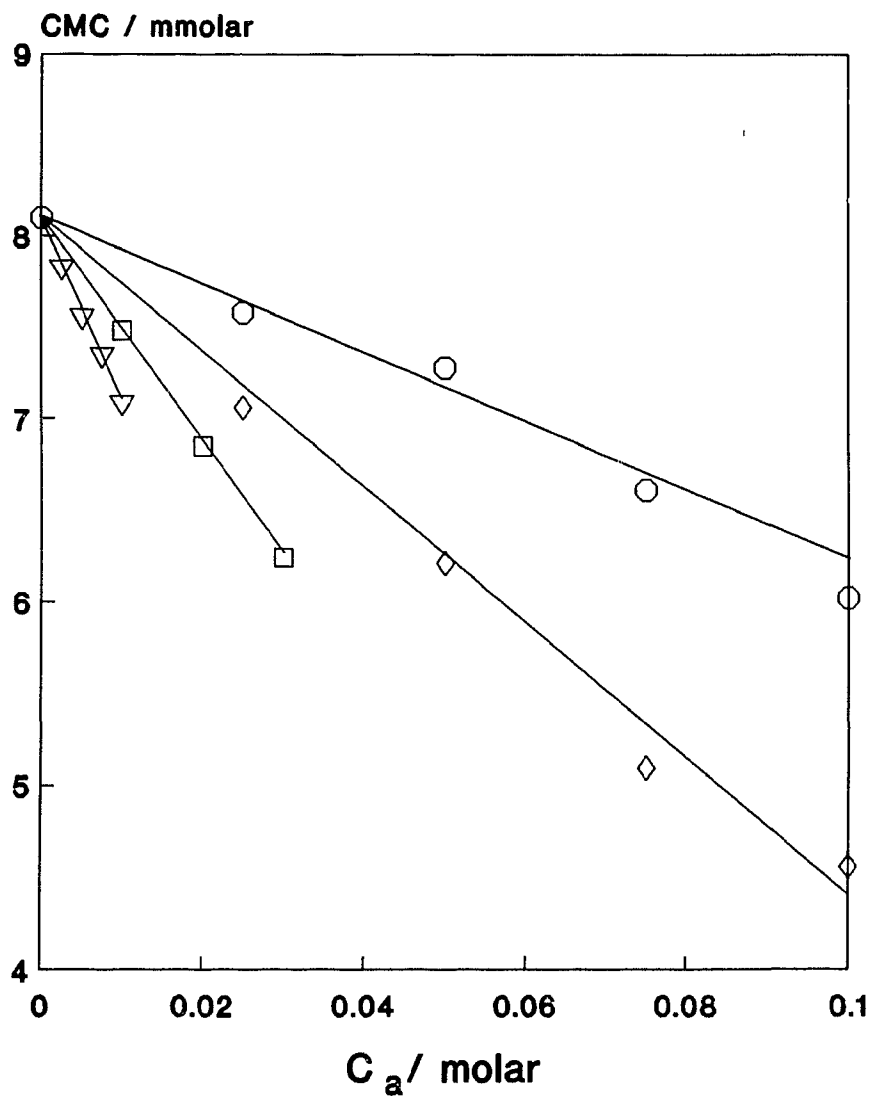


Figure 4.3. CMC values (± 0.2 mmolar, Conductance Measurements) for SDS/alkoxyethanol mixed micelles as a function of c_a . $\circ C_4E_0$; $\diamond C_4E_1$; $\square C_4E_2$; ∇C_4E_3 .

decrease in the *CMC* values of SDecS and SDS/alkoxyethanol mixed micelles as the concentration of the alcohol is increased. More importantly, it can be seen from Figures 4.2 and 4.3 that for a given alcohol concentration, there is a steady decrease in the *CMC* values from SDecS/C₄F₀ mixed micelles to SDecS/C₄E₃ and SDS/C₄E₀ mixed micelles to SDS/C₄E₃ mixed micelles. This effect of added ethoxylate groups is in very good agreement with the previous results of Manabe et al.²⁰⁴ and Yamashita et al.^{88,89}

Shinoda⁷⁸ has noted that the decrease in the *CMC* of alcohol/surfactant mixed micelles is linear with the total concentration of alcohol, c_a . From the data in Table 4.1, the rates of change of the *CMC* of SDecS/alkoxyethanol mixed micelles with the total concentration of added alkoxyethanol, $d CMC/d c_a$ values, are calculated to be 0.0794 for C₄E₀, 0.132 for C₄E₁, 0.191 for C₄E₂, and 0.254 for C₄E₃/SDecS mixed micelles. The $d CMC/d c_a$ values for SDS/alkoxyethanol mixed micelles are calculated from the data in Table 4.2 to be 0.0210 for C₄E₀, 0.0415 for C₄E₁, 0.0652 for C₄E₂, and 0.101 for C₄E₃/SDS mixed micelles. The $d CMC/d c_a$ values for SDS/alkoxyethanol mixed micelles are in agreement with the results of Manabe et al.²⁰⁴ The rates of change can be related to the free energy of transfer of the alcohol hydrophobic group from the aqueous phase to the micellar phase⁷⁸

$$\ln \frac{d CMC}{d c_a} = \frac{mw}{kT} + c_o \quad (4.7)$$

where w is the transfer free energy of the alcohol hydrophobic group from the aqueous to the micellar phase, and c_o is a constant related to the free energy of micellization of the pure surfactant micelles. Since the difference in the above series of alkoxyethanols

is an increase in the number of alcohol EO groups, at a constant alkyl chain length, equation 4.7 can be applied to the $d CMC/d c_e$ values in order to obtain estimates of the transfer free energy of the EO group, w_{EO} , from water to the anionic micellar interior. From the rates of change reported above, the average value of w_{EO} is estimated to be 0.46 ± 0.10 kT or 1.1 ± 0.30 kJ mol⁻¹.

Shinoda⁷⁸ has already postulated that alcohols solubilize into surfactant micelles with the head group in the palisade layer of the micelle and the hydrocarbon tail among the surfactant chains. The alcohol head group, being nonionic, serves to lessen the electrostatic interactions between neighbouring charged surfactant head groups, while the alcohol chain makes an additional contribution to the hydrophobic interactions. These two effects result in the observed decrease in the *CMC* with an increase in the alcohol concentration.

The decrease in the free energy of micellization, calculated from the decrease in the *CMC* values, is larger for the ethoxylated alcohol/anionic surfactant mixed micelles than for the corresponding n-alcohol/anionic surfactant mixed micelles. Two explanations are consistent with this observation. The first is that the ethoxylate head group occupies a larger surface area in the head group region of the mixed micelles, reducing the electrostatic interactions between the surfactant head groups by increasing the distance between them. In this model, the calculated value of w_{EO} represents an electrostatic contribution to the reduction in free energy.^{200,204} This is similar to the explanation used by Manabe et al.²⁰⁴ to account for the observed trends in the *CMC* values of SDS/alkoxyethanol mixed micelles as a function of the EO chain length of the alcohol.

An alternate way of interpreting the decrease in the *CMC* values is to propose that the EO group has a small, but significant contribution to the hydrophobic interactions. Unlike what was proposed by Manabe et al.,²⁰⁴ this implies that there would be an increase in the solubilization of ethoxylated alcohols into surfactant micelles as the number of EO groups is increased. Solubilization data for alkoxyethanols in anionic micelles are reported below in Chapter 5; a discussion of the role of the EO group in the formation of mixed micelles composed of anionic surfactants and alkoxyethanols (i.e., electrostatic or hydrophobic) is deferred until Chapter 5.

ii) Cationic Surfactant/Alkoxyethanol Mixed Micelles

As was noted in the introductions of both this thesis and this chapter, Mukerjee and Mysels²⁴ have noted that the *CMC* values obtained from different methods can be slightly different. As an example, the reported *CMC* values for DTAB micelles at 298 K range from 0.0140 molar (surface tension log plot) to 0.0164 molal (refractive index). These differences are evident in the *CMC* values for DTAB/alkoxyethanol mixed micelles, obtained from the two methods used in this chapter. For the DTAB/H₂O system (Figure 4.4), the *CMC* values, obtained from the plots of EMF vs. $\log c_{surf,t}$ and conductance vs. $c_{surf,t}$, are 15.5 mmolal and 16.3 mmolar, respectively; from the known density values, the conductance derived *CMC* value is calculated to be 15.7 mmolal. Therefore, the *CMC* values for DTAB/H₂O micelles, obtained from the two techniques, are in very good agreement. However, the *CMC* values for the DTAB/0.300 molal C₄E₃ mixed micellar system, obtained from the breaks in the EMF vs. $\log c_{surf,t}$ and conductance vs.

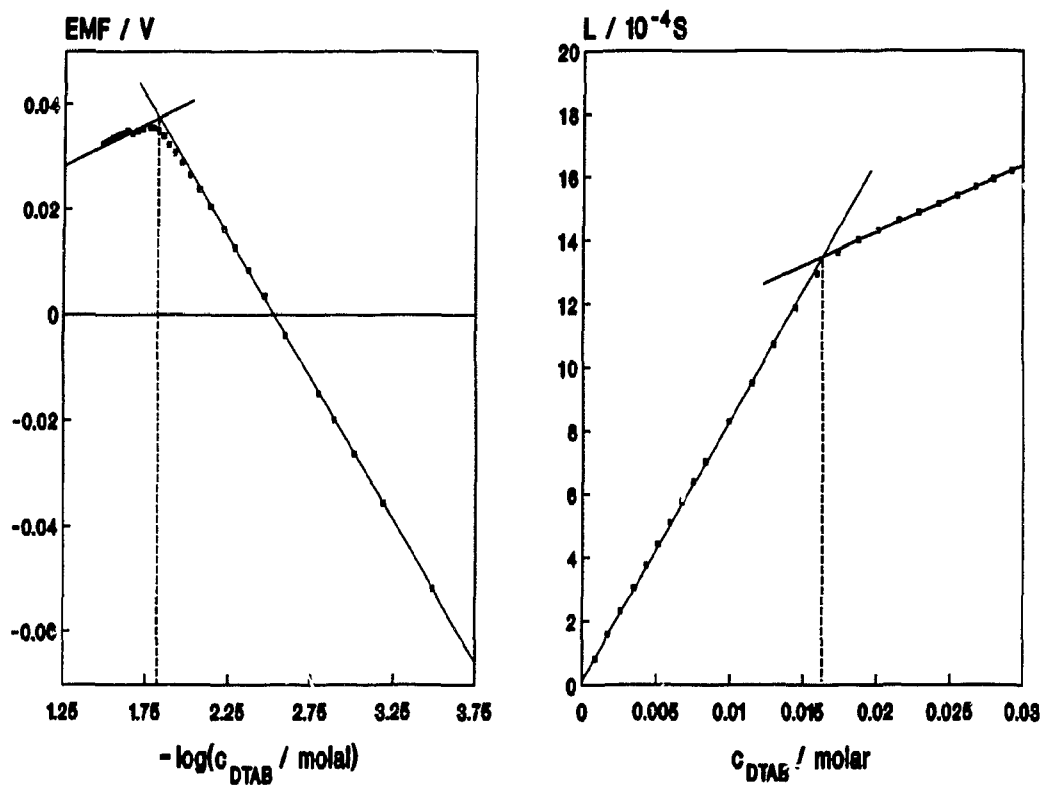


Figure 4.4. CMC values for DTAB/H₂O micelles determined from EMF and conductance measurements.

$c_{surf,t}$ plots (Figure 4.5), are in poor agreement. The deviation here is larger than the slight disparity observed previously for the DTAB/H₂O micelles. A possible explanation for this may be obtained from Figure 4.4 and 4.5, where the experimental plots of the physico-chemical property vs. surfactant concentration, used in the determination of the *CMC* values, are shown for the DTAB/H₂O and DTAB/0.300 molal C₄E₃ micellar systems. In Figure 4.4, the breaks in both the EMF and conductance curves for DTAB/H₂O micelles are fairly sharp. For the DTAB/0.300 molal C₄E₃ mixed micellar system, it can be clearly seen from Figure 4.5 that the break in the EMF vs. $\log c_{surf,t}$ curve appears at a slightly lower surfactant concentration (8.5 mmolar) than the break in the conductance vs. $c_{surf,t}$ plot (12.2 mmolar). As well, the breaks in both curves are not as sharp; the discontinuity occurs over a much broader range of surfactant concentrations, resulting in an additional uncertainty in its location. When the equivalent conductance is plotted against $c_{surf,t}^{1/2}$ for the DTAB/0.300 molal C₄E₃ system, a sharp break in the curve occurs at 9.4 mmolar (Figure 4.6). Differences in the *CMC* values obtained from the various ways of treating the conductance data have been noted previously.²⁴ According to Mukerjee and Mysels, graphing the equivalent conductance against $c_{surf,t}^{1/2}$ is the preferred method for plotting the conductance data in order to obtain the *CMC* values, since the break in the plot is usually unambiguous compared with the conductance vs. $c_{surf,t}$ curves, which may exhibit much curvature in the *CMC* region.

CMC values for the DTAB/alkoxyethanol mixed micelles, determined from the break in the EMF_{DTA+} vs. $\log c_{surf,t}$ curve and from the break in the conductance vs. $c_{surf,t}$ curve, are plotted in Figures 4.7 and 4.8, respectively, as a function of the total alcohol

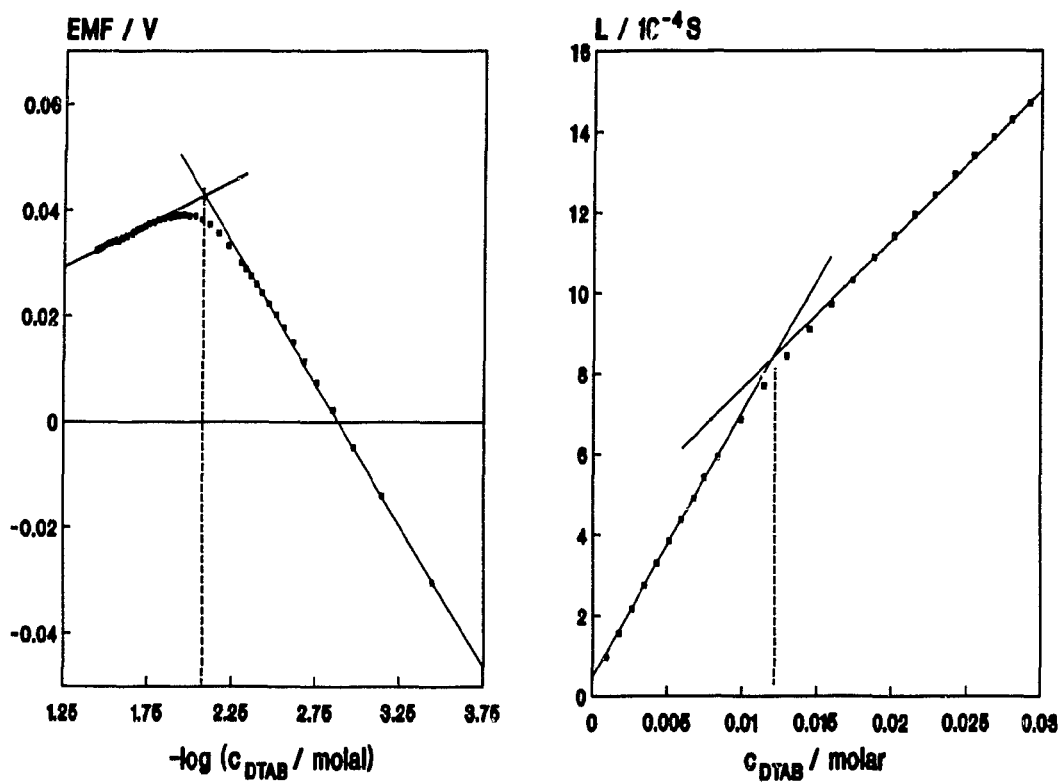


Figure 4.5. CMC values for DTAB/0.300 molal C_4E_3 mixed micelles determined from EMF and conductance measurements.

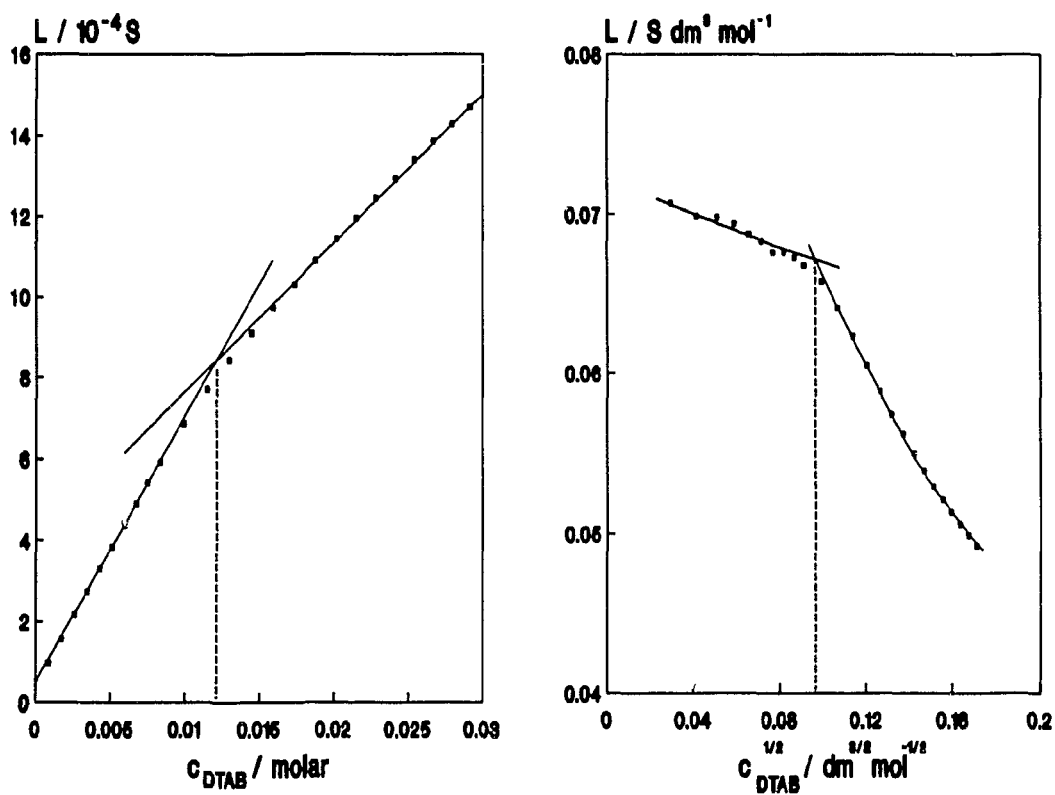


Figure 4.6. CMC values for DTAB/0.300 molal C_4E_3 mixed micelles determined from plots of conductance vs. $c_{\text{surf},t}$ and equivalent conductance vs. $c_{\text{surf},t}^{1/2}$.

Table 4.3. CMC values (± 0.5 mmolal, EMF measurements) for DTAB/Alkoxyethanol Mixed Micelles as a Function of the Total Concentration of Added Alcohol.

c_1 /molal	C_4E_0	C_4E_1	C_4E_2	C_4E_3
0.000	15.5	15.5	15.5	15.5
0.050	14.4	14.0	13.9	14.1
0.100	13.6	12.9	12.9	13.0
0.150	12.3	11.5	11.6	12.2
0.200	11.6	10.2	10.5	10.7
0.250	10.5	8.9	9.3	9.5
0.300	9.6	8.2	8.3	8.5

Table 4.4. CMC values (± 0.5 mmolar, Conductance measurements) for DTAB/Alkoxyethanol Mixed Micelles as a Function of the Total Concentration of Added Alcohol.

c_t /molal	C_4E_0	C_4E_1	C_4E_2	C_4E_3
0.000	16.3	16.3	16.3	16.3
0.050	14.8	14.6	14.9	14.9
0.100	14.0	13.3	13.8	13.9
0.150	13.0	12.4	12.9	13.5
0.200	11.9	11.4	12.2	12.9
0.250	11.1	10.9	11.7	12.2
0.300	10.3	10.2	11.3	12.2

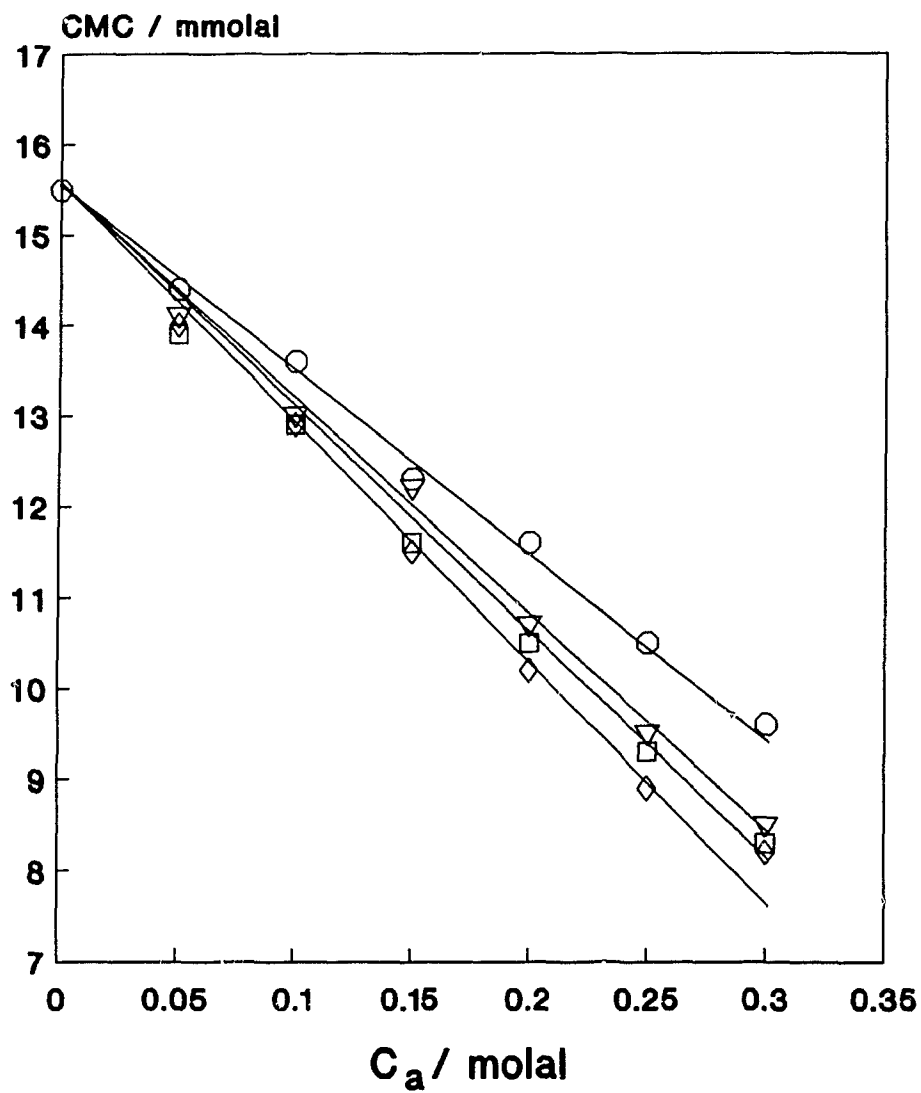


Figure 4.7. CMC values (± 0.5 mmolal, EMF measurements) for DTAB/alkoxyethanol mixed micelles. \circ C_4E_0 ; \diamond C_4E_1 ; \square C_4E_2 ; ∇ C_4E_3 .

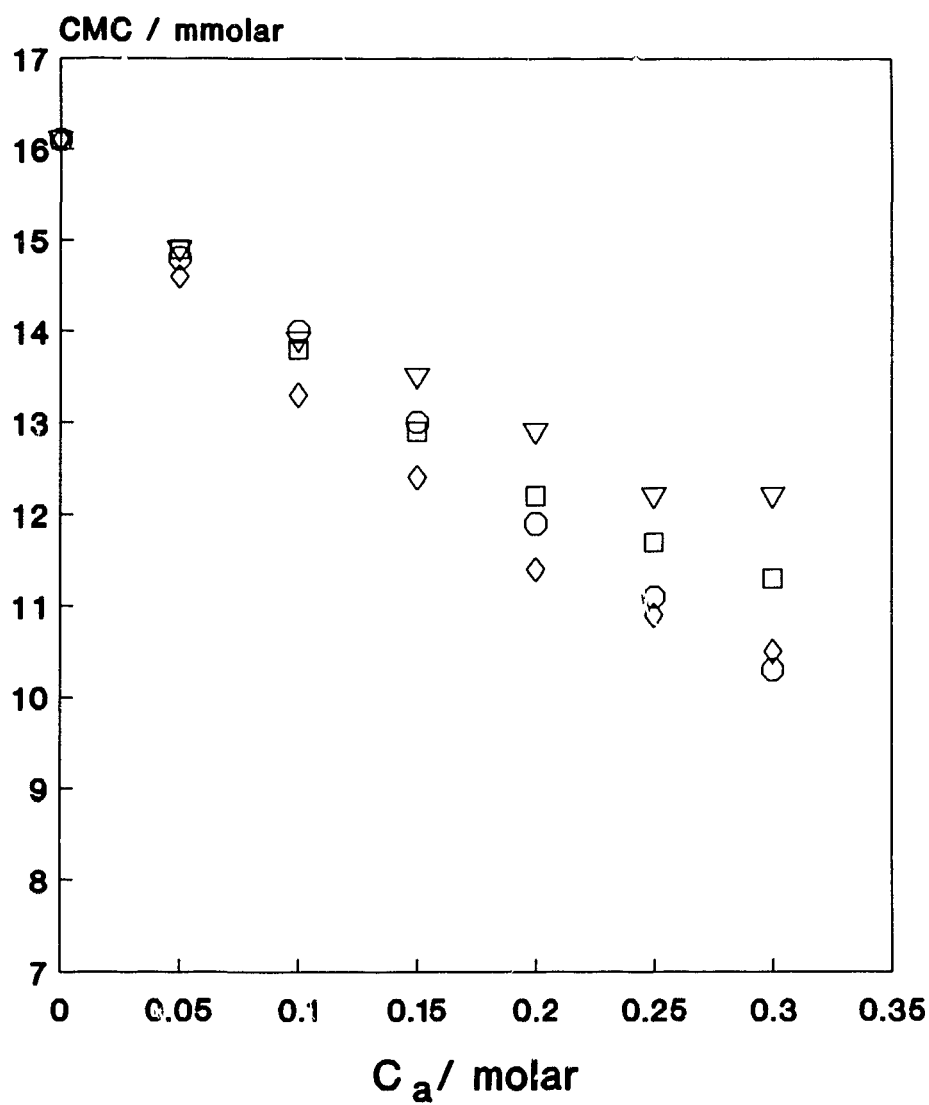


Figure 4.8. CMC values (± 0.5 mmolar, conductance measurements) for DTAB/alkoxyethanol mixed micelles. \circ C_4E_0 ; \diamond C_4E_1 ; \square C_4E_2 ; ∇ C_4E_3 .

concentration. Figures 4.7 and 4.8 clearly show that the addition of an EO group to the alcohol does not result in an additional decrease of the *CMC* values of the mixed micelles at the same concentration of alcohol. The rates of change of the *CMC* values with the alcohol concentration, the $d\ CMC/d\ c_a$ values, have been determined to be 0.0194 for DTAB/ C_4E_0 mixed micelles (in excellent agreement with the value of 0.0194, calculated from the *CMC* values reported by Zana²⁰⁰, and in very good agreement with the value of 0.0192 obtained for dodecylammonium chloride/ C_4E_0 mixed micelles by Herzfeld et al.¹⁵⁹), 0.0248 for DTAB/ C_4E_1 , 0.0237 for DTAB/ C_4E_2 , and 0.0231 for DTAB/ C_4E_3 mixed micelles. Unlike the trend that was observed in the SDecS and SDS/alkoxyethanol mixed micelles, the $d\ CMC/d\ c_a$ values do not increase in a regular fashion as the number of EO groups in the alcohol is increased. The insensitivity of the observed $d\ CMC/d\ c_a$ values of DTAB to the number of EO groups in the added alcohol indicates a negligible free energy contribution from the EO group in the formation of cationic DTAB/alkoxyethanol mixed micelles.

b) β Values

The β values, calculated from the slopes of the conductance vs. $c_{surf,t}$ above and below the *CMC*, are presented in Tables 4.5 for SDS/alkoxyethanol mixed micelles and in Table 4.6 for DTAB/alkoxyethanol mixed micellar systems. For the addition of alcohols to ionic micellar solutions, the slopes of the conductance vs. $c_{surf,t}$ plots below the *CMC* (S_1) were relatively constant, while the slopes of the conductance vs. $c_{surf,t}$ plots above the *CMC* (S_2) increase as the concentration of alcohol in the mixed micelle is

Table 4.5. Degrees of Counterion Binding ($\beta \pm 0.02$) for SDS/Alkoxyethanol Mixed Micelles as a Function of the Total Concentration of Added Alcohol.

c_a /molal	C_4E_0	C_4E_1	C_4E_2	C_4E_3
0.0000	0.62	0.62	0.62	0.62
0.0025	----	----	----	0.61
0.0050	----	----	0.61	0.59
0.0075	----	----	----	0.57
0.0100	----	----	0.58	0.55
0.0150	----	----	0.56	0.53
0.0200	----	----	0.51	0.50
0.0250	0.59	0.56	----	----
0.0300	----	----	0.48	----
0.0500	0.56	0.47	0.44	0.39
0.0750	0.54	0.39	0.42	0.34
0.1000	0.51	0.35	0.34	0.31
0.1500	0.44	0.31		
0.2000	0.39	0.23		
0.3000	0.30	0.18		

Table 4.6. β values (± 0.02) for DTAB/Alkoxyethanol Mixed Micelles as a Function of the Total Concentration of Added Alcohol.

c_a /molal	C_4E_0	C_4E_1	C_4E_2	C_4E_3
0.000	0.75	0.75	0.75	0.75
0.050	0.72	0.70	0.69	0.69
0.100	0.77	0.65	0.64	0.63
0.150	0.68	0.60	0.60	0.58
0.200	0.65	0.56	0.55	0.54
0.250	0.62	0.54	0.51	0.49
0.300	0.59	0.49	0.46	0.45

increased. Applying the principles of the ratio of slopes method, this indicates a decrease in β as a result of the addition of alcohols to the micelles. The degrees of counterion binding were found to decrease with alcohol concentration for all the alcohol/surfactant mixed micellar systems studied.

From the plot of the values of β vs. the total alcohol concentration for SDS/alkoxyethanol mixed micelles (Figure 4.9), it can be inferred that the surface charge density decreases with an increase in the number of EO groups in the alkoxyethanol, at a similar concentration of alcohol. However, from the plot of the β values measured in DTAB/alkoxyethanol mixed micelles against the alcohol concentration (Figure 4.10), it is readily apparent that the surface charge density of DTAB/alkoxyethanol mixed micelles is unaffected by the addition of EO groups to the cosurfactant, at identical alcohol concentrations. These results can be explained as follows. In the anionic surfactant/alkoxyethanol mixed micellar systems, the surface properties of the mixed micelles indicate that the alkoxyethanol cosurfactant behaves as a longer chain alcohol as the number of EO groups in the alcohol are increased, at similar alcohol concentrations. However, the results for DTAB/alkoxyethanol mixed micelles indicate that the surface properties of these mixed micellar systems are independent of the increase in the number of alcohol EO groups; the mixed micelles continue to behave as if the cosurfactant were the n-alcohol. These results, however, are inconclusive as to the nature of the interaction of the EO group with anionic or cationic micellar systems. It should be noted that these trends are in line with the *CMC* values presented previously.

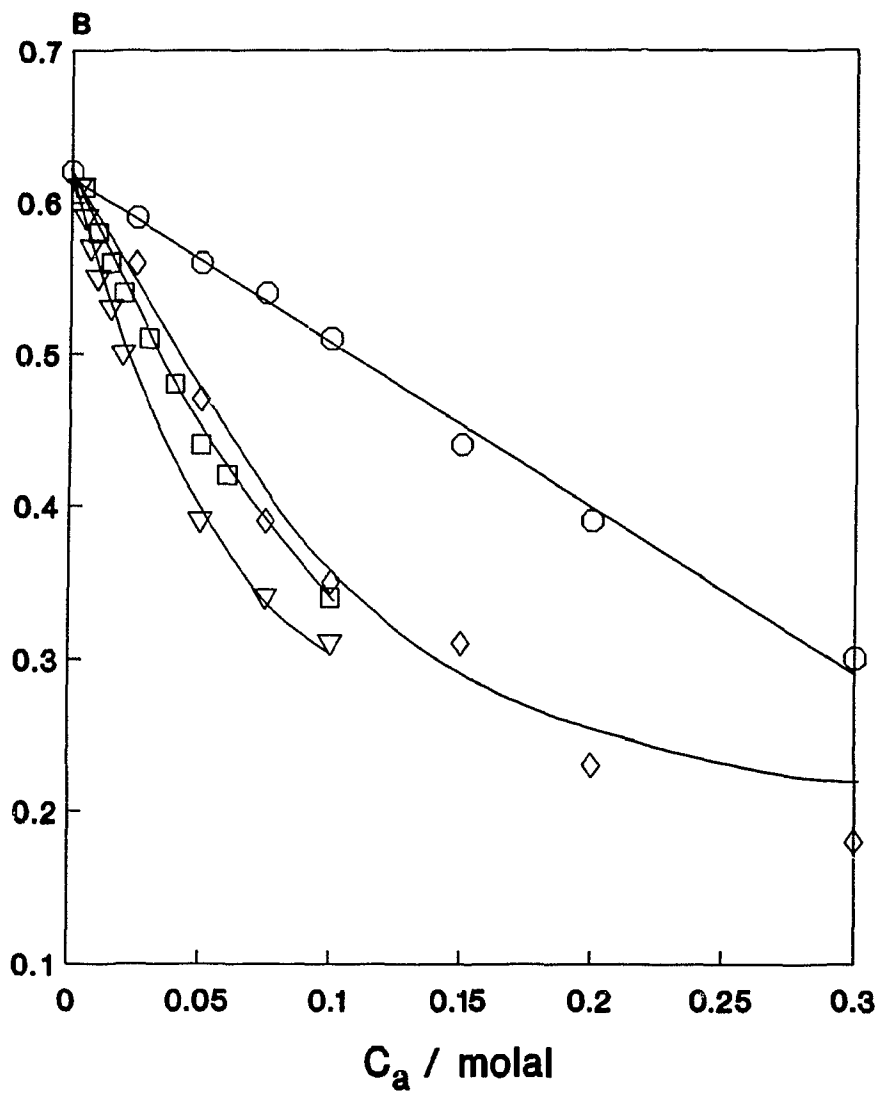


Figure 4.9. β values (± 0.02) for SDS/alkoxyethanol mixed micelles as a function of c_a . \circ C_4E_0 ; \diamond C_4E_1 ; \square C_4E_2 ; ∇ C_4E_3 .

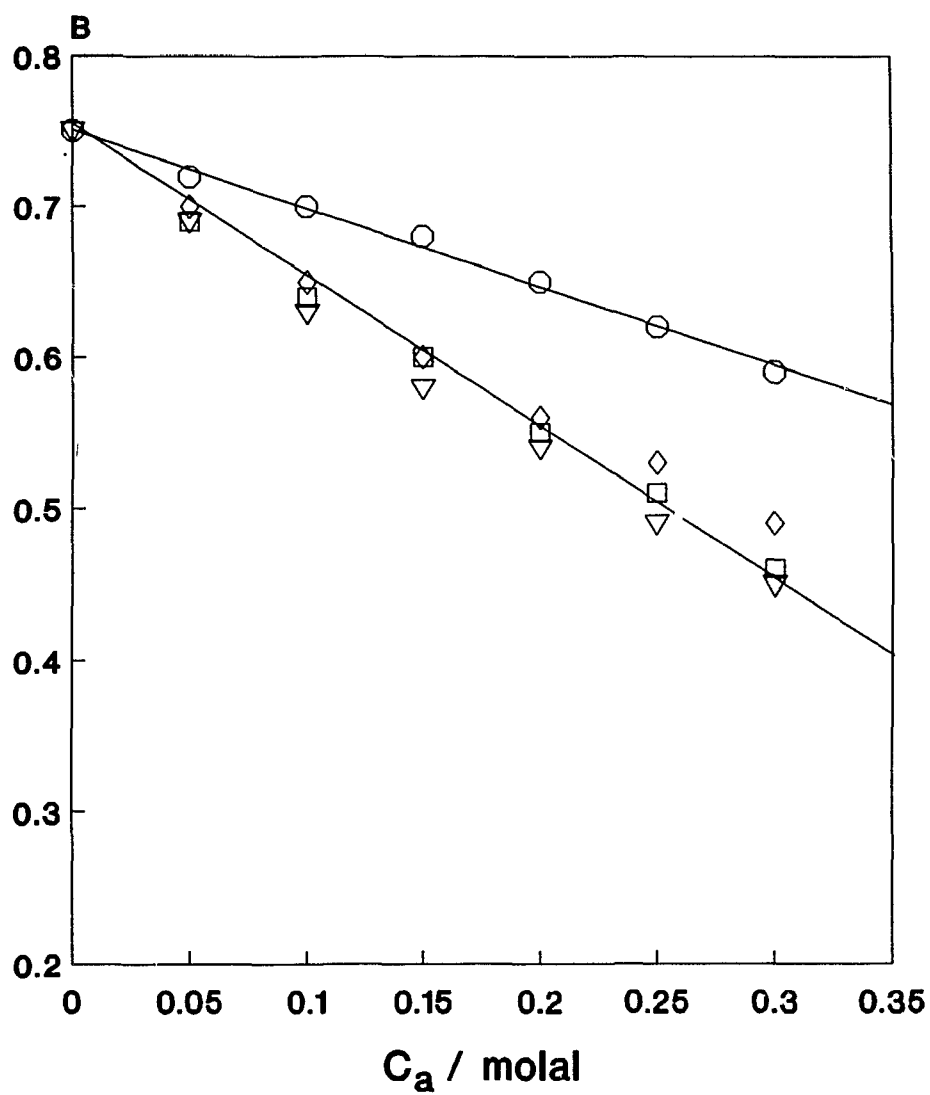


Figure 4.10. β values (± 0.02 , conductance measurements) for DTAB/alkoxyethanol mixed micelles. \circ C_4E_0 ; \diamond C_4E_1 ; \square C_4E_2 ; ∇ C_4E_3 .

4.3 Conclusions

From the results of *CMC* determinations in ionic surfactant/alkoxyethanol mixed micelles, the following conclusions can be drawn:

- 1) In anionic surfactant/alkoxyethanol mixed micellar systems, the *CMC* values and the β values of SDS and SDecS/alkoxyethanol mixed micelles decrease in the direction of an increasing number of EO groups in the alkoxyethanol, at a constant alcohol concentration. At this point in the thesis, it is unclear whether or not this is due to an electrostatic contribution, or, possibly, a contribution from the EO group to the hydrophobic interactions.
- 2) In cationic surfactant/alkoxyethanol mixed micelles, the *CMC* and β values of DTAB/alkoxyethanol mixed micelles, within the series $C_4E_1 \rightarrow C_4E_3$, are independent of the number of EO groups in the alcohol. These results indicate that the EO group has a negligible contribution to the interactions between cationic surfactants and ethoxylated alcohols.

Chapter 5

NMR Studies of the Solubilization of Alkoxyethanols in Anionic and Cationic Micellar Systems

5.1 Introduction

Since the micellar interior is hydrophobic, micelles have the ability to solubilize many compounds which are either sparingly soluble or insoluble in water. The phenomenon of solubilization is of paramount importance in the physical chemistry of surfactant solutions.^{3,6-23} Of particular importance is the fraction of the solubilize located in the micellar phase, i.e., the distribution constant or the p -value. It was stated in Chapter 3 that a number of experiments are available for determining the p -value of a solubilize, including vapour pressure measurements,⁹⁷⁻⁹⁹ total solubility,¹⁰⁰⁻¹⁰⁶ and the two NMR experiments, the FT-PGSE,¹⁵⁰ and the NMR paramagnetic relaxation experiment.^{139,153} The NMR paramagnetic relaxation experiment has been discussed extensively in Section 1.3 and Chapter 3.

Since NMR parameters are sensitive to changes in microenvironment, NMR techniques have been used extensively in the study of micellar solutions and other aggregated systems.^{138,150} Since the development of the current version of the FT-PGSE experiment by Stilbs, the solubilization equilibria for a number of organic molecules (particularly n -alcohols and other polar compounds) in surfactant solutions have been determined.^{84-86,132-134,150} In this chapter, the recently developed NMR paramagnetic relaxation experiment, which allows the distribution coefficient for a solubilize in the

micellar phase to be determined on any FT spectrometer,¹³⁹ will be used to determine to determine the *p*-values of a number of ethoxylated alcohols some typical anionic and cationic surfactant micelles; specifically, the degree of solubilization of alkoxyethanols in DTAB, DPC, SD, and SDS micelles has been determined using the NMR paramagnetic relaxation experiment. From the calculated values of the distribution coefficients and the transfer free energies of alkoxyethanols from the aqueous to the micellar phase, the contribution of the EO group to the hydrophobic interactions in both anionic and cationic micellar systems will be examined. These data will be useful in interpreting the effect of the addition of EO groups to alcohols. Addition of EO groups leads to a decrease in the free energy of micellization in anionic surfactant/alkoxyethanol mixed micelles, but has little effect in cationic surfactant/alkoxyethanol mixed micellar systems.

5.2 Results and Discussion

The distribution constants for the following alkoxyethanols, $C_2E_0 \rightarrow C_2E_3$, $C_4E_0 \rightarrow C_4E_3$, and C_6E_0 and C_6E_2 , have been calculated from the 1H relaxation time data, using equation 3.3. These values are given in Table 5.1 for anionic SDS and SD micelles. For the experiments in SDS micelles, the surfactant concentration was 70 mg/g D_2O (0.243 molal), while the amount of added alcohol was deliberately kept low (6 $\mu L/g$ solvent, corresponding to about 0.05 molal, or less than 10 wt% of the surfactant), in order to avoid significant perturbations in the micellar structure.^{84,85,134} For the experiments in SD micelles, the surfactant concentration was 90 mg SD/g D_2O , while the

Table 5.1. Distribution Coefficients and Free Energies of Transfer for Several Alcohols in SDS¹ and SD² Micellar Solutions.

Alcohol	p	K_x	$-\Delta G_t^\circ/(\text{kJ/mol})$
SDS			
C ₂ E ₀	0.00 ± 0.06	-----	-----
C ₂ E ₁	0.11 ± 0.06	25 ± 15	8.0 ± 1.5
C ₂ E ₂	0.22 ± 0.05	55 ± 16	10.0 ± 0.7
C ₂ E ₃	0.28 ± 0.05	93 ± 22	11.2 ± 0.6
C ₄ E ₀	0.42 ± 0.04	134 ± 24	12.1 ± 0.4
C ₄ E ₁	0.54 ± 0.03	219 ± 29	13.4 ± 0.3
C ₄ E ₂	0.66 ± 0.03	364 ± 47	14.6 ± 0.3
C ₄ E ₃	0.72 ± 0.03	487 ± 71	15.3 ± 0.4
C ₆ E ₀	0.82 ± 0.02	806 ± 107	16.6 ± 0.3
C ₆ E ₂	0.89 ± 0.03	1502 ± 455	18.1 ± 0.8
SD			
C ₂ E ₀	0.06 ± 0.06	7 ± 7	4.7 ± 2.6
C ₂ E ₁	0.14 ± 0.07	17 ± 10	7.1 ± 1.4
C ₂ E ₂	0.20 ± 0.07	26 ± 11	8.1 ± 1.1
C ₂ E ₃	0.25 ± 0.07	35 ± 13	8.8 ± 0.9
C ₄ E ₀	0.34 ± 0.05	53 ± 12	9.8 ± 0.4
C ₄ E ₁	0.47 ± 0.05	91 ± 18	11.2 ± 0.5
C ₄ E ₂	0.54 ± 0.05	121 ± 24	11.9 ± 0.5
C ₄ E ₃	0.59 ± 0.05	150 ± 37	12.5 ± 0.5

1. C_{SDS} = 0.243 molal; T = 298 K; C(proxy) = 0.010 molal; C_a ≈ 0.050 molal.

2. C_{SD} = 0.463 molal; T = 298 K; C(proxy) = 0.015 molal; C_a ≈ 0.050 molal.

alcohol concentrations were the same as for the experiments in SDS. The paramagnetic ion concentrations (3-carboxylate-proxyl) used in these experiments were 0.010 molal and 0.015 molal for measurements in SDS and SD micelles, respectively.

The relaxation time of the α -CH₂ protons in a 0.243 m SDS/0.010 m proxyl solution was 0.78 seconds, compared to a relaxation time of 0.81 seconds for the same protons measured in a 0.243 m SDS solution in the absence of 3-carboxylate-proxyl free radicals. This indicates that the assumption that the paramagnetic ion does not influence the relaxation of micellar bound solubilizates is reasonable. The error in the calculated value of p has been estimated using equation 3.4, where the errors in the ¹H T_1 data are approximately 4%; these error estimates again represent the reproducibility of the T_1 data in a separate series of measurements. Direct comparisons of some of the present results with those of the FT-PGSE experiment are possible (i.e., for C₂E₀, C₄E₀, and C₆E₀ in SDS micelles). In 0.243 m SDS solution, the measured p -values for C₂E₀, C₄E₀, and C₆E₀ (0.00, 0.42, and 0.82) are in good agreement with those obtained from the FT-PGSE experiment (0.03, 0.44, and 0.92), under identical conditions of temperature and concentration of surfactant and solubilizate.^{84,85} Good agreement between the distribution constants obtained using the FT-PGSE experiment and the NMR paramagnetic relaxation experiment has been observed previously.^{139,153}

From the results in Table 5.1, it is apparent that the distribution constants of alkoxyethanols in SDS micelles increase in the order of increasing number of EO groups, at a constant alkyl chain length. These results are particularly striking in that they indicate these alkoxyethanols have a preference for the micellar phase over their n-

alcohol counterparts. The distribution coefficients (K_x values) of the solubilize between the aqueous and micellar phases are calculated as in Chapter 3 (equation 3.5); from the K_x values, the transfer free energies of alkoxyethanols from water to the interior of anionic micelles have been calculated. These values, along with the distribution coefficients, are also presented in Table 5.1 for alkoxyethanol/SDS and alkoxyethanol/SD mixed micellar systems.

The decrease in the free energy of transfer in the two series of alkoxyethanols (i.e., $C_2E_0 \rightarrow C_2E_3$ and $C_4E_0 \rightarrow C_4E_3$ in SDS and SD micellar systems), and from C_6E_0 and C_6E_2 in SDS micelles, indicates that the transfer of ethoxylated alcohols to the micelles becomes more favourable as the number of ethylene oxide groups in the alcohol is increased, which may be due to the contribution of the EO groups to the hydrophobic interactions. Although C_4E_1 , C_4E_2 , and C_4E_3 are more water soluble than C_4E_0 ,^{206,207} and the solubility of C_6E_2 in water is greater than that of C_6E_0 ,²²⁰ the alcohols containing EO groups exhibit a marked preference for the micellar phase. If the free energy of transfer of alkoxyethanols were plotted against the number of EO groups in the alcohol, the slope would be equal to the free energy of transfer of an EO group from the aqueous to the micellar phase. The averages of the slopes of these plots, shown in Figures 5.1 and 5.2 for the two series of alkoxyethanols in SDS and SD micelles, are 1.21 ± 0.40 kJ/mol for SDS and 0.87 ± 0.30 kJ/mol for SD, respectively. Also plotted in Figure 5.1 are the transfer free energies of C_6E_0 and C_6E_2 . It can be easily seen from Figure 5.1 that the decrease in ΔG_t° for C_6E_2 over C_6E_0 is in line with the above estimate for the transfer free energy of the EO group.

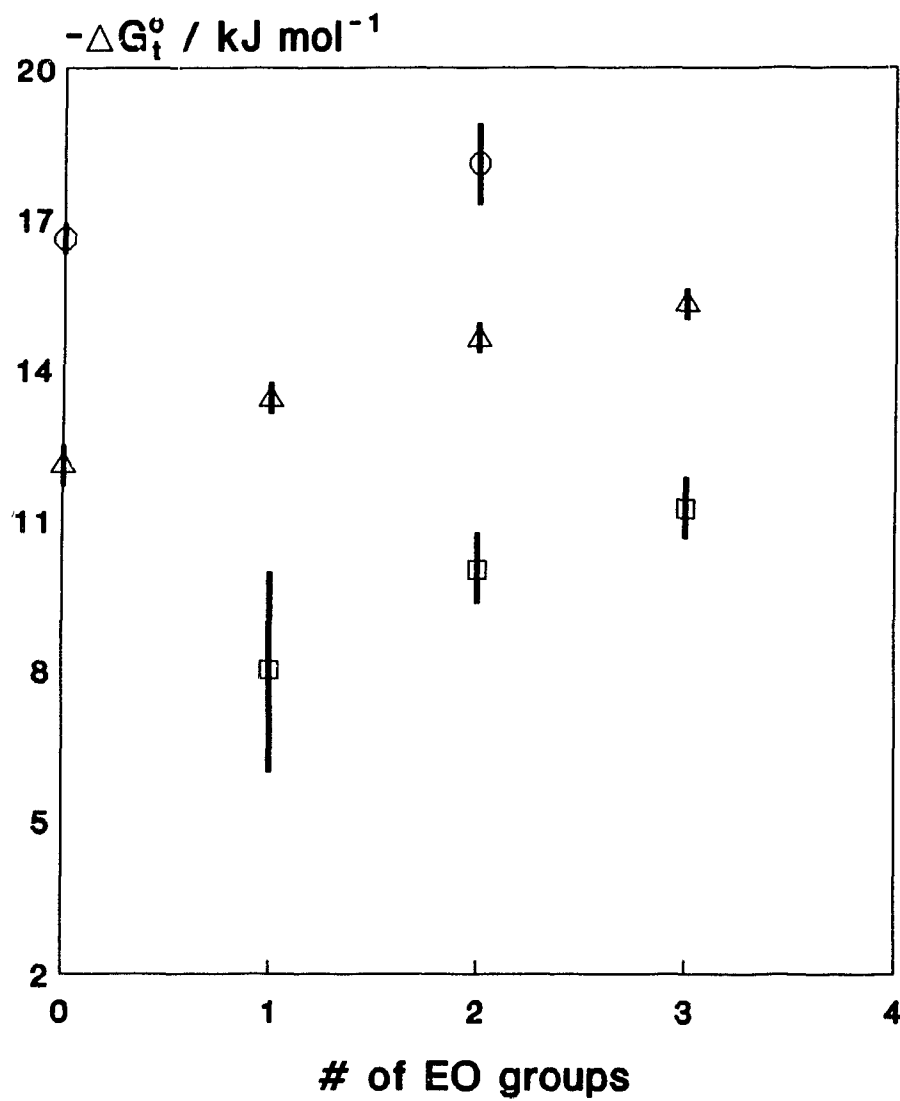


Figure 5.1. Transfer free energy of ethoxylated alcohols from water to SDS micelles.
□ $C_2E_0 \rightarrow C_2E_3$; Δ $C_4E_0 \rightarrow C_4E_3$; ○ C_6E_0, C_6E_2 .

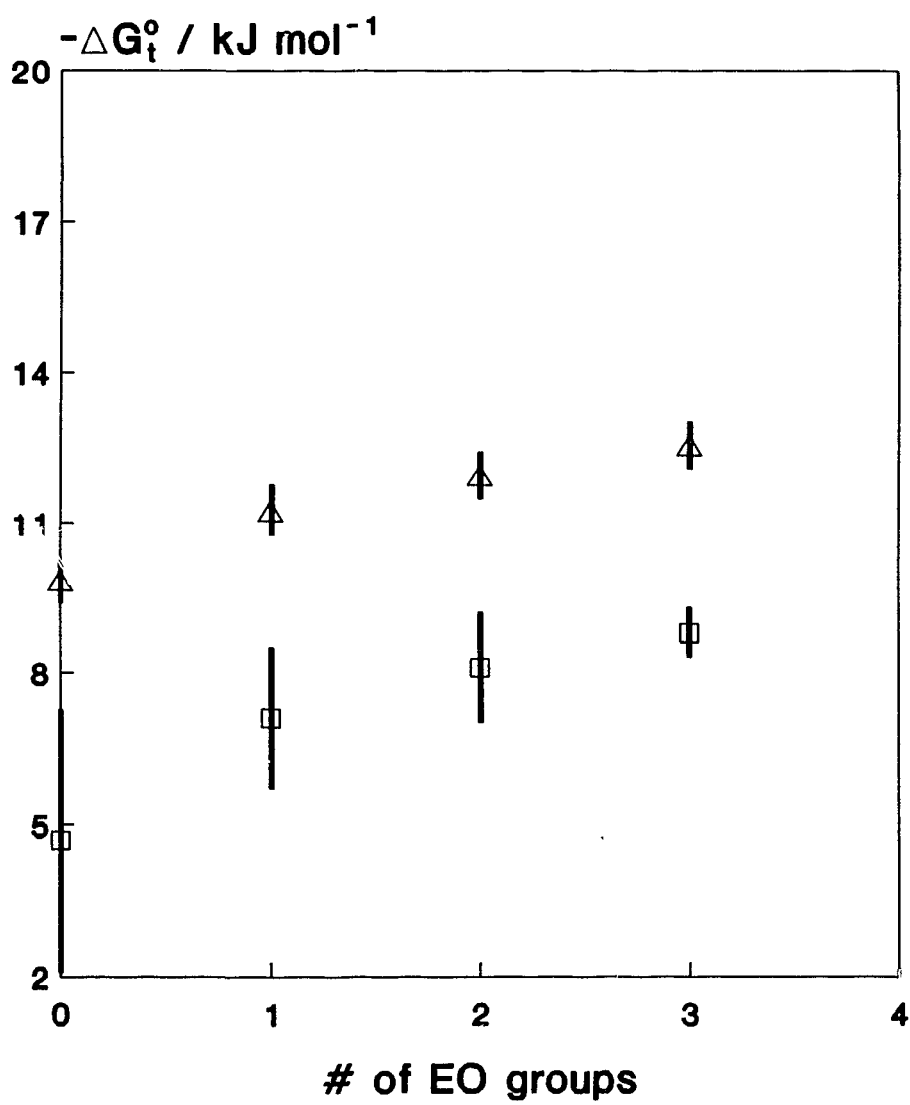


Figure 5.2. Transfer free energy of ethoxylated alcohols from water to SD micelles.
 \square $\text{C}_2\text{E}_0 \rightarrow \text{C}_2\text{E}_3$; \triangle $\text{C}_4\text{E}_0 \rightarrow \text{C}_4\text{E}_3$.

The estimate of the transfer free energy of the EO group is roughly half that for the free energy of transfer of a methylene group from the aqueous to the micellar phase, which is -2.6 ± 0.3 kJ/mol.^{84,153} Also, the decrease in the free energy of transfer with an increase in the number of CH₂ groups (e.g., from C₂E₁ to C₄E₁ or from C₂E₂ to C₄E₂) is about 5 kJ/mol. This estimate of the transfer free energy of the methylene group to the micellar phase is in very good agreement with the results of Chapter 3, where the transfer free energy of the CH₂ group was estimated from the solubilization of n-alcohols in SDS and SD micelles. As well, the estimate for the free energy of transfer of the EO group, as calculated from the NMR paramagnetic relaxation experiment (≈ -1.1 kJ/mol), is in good agreement with the value of w (0.85 ± 0.3 kJ/mol), calculated in Chapter 4 from the $\ln(d\ CMC/d\ c_a)$ vs. the number of EO groups in the alcohol.

The results from the solubilization of alkoxyethanols in SDS micelles indicate that the dominant effect in the decrease of CMC 's and the degrees of counterion binding, reported in Chapter 4, is the contribution of the EO group to the hydrophobic interactions. The increased solubilization of alkoxyethanols over their n-alkanol counterparts would dilute the surface charge density of the mixed micelle, decreasing β . As well, the increase in the hydrophobic interactions would result in a lower free energy of micellization, i.e, a lower CMC . These results also agree with the conclusions of Schwuger,²¹⁵ who stated that the EO group may, in certain cases, increase the hydrophobic interactions. This results in a decrease in the CMC 's of alkyl ether sulphate micellar solutions as a function of the number of EO groups between the sulphate head group and the hydrocarbon chain.

For the NMR paramagnetic relaxation experiments in cationic DTAB and DPC micellar solutions, the solubilization equilibria of ethoxylated alcohols were determined at surfactant concentrations of 0.162 molal and 0.166 molal, respectively. The solubilize concentration was the same as for the experiments in anionic SDS and SD micelles, 6 μL of alcohol per g of solvent. At a paramagnetic ion concentration of 1 mmolal, no decrease in the T_1 for either the $\alpha\text{-CH}_2$ protons, or of the methyl protons in the surfactant headgroup in DTAB, was observed, again indicating that the $\text{Mn}(\text{D}_2\text{O})_6^{2+}$ resides exclusively in the bulk solution away from the micellar surface. The p -values are tabulated in Table 5.2 for $\text{C}_4\text{E}_0 \rightarrow \text{C}_4\text{E}_3$ in DTAB and DPC micelles, along with the errors in p , using 4% as the random error in the T_1 measurements. It can be seen from Table 5.2 that for the cationic DTAB and DPC micelles, the distribution constants are independent of the number of EO groups in the alcohol. It is also clear from Figure 5.3 that the transfer free energy of ethoxylated alcohols in cationic DTAB and DPC micelles is insensitive to the number of EO groups in the alcohols, i.e., in cationic micelles, the ethoxylated alcohols behave as if they were a four carbon n -alcohol. The p -values for the series C_4E_0 to C_4E_3 are constant in both cationic micellar systems, with values of about 0.32 in DTAB and 0.40 in DPC. These results appear to indicate that the EO group does not contribute to the hydrophobic interactions in the cationic micellar systems studied here. These results are in sharp contrast with the trends for the SDS and SD/alkoxyethanol mixed micellar systems reported above, indicating a negligible interaction between the cationic micelles and the ethylene oxide unit. This type of behaviour parallels the interaction of PEO and other neutral polymers with cationic and

Table 5.2. Distribution Coefficients and Free Energies of Transfer for Several Alcohols in DTAB¹ and DPC² Micellar Solutions.

Alcohol	p	K_x	$-\Delta G_i^\circ/(\text{kJ/mol})$
DTAB			
C ₄ E ₀	0.32 ± 0.04	128 ± 32	12.4 ± 0.4
C ₄ E ₁	0.37 ± 0.05	163 ± 33	13.1 ± 0.5
C ₄ E ₂	0.32 ± 0.07	141 ± 42	12.7 ± 0.7
C ₄ E ₃	0.31 ± 0.03	131 ± 41	12.5 ± 0.7
C ₆ E ₀	0.80 ± 0.03	995 ± 179	17.7 ± 0.5
C ₆ E ₂	0.72 ± 0.06	700 ± 202	16.8 ± 0.7
DPC			
C ₄ E ₀	0.36 ± 0.05	148 ± 32	12.8 ± 0.5
C ₄ E ₁	0.42 ± 0.05	195 ± 38	13.5 ± 0.5
C ₄ E ₂	0.41 ± 0.07	192 ± 53	13.5 ± 0.7
C ₄ E ₃	0.40 ± 0.07	188 ± 53	13.4 ± 0.7

1. $c_{\text{DTAB}} = 0.162$ molal; $T = 308$ K; $c(\text{MnCl}_2) = 0.0010$ molal; $c_a \approx 0.050$ molal.

2. $c_{\text{DPC}} = 0.166$ molal; $T = 308$ K; $c(\text{MnCl}_2) = 0.0010$ molal; $c_a \approx 0.050$ molal.

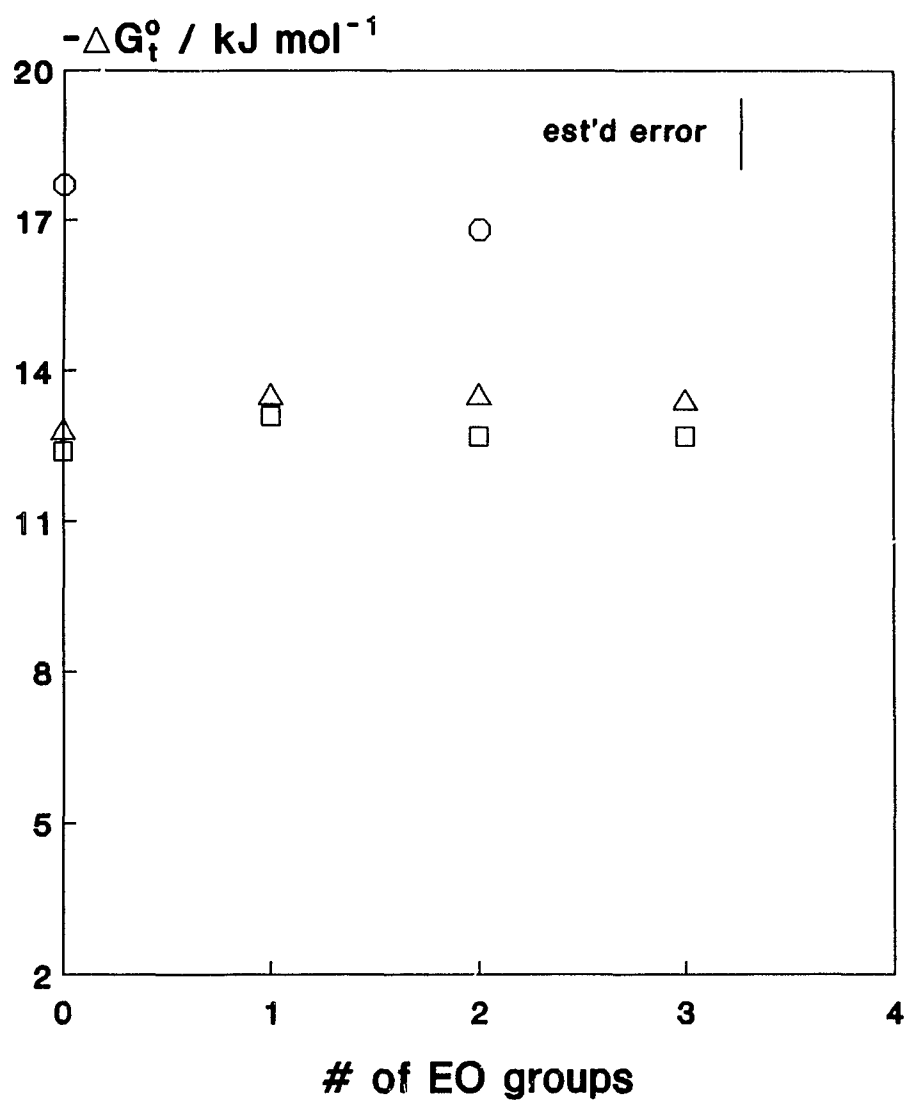


Figure 5.3. Transfer free energies of alkoxyethanols in DTAB and DPC micelles.
 \square $C_4E_0 \rightarrow C_4E_3$, \circ C_6E_0, C_6E_2 in DTAB; \square $C_4E_0 \rightarrow C_4E_3$ in DPC.

anionic micelles; i.e, PEO binds to or solubilizes in anionic micelles, but does not bind to cationic micelles.²⁰⁹

In Table 5.3, the interaction of TEG and TGD with anionic SDS and cationic DTAB micelles have been examined using the NMR paramagnetic relaxation experiment, in order to investigate the effect of changing the hydrophilic OH group for a more hydrophobic end group, the methoxy group, OCH₃. It can be seen on examining Table 5.3 that the nature of the end group may have a dramatic effect on the solubilization of neutral polymers containing small numbers of repeating units. For TEG, the results from the NMR paramagnetic relaxation experiment indicate a negligible interaction for both SDS and DTAB micelles. This is not unexpected since TEG contains two OH groups and a small number of EO chains, i.e., the driving force for the transfer of TEG to the SDS micelle interior (the transfer free energy of the EO group) would be overwhelmed by the interaction of the two OH groups with water. However, a much more favourable interaction is observed for TGD with SDS micelles, due to the replacement of the hydrophilic OH groups with the more hydrophobic OCH₃. This is, in part, due to the contribution of the EO groups to the hydrophobic interactions, and a possible hydrophobic effect due to the OCH₃ groups, i.e., substituting the methoxy groups for the OH group results in a loss of favourable hydrogen bonding between the ether OH groups and the water molecules surrounding them, *vide infra*. However, the transfer of either TGD or TEG from water to the interior of cationic micelles is energetically unfavourable (i.e., $p(\text{TGD}) \approx p(\text{TEG}) \approx 0$), which is related to the inability of the EO groups to penetrate the palisade layer of cationic micelles.

Table 5.3. Distribution Coefficients and Free Energies of Transfer for TEG and TGD in SDS¹ and DTAB² Micellar Solutions.

Alcohol	p	K_x	$-\Delta G_t^0/(\text{kJ/mol})$
SDS			
TEG	0.00 ± 0.07	-----	-----
TGD	0.44 ± 0.04	161 ± 33	12.6 ± 0.5
DTAB			
TEG	0.00 ± 0.14	-----	-----
TGD	0.05 ± 0.09	16 ± 16	7.1 ± 2.6

1. $c_{\text{SDS}} = 0.243$ molal; $T = 298$ K; $c(\text{proxyl}) = 10$ mmolal; $c_a \approx 0.050$ molal.
2. $c_{\text{DTAB}} = 0.162$ molal; $T = 308$ K; $c(\text{MnCl}_2) = 1.0$ mmolal; $c_a \approx 0.050$ molal.

5.3 Conclusions

The NMR paramagnetic relaxation experiment has given some valuable insight into the nature of the solubilization process. In anionic micelles, an increase in the p -value of the alkoxyethanols $C_2E_1 \rightarrow C_2E_3$, $C_4E_1 \rightarrow C_4E_3$, and C_6E_2 over their monohydroxy counterparts was interpreted in terms of the contribution of the EO group in the alcohol to the hydrophobic interactions. The free energy of transfer of an EO group from the aqueous to the micellar phase was calculated to be $\approx -1.1 \pm 0.3$ kJ/mol, in very good agreement with the free energy of transfer calculated from the decrease in the CMC 's as a function of alcohol concentration in Chapter 4.

However, for cationic micelles there is no increase in solubilization for the alkoxyethanols over their n -alkanol counterparts, indicating that the EO group has a negligible contribution to the hydrophobic interactions in cationic micellar systems. This is similar to the observation that PEO and other neutral polymers bind to anionic micelles, while not binding to cationic micelles.

The solubilization of TEG and TGD in anionic and cationic micelles indicates the importance of the end groups in the interaction of small, water soluble, nonionic polymers with micelles. TEG interacts very little with either SDS or DTAB, while TGD interacts very strongly with SDS and weakly with DTAB. The interaction with SDS micelles is due to the hydrophobic effect of the OCH_3 group and the favourable transfer free energy of the EO groups from D_2O to the interior of anionic micelles.

Chapter 6

The Determination of the Aggregation Numbers of Surfactant and Alcohol in Ionic Surfactant/Alcohol Mixed Micelles Using the Static Fluorescence Quenching Experiment

6.1 Introduction

(a) The Static Fluorescence Quenching Experiment

The ability of aqueous micellar solutions to solubilize organic molecules otherwise sparingly soluble or insoluble in water is well known. It has been discussed in the preceding chapters of this thesis that the presence of solubilizates may have a profound effect on the properties of the host micelles, e.g., the *CMC*'s and the degrees of counterion binding (β 's). It is well known that the presence of solubilizates also affects the aggregation number of the host surfactant system, the manner in which this perturbation occurs depends on the structure and polarity of the solubilizate, and whether the solubilization occurs deep within the micelle, or in the palisade layer (the headgroup region).

A number of methods are available in the literature to determine the surfactant aggregation number including dynamic light scattering (DLS),¹⁹⁷ self-diffusion measurements, and ¹³C NMR chemical shifts.²²¹ The fundamental property measured in dynamic light scattering experiments is the micellar self-diffusion coefficient. It should be noted here that the measurement of micellar diffusion coefficients, either by DLS or

NMR self-diffusion experiments, is a determination of a property of the whole micelle from which the micellar radius is estimated from the Stokes-Einstein equation

$$r_{mic} = \frac{k_B T}{6 \pi \eta D_{mic}} \quad (6.1)$$

where r_{mic} is the micellar radius, T is the absolute temperature, η is the viscosity of the continuous medium, and k_B is the Boltzmann constant. The aggregation number of the surfactant is then estimated from the micellar radius by assuming *a priori* a micelle shape. Measured values of the micellar self-diffusion coefficient must be corrected for obstruction effects; the micelle does not diffuse in a continuous medium (implicitly assumed in equation 6.1) and encounters other particles (micelles) present in solution. Accounting for obstructions to the diffusion of spherical micelles is approximate at best, and, in the case of mixed micelles, the presence of the solubilize influences the composition and, possibly, the micellar structure. This changes not only the volume fraction of obstructing particles, but may alter their shape as well, leading to difficulties in accounting for the effects of solubilizes in the micelles, and, hence, errors in the determination of the aggregation number.

^{13}C NMR chemical shifts have also been used to determine the micellar aggregation number.²²¹ It was stated in Section 1.3 (b) that the formation of micelles is accompanied by a change in NMR parameters, such as spin-lattice relaxation times (T_1 's) and chemical shifts (δ 's). By computer fitting the ^{13}C chemical shifts of the methylene carbons in SDS micelles to the mass action model, under the assumption of a single aggregation number at all micelle concentrations, Söderman obtained an average surfactant aggregation

number of 29 for SDS micelles. Clearly, this estimate of N_s is in poor agreement with literature results obtained from other methods. Fitting ^{13}C chemical shifts to the mass action model to obtain surfactant aggregation numbers has been criticized on several counts,^{3,138,221} and is generally not recommended for obtaining N_s .

The use of luminescence probing techniques to determine the surfactant aggregation number is a relatively recent development.^{42,178,179,181} The main advantage of luminescence probing techniques is that they can be used at any surfactant concentration, and do not require *a priori* a knowledge of the micellar shape or fitting an experimental observable to a micellar model, as in the case of ^{13}C NMR chemical shifts. As well, luminescence probing techniques are not expected to be affected by intermicellar interactions. The disadvantage with these techniques is the need for solubilized probes and quenchers, the influence of which on the micellar concentration has been briefly discussed in the introduction.

Two luminescence probing techniques for determining the aggregation number are available, the static and the time-resolved (or lifetime) methods. In general, the lifetime method is the preferred technique for determining the micellar concentrations, and, hence, the aggregation number of the surfactant. A disadvantage of using the lifetime method is the need for a single-photon-counting instrument, and larger random errors in the determined values of the aggregation number.

The static quenching method, proposed originally by Turro and Yekta,¹⁷⁰ has been used extensively in the literature for the determination of the surfactant aggregation number in the presence of additives. These authors derived a simple Stern-Volmer type

relationship between the bulk quencher concentration and the logarithm of the fluorescent intensities as a function of the quencher concentration, shown previously in Chapter 1

$$\ln \left[\frac{I_0}{I} \right] = \frac{[Q]}{[M]} \quad (6.2)$$

The advantage of the static quenching method is in its ease of implementation (it can be used routinely on any emission spectrophotometer). However, the success of the static quenching method depends on compliance with the following three experimental criteria:

- 1) *both the luminescent probe and quencher are associated with the micelle during the luminescent lifetime of the probe (i.e., immobile probes and quenchers),*
- 2) *in the presence of increasing quencher concentrations, the lifetime of the non-quenched luminescent probes is the same as in the absence of quencher.*
- 3) *luminescence is observed only from micelles containing a solubilized probe and no quencher (i.e., the static quenching condition).*

It has been stated in the introduction of this thesis (Section 1.4 (g)) that both pyrene and CP⁺ ion are associated with the micelles on the order of 10 → 50 μs,^{192,222} while the fluorescent lifetimes are on the order of 200 → 360 ns,¹⁹⁵ thereby satisfying condition 1. Turro and Yekta, in their original paper describing the application of this method, determined the fluorescent lifetimes of the micelle bound probe, ruthenium tris-bipyridyl chloride, in the presence of increasing concentrations of the micelle solubilized quencher, 9-methylanthracene.¹⁷⁰ The fluorescent decay curves of micellar bound probes and quencher clearly show the existence of processes occurring with two distinct lifetimes; a shorter lifetime due to the interaction of the luminescent probe with a quencher

molecule occupying the same micelle, and a longer lifetime corresponding to the unquenched luminescent probe.^{42,161,163,167,170,195} The results of Turro and Yekta¹⁷⁰ confirmed that the lifetime of the unquenched luminescent probe remained constant at 480 ± 16 ns, indicating that condition 2 was fulfilled for the ruthenium tris-bipyridyl/9-methylanthracene probe/quencher pair. Lang et al.,¹⁹⁵ and more recently DeSchryver et al.²²³ have shown that, even if the quencher concentration is quite close to the micellar concentration, the lifetime of the remaining unquenched probes is the same as in the absence of added quencher.

Some additional insight into condition 3 can be obtained from the functional form of equation 1.40, by examining the variation in $\ln(I_o/I)$ versus the average quencher occupancy number. Figure 6.1 is a plot of calculated $\ln(I_o/I)$ values for $k_q\tau_o$ values ranging from 0.1 to ∞ (i.e., the static limit). It is obvious on examining Figure 6.1 that the value of $\ln(I_o/I)$ is strongly influenced by the value of the kinetic ratio, $R = k_q\tau_o$. At intermediate values of the kinetic ratio (e.g., $R = 1, 10, 18$) curvature in the plots is apparent. Taking $R = 10$ as an example, the difference between the static limit ($R = \infty$) and $R = 10$ at $\langle Q \rangle = 0.2$ is approximately 10%, while at $\langle Q \rangle = 1.0$, the error increases slightly to about 12%. The error at $\langle Q \rangle = 2.0$ (not shown in Fig. 6.1) is about 14%. For $R = 18$, the literature value for the kinetic ratio of pyrene/CP⁺ ion in SDS micelles,¹⁹⁴⁻¹⁹⁶ the situation is improved somewhat. At $\langle Q \rangle = 0.2$, the difference in the $\ln(I_o/I)$ values for the curves represented by $R = 18$ and $R = \infty$ is now about 5%, while at $\langle Q \rangle = 1.0$, the difference now amounts to approximately 7%. It is evident from Fig. 6.1 and the preceding discussion that the use of the static

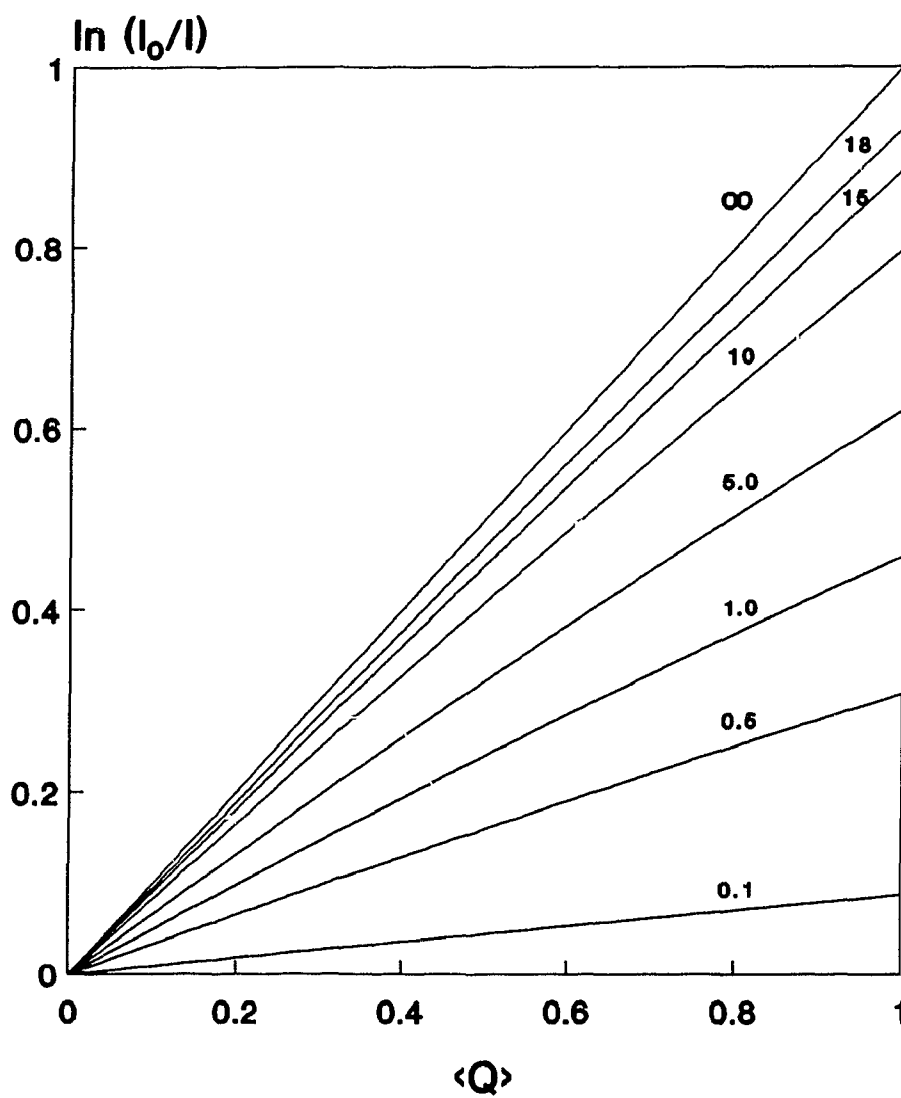


Figure 6.1. Plot of calculated values of $\ln(I_0/I)$ vs. $\langle Q \rangle$ at different kinetic ratios, $k_4 \tau_0$.

quenching method results in an inherent overestimation of the number of micelles of the order of 5-7%, using the probe quencher pair pyrene/CP⁺ ion in SDS micelles, and 6-8%, using the same probe/quencher pair in DTAC and DTAB micelles (i.e., $R \approx 15$).^{195,196} However, the resulting systematic error of about 5-8% is less than the random error usually quoted for the time-resolved experiments, generally 10-12%.^{42,193} However, the use of the pair pyrene/CP⁺ ion is acceptable for the routine estimation of the surfactant aggregation numbers of both SDS/alcohol and DTAB/alcohol mixed micelles, provided the ratio of quenchers to micelles, and the surfactant concentration, is kept low.

Additional support for the use of the static method can be found in the paper by Grätzel et al.,¹⁸⁵ in which the surfactant aggregation number of alkylsulfonic acids (C₁₂, C₁₄, and C₁₆) were determined by both time-resolved and static fluorescence quenching methods, using the pyrene/CP⁺ probe/quencher pair. The surfactant aggregation numbers obtained from both methods were in excellent agreement with each other. As well, Anderson and Kwak²²⁴ have determined the aggregation number of SDS and SD, at various surfactant concentrations, using both the static and the time-resolved fluorescence quenching experiment. The results obtained from both luminescence quenching experiments were in excellent agreement with each other.

In Table 6.1 and Fig 6.2, a number of experimental determinations of N_s for SDS and DTAC micelles, using the static quenching method, are compared to literature values for SDS at 0.025, 0.05, 0.075, and 0.100 molal, and for DTAC at 0.031, 0.050, and 0.100 molal.^{39,42,161,222,223} DTAC has been chosen for the cationic micelle comparison, since a number of time-resolved luminescent quenching determinations of the surfactant

Table 6.1. Aggregation Numbers of DTAC and SDS Micelles¹ as a Function of the Surfactant Concentration, as Determined by the Static Fluorescence Quenching Experiment.

$C_{\text{surf}}/\text{molal}$	DTAC			SDS		
	N_s	$N_s(\text{lit.})$	Ref.	N_s	$N_s(\text{lit.})$	Ref.
0.020	--	--	---	--	65	194
0.025	--	--	---	61	--	---
0.031	54	47	161	--	--	---
0.050	49	--	---	66	71	223
0.075	51	--	---	75	--	---
0.100	51	51	39, 161, 223	77	75	39
0.200	--	57	195	--	--	---
0.500	--	62	195	--	--	---

1. $N_s \pm 3$.

2. Additional literature values for SDS (concentration not given):

59, 64¹⁸⁵; 62^{40,165,167,171}; 74¹⁷⁸.

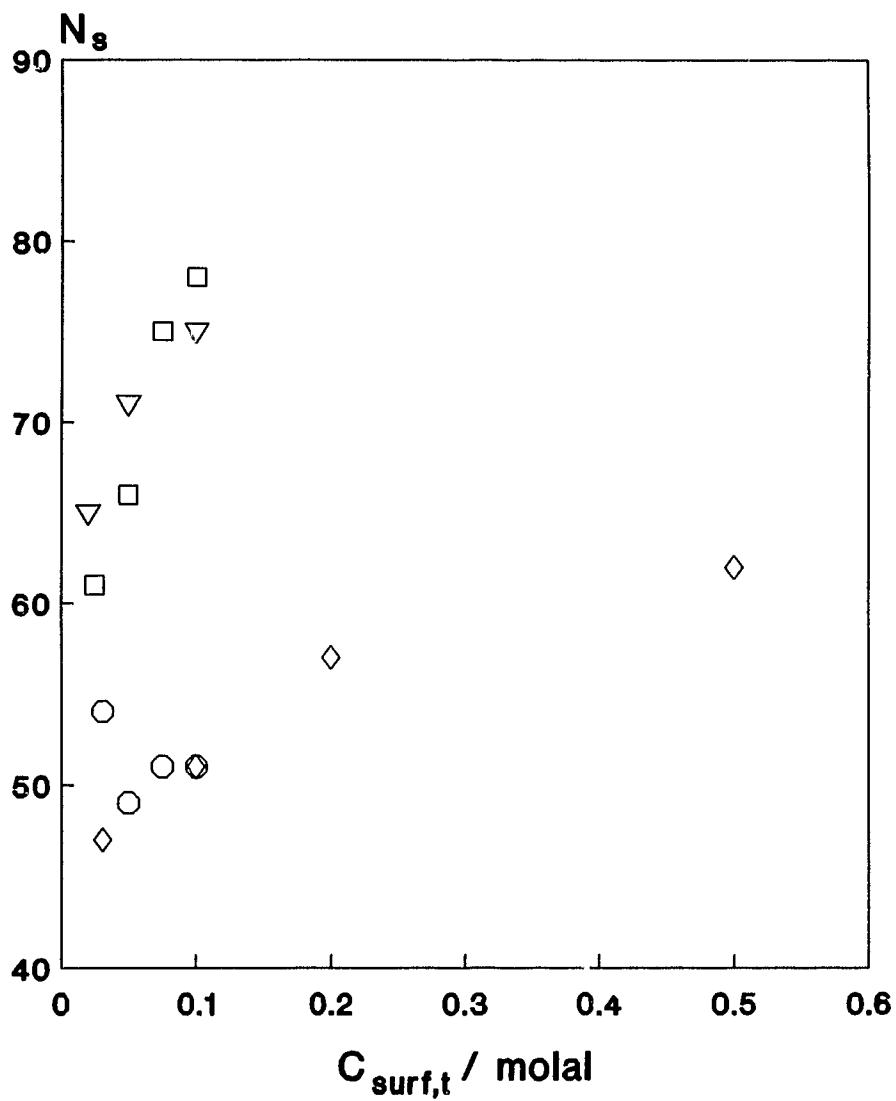


Figure 6.2. Aggregation numbers of DTAC and SDS at different surfactant concentrations. \circ DTAC (present data); \diamond DTAC (lit. values); \square SDS (present data); ∇ SDS (lit. values).

aggregation number were available in the literature, while relatively few aggregation number determinations of DTAB by luminescence probing methods were found. It can be seen clearly from Table 6.1 and Fig. 6.2 that the N_s values determined here are in good agreement with the literature results for SDS and DTAC micelles.

It should be noted that Almgren and Swarup have stated that for SDS, N_s is underestimated when the surfactant concentration is higher than ≈ 0.200 molal.¹⁷⁶ This is due to the decreased magnitude of k_q ; the increase in the aggregation number of SDS at concentrations higher than ≈ 0.200 molal is large enough to increase significantly the time for the quencher to diffuse over the micellar surface. In terms of the aggregation number of SDS, determined from the static quenching method, this places an upper limit of ≈ 80 as an experimentally accessible number.

It should be noted here that if the kinetic ratio, R , is known, it is not necessary to adhere to the condition that R be as large as possible, if R has been accurately determined from independent measurements, which, in the case of fluorescent quenching necessitates the use of time-resolved experiments. From the R value determined with the lifetime experiments, the $\ln(I_0/I)$ data can be fitted to equation 1.40 in order to correct for the underestimation in the micelle concentration. As an example, for the system SDS/pyrene/CP⁺, the experimental value of the kinetic ratio is 18. The slope of the $\ln(I_0/I)$ vs. $[Q]$ curve yields an estimate of the micellar concentration, $[M]$, of 0.660 mmolal, from which an aggregation number of 67 is estimated. Using equation 1.40, the corrected micellar concentration is 0.628 mmolal, resulting in an aggregation number of 70; without correction, N_s is underestimated by 4%. Published values of N_s for

0.0500 molal SDS ranges from about 64 to 73.^{39,40,164,167,169} It can be easily seen that the aggregation number estimated from the steady state method, even without the correction, is within the random error of the time resolved method ($\approx 10 - 12\%$).

According to Zana,⁴² the limitation of a finite R value suggests that time-resolved (or lifetime) experiments are preferred for determining the micellar concentrations. However, Zana⁴² and Malliaris¹⁹³ state that the application of the static method is perfectly acceptable when immobile probes and quenchers (e.g., pyrene and CP^+ ion) are used, and the surfactant aggregation number is less than ≈ 70 .

As a final comment concerning the use of the static quenching method for determining the micellar concentrations, and, thus, the surfactant aggregation numbers, in mixed solvent systems, the value of $k_q\tau_o$ should increase as alcohols are added to ionic surfactant solutions. Both k_q and τ_o were found to increase when alcohols were added to SDS micellar solutions,²²³ indicating the determination of surfactant aggregation numbers at low to moderate alcohol concentrations is somewhat more favourable. On the other hand, at still higher alcohol concentrations, the decrease in the surface charge density of the micelle results in lower intermicellar repulsion potentials, increasing the possibility of intermicellar exchange of solubilized probe and quencher molecules on the timescale of the fluorescent lifetime.^{222,223} In some cases, this may result in a violation of condition 1, rendering the static method unusable at higher alcohol concentrations.

(b) Literature Studies and Present Work

A number of studies in the literature have used the static quenching method to determine the effects of solubilizates on N_s . Perhaps the most complete study is a series of papers by Almgren and Swarup which focussed on the influence of added alcohols, alkanes, and a number of other polar and nonpolar solubilizates on the surfactant aggregation number, N_s , of SDS micelles.^{176,202,203} Using the probe/quencher pair, ruthenium tris-bipyridyl chloride/9-methylanthracene, proposed originally by Turro and Yekta,¹⁷⁰ these authors determined the surfactant aggregation number of SDS micelles as a function of the concentration of both the surfactant and solubilizate. A number of trends were reported in these studies, including the decrease in N_s brought about by the addition of alcohols; the addition of alkanes and aromatic hydrocarbons tended to increase the surfactant aggregation number. For a given concentration of surfactant, the rate of the decrease in N_s with an increase in the alcohol concentration was observed to be larger for the longer chain alcohols. For the alkane or aromatic solubilizates, the rate of increase of N_s with an increase in the solubilizate concentration (either alkane or aromatic) was found to be larger for the longer chain solubilizates. From the distribution constants of the solubilizates, p , obtained by Stilbs using the FT-PGSE experiment,¹³⁴ and the micellar concentration from the static quenching method, the aggregation number of the additives, N_a , was calculated from the following relationship

$$N_a = \frac{pC_{a,t}}{[M]} \quad (6.3)$$

In the case of alcohols, N_a was observed to increase slowly for solubilizates with small alkyl chain lengths, while for the longer chain length alcohols, N_a increased more quickly, so that the total aggregation number, $N_t = N_s + N_a$, remained relatively constant or increased slowly. For SDS/alkane mixed micelles, N_t was observed to increase for all the SDS/alkane systems studied, even at small alkane concentrations. These authors postulated that the decrease, or increase, in N_s could be readily explained by taking into account the effect of the solubilizate on the surface charge density (σ/e) of the micelle. In fact, a plot of the calculated estimate of the surface charge density against the mole fraction of the micellar solubilized additive indicated that the decrease in N_s was independent of the nature of the polar additive, in spite of the variety of alcohols and polar compounds examined. Addition of non-polar compounds, both alkanes and aromatic solubilizates, induced micellar growth. However, the surface charge density of the SDS/alkane mixed micelles was unchanged from SDS micelles without additives.

Malliaris¹⁹³ examined the effects of the addition of solubilizates (n-alcohols, alkanes, and alkyl ketones) on the aggregation number of 0.0400 molal SDS micelles, using the static quenching method with pyrene and CP^+ ion as the probe/quencher pair. In agreement with the results of Almgren and Swarup,^{176,202,203} the addition of alcohols to SDS micellar solutions decreased the surfactant aggregation number, while the addition of alkanes promoted micelle growth. The rate of decrease of N_s with the increased alcohol concentration (and, conversely, the increase in N_a) was again found to be largest for the longer chain alcohols. The addition of alkyl ketones decreased N_s , with the rate of decrease of N_s with the concentration of added ketone being largest for the longer

chain alkyl ketones. Malliaris concluded that the ketone results were consistent with the polarity of the alkyl ketones, i.e., the carbonyl group would be expected to occupy part of the interfacial region and the hydrocarbon chain would be oriented towards the centre of the micelle. The additive aggregation number, N_a , was calculated in these systems as described above in Almgren and Swarup's work.^{176,202,203} The values of N_a increased for all the solubilizates studied; the rate of increase of N_a with the additive concentration was again found to be strongly dependent on the p -value of the solubilizates.

Lianos et al.²⁰⁰ have studied the effect of n -alcohol addition on long chain n -alkyltrimethylammonium micelles (C_{12} - C_{16}), using a variety of techniques, including time-resolved fluorescence quenching, in order to obtain a complete picture of the effects of alcohols on the properties of these typical cationic surfactant micelles.

In this chapter, the effects of the addition of alcohols and alkoxyethanols on the N_s of typical ionic micelles (SDS and DTAB) are determined using the static fluorescence quenching method. In addition, the additive aggregation number (in this case alkoxyethanols), N_a , and the total micelle aggregation number, N_t , are estimated from the micelle concentrations determined from the static quenching method, and the distribution constants of the alcohols and alkoxyethanols obtained from the paramagnetic relaxation experiment, described in Chapter 5. These results, along with the I_1/I_3 ratios (indicative of the micropolarity sensed by the luminescent probe), will be interpreted in terms of the EO group contribution to the formation of mixed micelles, the possible location of the EO chains in the mixed micelles, and the differences in the interactions of ethoxylated alcohols with anionic and cationic micelles.

6.2 Results and Discussion

(a) SDS/Alkoxyethanol Mixed Micelles

As a typical example of the methodology used, in Figure 6.3, the emission intensities of micellar solubilized pyrene at 373 nm are plotted against the quencher concentration (equation 6.1) for two different micellar systems, 0.0500 molal SDS and 0.0500 molal SDS/0.200 molal C₁E₂. The pyrene concentration for both these experiments is 0.010 mmolal. The slopes of the respective straight lines are the reciprocals of the micelle concentrations, $[M]$. The slope and the relative error in the slope were calculated by least-squares methods. Good linearity was found for all plots of $\ln(I_0/I)$ versus $[Q]$, as indicated by the small relative error in the slope (generally around 2-3%). The aggregation numbers of the surfactant were calculated from the simple relationship

$$N_s = \frac{[surf]_{mic}}{[M]} \approx \frac{c_{surf,t} - CMC}{[M]} \quad (6.4)$$

where the CMC estimates are those of the mixed micelles, reported previously in Chapter 4. It can be easily seen from Figure 6.3 that $[M]$ is much higher in the surfactant solution containing alcohol, indicating a change in the aggregation properties of the micellar system. A number of authors have indicated that quenching of the pyrene fluorescence by molecular oxygen from dissolved air can have a significant effect on luminescence intensity in these systems.^{42,178,196} In a trial experiment, the slope of a plot

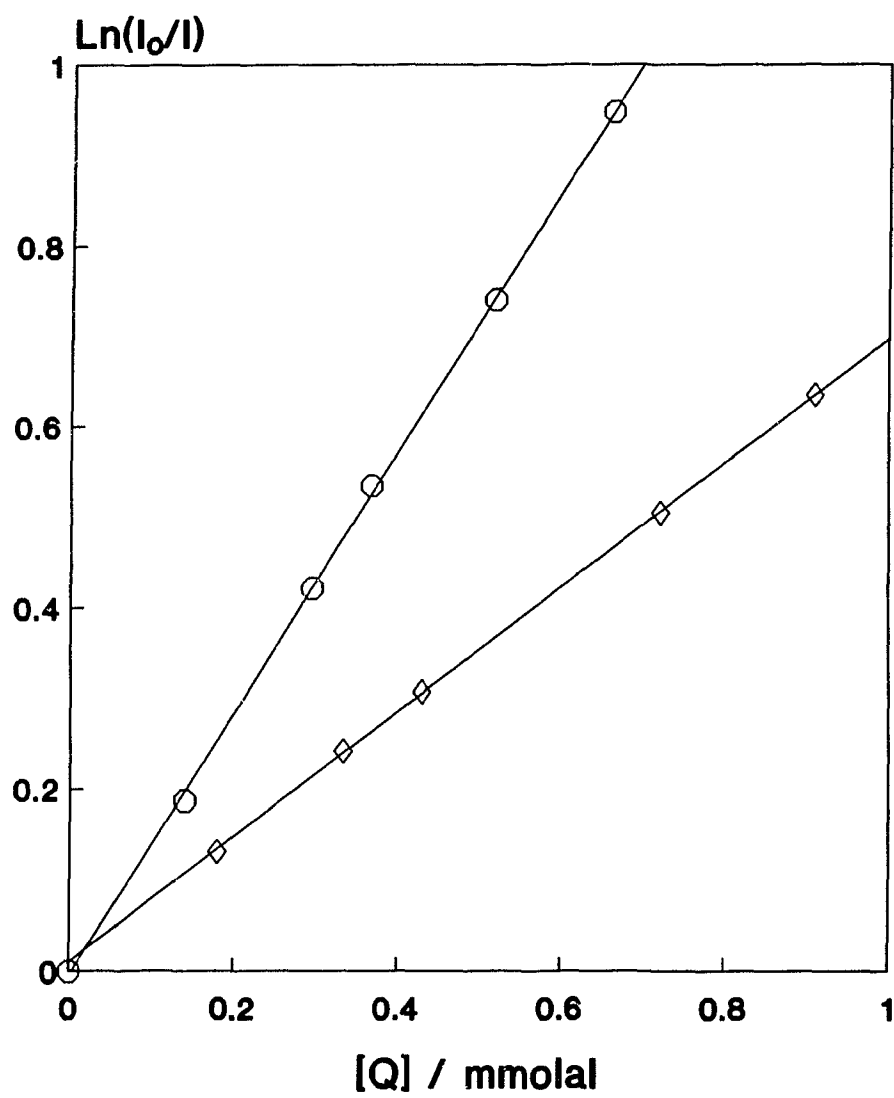


Figure 6.3. Plot of $\ln(I_0/I)$ vs. $[Q]$ for the pyrene/ CP^+ probe quencher pair in micellar solutions. ○ 0.0500 molal SDS; ◇ 0.0500 molal SDS/0.200 molal C_4E_2 .

of $\ln(I_0/I)$ vs. $[Q]$ was determined for two sets of 0.0500 molal SDS solutions, one set in which the solutions were degassed by bubbling with nitrogen gas, the other set without degassing. Although some differences were noticed in the luminescent intensity of the probe at the same quencher concentrations, the quenching slopes for the two sets of solutions were in excellent agreement (1516 kg mol⁻¹ in the absence of degassing and 1501 kg mol⁻¹ with degassing). Therefore, most of the subsequent experiments were done without degassing. The equivalence of the quenching slopes with and without degassing was periodically checked throughout the course of the measurements.

It should be noted here that in light of the discussion presented in the Introduction of this chapter, the aggregation numbers reported here (and the numbers to be reported later for DTAB/alcohol mixed micelles) are most likely underestimated by 5-8%, and are, therefore, reported as apparent aggregation numbers. Despite the finite value of the kinetic ratio, R , no corrections have been made to the estimates of the micellar concentration determined from the static quenching experiment for either SDS/alcohol or DTAB/alcohol mixed micelles.

Surfactant aggregation numbers, N_s , for 0.0500 molal SDS/alkoxyethanol mixed micelles are presented in Tables 6.2 - 6.3 and plotted in Figs. 6.4 - 6.5. The errors reported here are determined from the relative error in the slope of the plot of $\ln(I_0/I)$ vs. $[Q]$ calculated at the 90% confidence level, regarding all deviations from N_s as random errors. The aggregation number for 0.0500 molal SDS micelles, in the absence of added alcohol, is in excellent agreement with both time-resolved and static experiments involving the same probe/quencher pair.^{42,193} The additive (alcohol) aggregation

numbers, N_a , were calculated from Eq. 6.2, using the micellar concentrations determined via the static fluorescence quenching experiment and the distribution constants obtained from the NMR paramagnetic relaxation experiment in 0.243 m SDS micelles (Chapters 3 and 5). The reported errors in N_a reflect the sum of the relative errors in the slope and the distribution constants (p -values) calculated at the 90% confidence interval, regarding all deviations from the calculated value of N_a as random errors. These numbers are also presented in Tables 6.2 - 6.3. The ratio of the first and third peaks of the pyrene emission spectrum, I_1/I_3 , are also presented in Tables 6.2 - 6.3. The errors in the I_1/I_3 ratios are estimated to be on the order of 1-2%.

A number of trends can be noted in Tables 6.2 - 6.3 and Figs. 6.4 - 6.5. The first of these is that the surfactant aggregation number, N_s , decreases when alcohols are added to 0.0500 molal SDS micelles, for all alcohols studied in the present thesis. It is also apparent from Tables 6.2 - 6.4 that the additive (alcohol) aggregation number, N_a , increases with an increase in the total alcohol concentration, in agreement with the findings of a number of previous authors. These trends are evident in Figure 6.6, where N_s , N_a , and N_t are plotted for the SDS/ C_4E_2 mixed micelles. It can be seen from Figure 6.6 and the tabulated values for the aggregation numbers presented previously that N_t remains relatively constant, or increases slightly. Other SDS/alkoxyethanol mixed micelles exhibit trends similar to those exhibited in Figure 6.7. For a given alcohol concentration, C_a , the additive (alcohol) aggregation number, N_a , is greatest for alcohols containing a longer hydrophobic chain, e.g., C_4E_2 , C_4E_3 , C_6E_0 , and C_6E_2 , and is smaller for alcohols like C_4E_0 and C_4E_1 . Since these alcohols all possess the same hydrophilic

Table 6.2. Aggregation Numbers of Surfactant and Alcohol¹ for 0.0500 molal SDS/Alkoxyethanol Mixed Micelles as a Function of the Concentration of Alcohol

C_s /molal	C_4E_0			C_4E_1			C_4E_2			C_4E_3		
	N_s	N_a	I_1/I_3									
0.000	66	0	1.26	66	0	1.26	66	0	1.26	66	0	1.26
0.025	--	--	----	--	--	----	53	9	1.21	48	10	1.23
0.050	59	9	1.20	53	11	1.18	46	15	1.21	41	16	1.23
0.075	--	--	----	--	--	----	42	21	1.21	37	22	1.24
0.100	55	16	1.19	47	20	1.18	38	26	1.22	34	36	1.23
0.150	48	21	1.14	42	27	1.18	33	32	1.23	31	36	1.23
0.200	46	26	1.12	34	29	1.15	30	38	1.21	21	41	1.23
0.250	43	31	1.11	31	33	1.15	27	44	1.22	--	--	----
0.300	41	34	1.10	29	38	1.14	26	51	1.20	20	51	1.24
0.400	35	41	1.07	23	42	1.14	--	--	----	--	--	----
0.500	30	44	1.05	20	46	1.14	--	--	----	--	--	----

1. $N_s \pm 2, N_a \pm 5$

Table 6.3. Aggregation Numbers of Surfactant and Alcohol¹ for 0.0500 molal SDS/C₆E₀ and SDS/C₆E₂ Mixed Micelles as a Function of the Concentration of Alcohol

C _s /molal	C ₆ E ₀			C ₆ E ₂		
	N _s	N _a	I ₁ /I ₃	N _s	N _a	I ₁ /I ₃
0.000	66	0	1.26	66	0	1.26
0.010	61	7	1.20	55	8	1.21
0.020	59	13	1.17	49	13	1.19
0.030	57	19	1.15	46	18	1.19
0.040	55	24	1.12	43	23	1.18
0.050	53	28	1.10	39	27	1.18
0.060	50	31	1.09	37	30	1.17
0.070	48	36	1.07	35	35	1.17
0.080	47	41	1.05	31	40	1.16

1. N_s ± 2, N_a ± 5

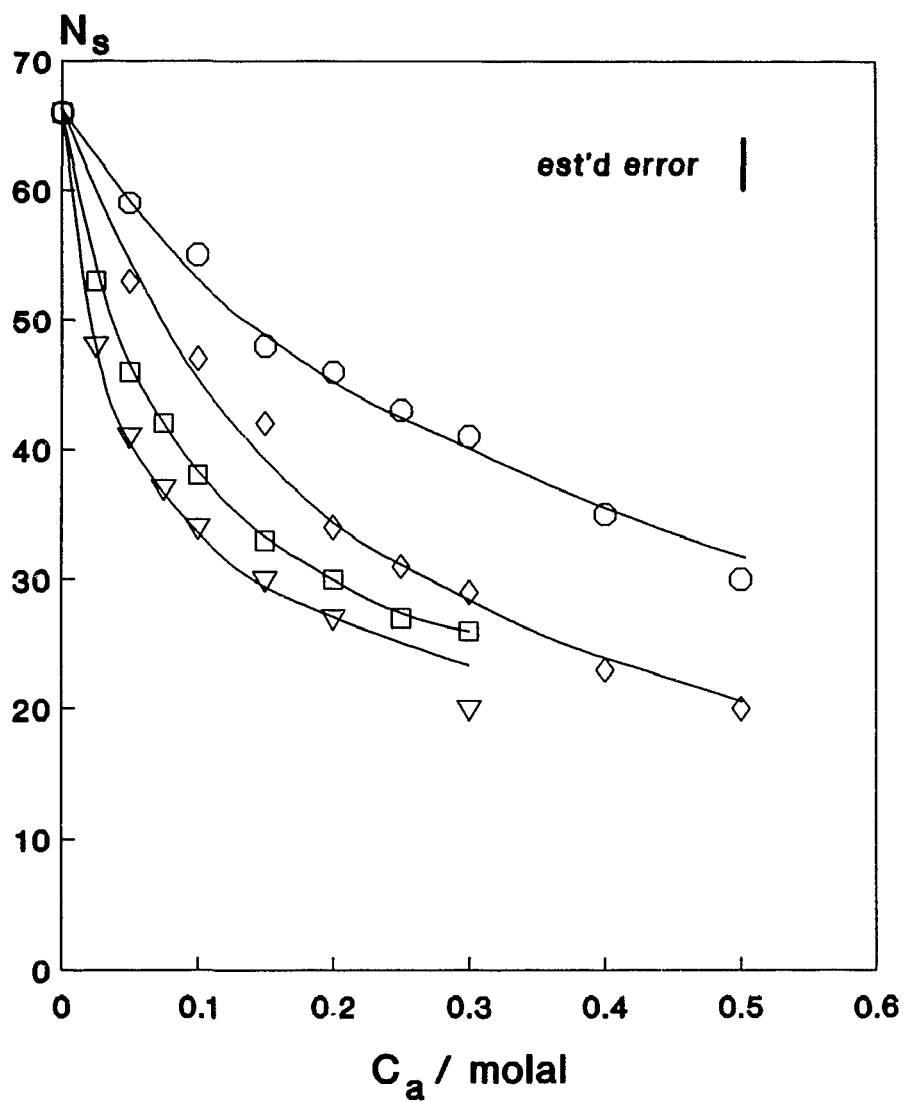


Figure 6.4. Surfactant aggregation numbers, N_s , for SDS/alkoxyethanol mixed micelles as a function of c_a . \circ C_4E_0 ; \diamond C_4E_1 ; \square C_4E_2 ; ∇ C_4E_3 .

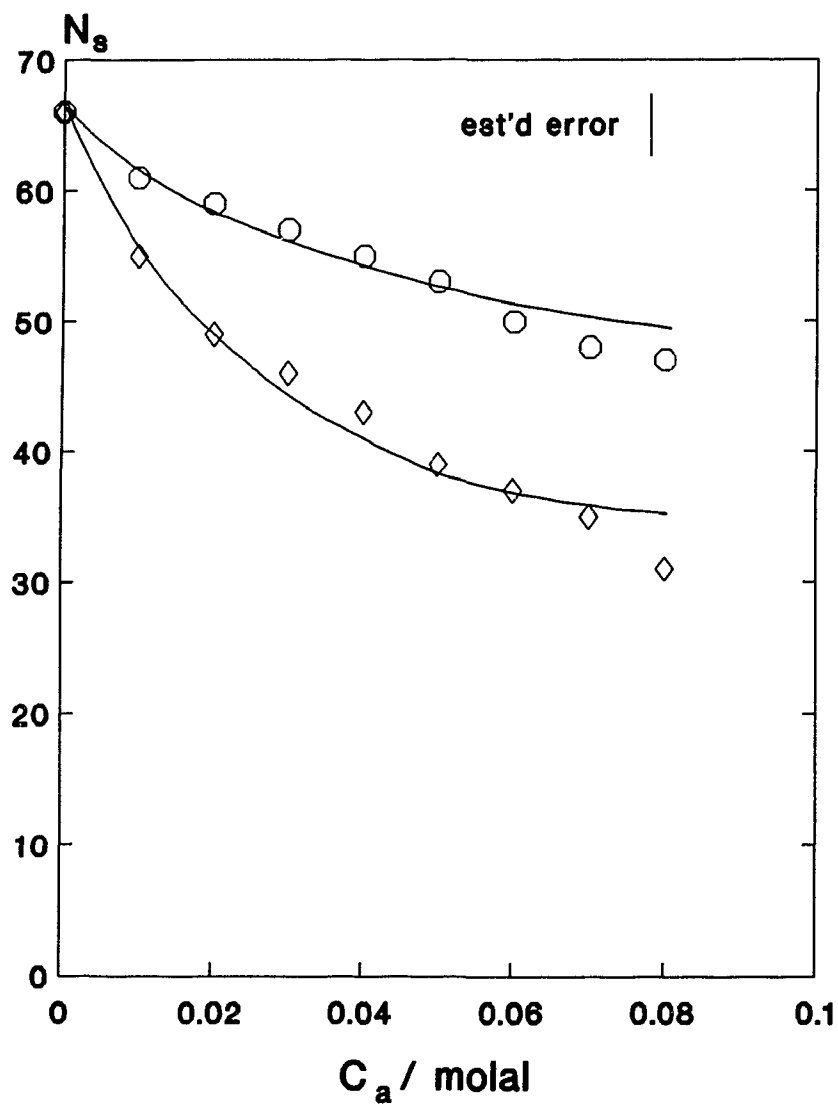


Figure 6.5. Surfactant aggregation numbers, N_s , for SDS/alkoxyethanol mixed micelles as a function of c_a . \circ C_6E_0 ; \diamond C_6E_2 .

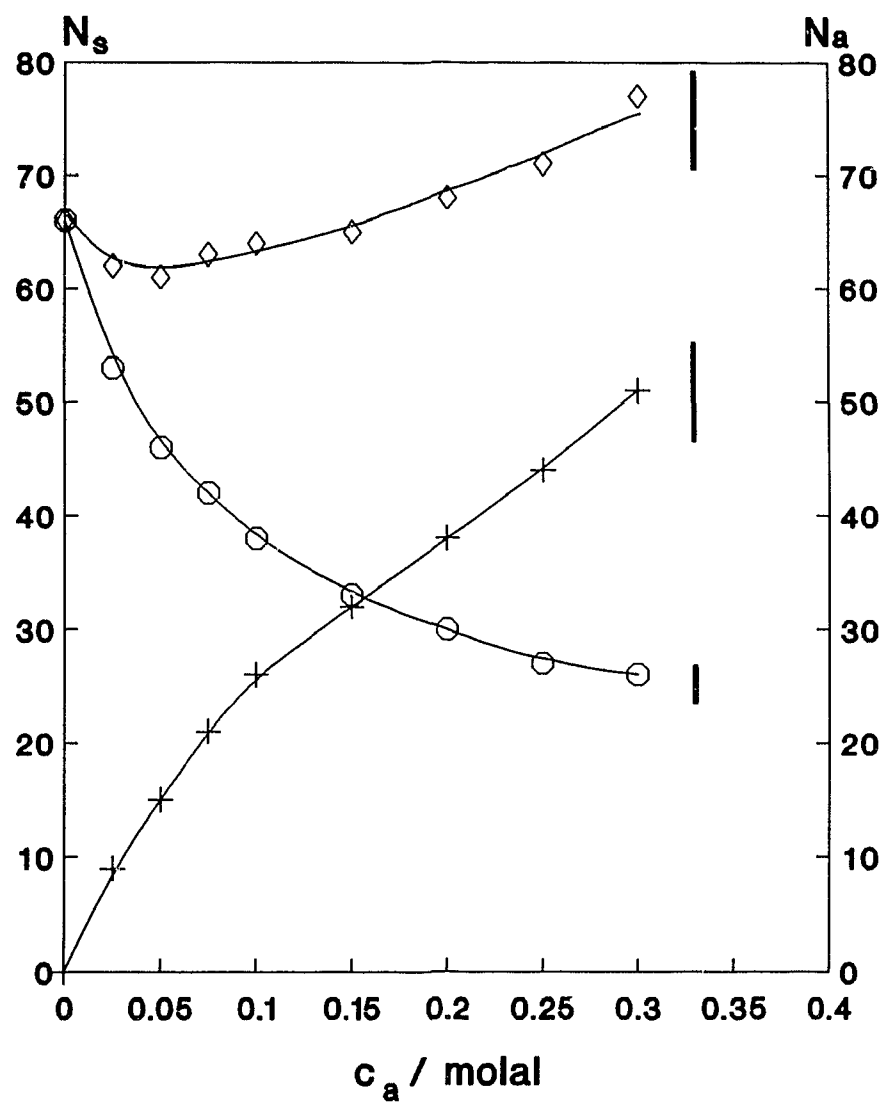


Figure 6.6. Surfactant aggregation numbers (O), alcohol aggregation numbers (+) and total aggregation numbers (\diamond) for 0.0500 molal SDS/ C_4E_2 mixed micelles.

group, i.e., the hydroxyl group, the observed differences in the increase in N_a reflect the differences in the hydrophobicity of the alkyl or alkyl + EO chain.

It can be seen from a comparison of the data in Tables 6.2 and 6.3 that, as expected, the surfactant aggregation numbers for 0.0500 m SDS/C₆E₀ are lower than for 0.0500 m SDS/C₄E₀ mixed micelles at the same concentration of alcohol. An interesting trend is observed in all the aggregation numbers, N_s , N_a , and N_t , in the two series C₄E₀ → C₄E₃ and C₆E₀ and C₆E₂. At the same total concentration of alcohol, the N_s values in the series SDS/C₄E₀ → SDS/C₄E₃ tend to decrease, while the opposite trend is observed for N_a , as the number of EO groups in the alcohol is increased. Similar conclusions can be made upon examining the N_s and N_a values for 0.0500 m SDS/C₆E₀ and C₆E₂ mixed micelles. Again, for alcohols with shorter alkyl or alkyl + EO chains, N_t , the total aggregation number, tends to increase slowly with an increase in the alcohol concentration, while for alcohols containing longer alkyl or alkyl + EO chains, N_t remains relatively constant with an increase in the alcohol concentration. This indicates that for all the 0.0500 m SDS/alcohol mixed micelles studied in this thesis, the overall radius of the micelle remains relatively constant, or decreases slightly. At the present range of alcohol concentrations, these results are not unexpected since the micelles would tend to retain their spherical geometry.²²³

Additional information about the structure of these mixed micelle can be obtained from an analysis of the pyrene I_1/I_3 ratios in Tables 6.2 and 6.3. As the concentration of alcohol in the micellar solution is increased, the pyrene I_1/I_3 ratios decrease with an increase in the alcohol concentration for mixed micelles of SDS and C₄E₀, C₄E₁, C₆E₀,

and C_6E_2 . Zana²⁰¹ and Thomas¹⁷⁹ have explained this trend in terms of a looser micelle structure, allowing the luminescent probe (in this case pyrene) to penetrate further into the micelle, thereby sensing a less polar environment. Recently, Gao et al.²²⁵ have examined the distribution of aromatic probe molecules, like pyrene, in anionic and cationic micelles. Their findings indicated that SDS solubilized probe molecules e.g., pyrene and naphthalene, are evenly distributed throughout the micelle. When a short chain alcohol (e.g., C_4E_0) is added to the micelles, this distribution is not expected to be altered, and, hence, the probe molecule would still sample the entire micelle volume, including the region close to the surface of the SDS micelle. Since the I_1/I_3 ratio decreases, this indicates that the presence of the alcohol blocks water penetration into the micelle. For the SDS/ C_4E_2 and the SDS/ C_4E_3 mixed micellar systems, the I_1/I_3 ratios are invariant with an increase in the concentration of cosurfactant (alcohol). An interesting trend in the I_1/I_3 ratios can be observed upon changing the cosurfactant from C_4E_0 to C_4E_3 in that the I_1/I_3 ratios increase upon addition of EO groups to C_4E_0 . This indicates that the pyrene senses a more polar environment, possibly due to the penetration of the EO groups in the micellar interior. This lends support to the idea advanced in previous chapters that the EO groups penetrate the palisade layer of the anionic SDS micelles, thereby mixing with the methylene chains of the surfactant. This mixing of the EO chains and the CH_2 groups of the surfactant would lead to a decrease in the free energy of the system. It is this mixing of the hydrophobic chains that is responsible for the decrease in the free energy of micelle formation (the *CMC*'s) and the free energies of transfer of ethoxylated alcohols from D_2O to the micellar phases of SDS and SD reported

in Chapter 5 of this thesis.

The volumes occupied by the hydrophobic tails of mixed micellar systems can be calculated from the aggregation numbers of the surfactant and additive, and a knowledge of their partial molar volumes

$$V_{mic} = N_s V_s + N_a V_a \quad (6.5)$$

where V_{mic} is the micellar volume, V_s is the volume of a surfactant tail in a micelle ($V_s = V_s^o/N_{avo}$) and V_a is the volume occupied by an alcohol tail in the micelles ($V_a = V_a^o/N_{avo}$). If a spherical micelle shape is assumed for mixed these micellar systems, i.e., $V_{mic} = 4/3\pi r_{mic}^3$, the micellar radius and the area occupied by the amphiphile ion in the palisade layer, A/N_s , can be estimated from simple geometric considerations. For all the SDS/alkoxyethanol mixed micellar systems studied above, the micellar radii has been estimated from the surfactant and alcohol aggregation numbers, and the volume contributions surfactant and alcohol chains. The volume contribution of the surfactant alkyl chains have been estimated from the hydrophobic volumes of a methyl group and methylene group (49\AA^3 and 28\AA^3 , respectively).^{176,202,203} For the cosurfactants containing EO groups, the volume contribution of the chain is calculated by including the EO groups as a part of the hydrophobic chain. The hydrophobic volume of an EO has been estimated from the partial molar volumes of ethoxylated alcohols and nonionic surfactants containing different numbers of EO groups, but the same alkyl chain length.^{220,226} From the calculated values of the micellar radii, A/N_s and its reciprocal ($N_s/A = \sigma/e$, the surface charge density) are determined. Fig. 6.7 is a plot of N_s/A against the moie

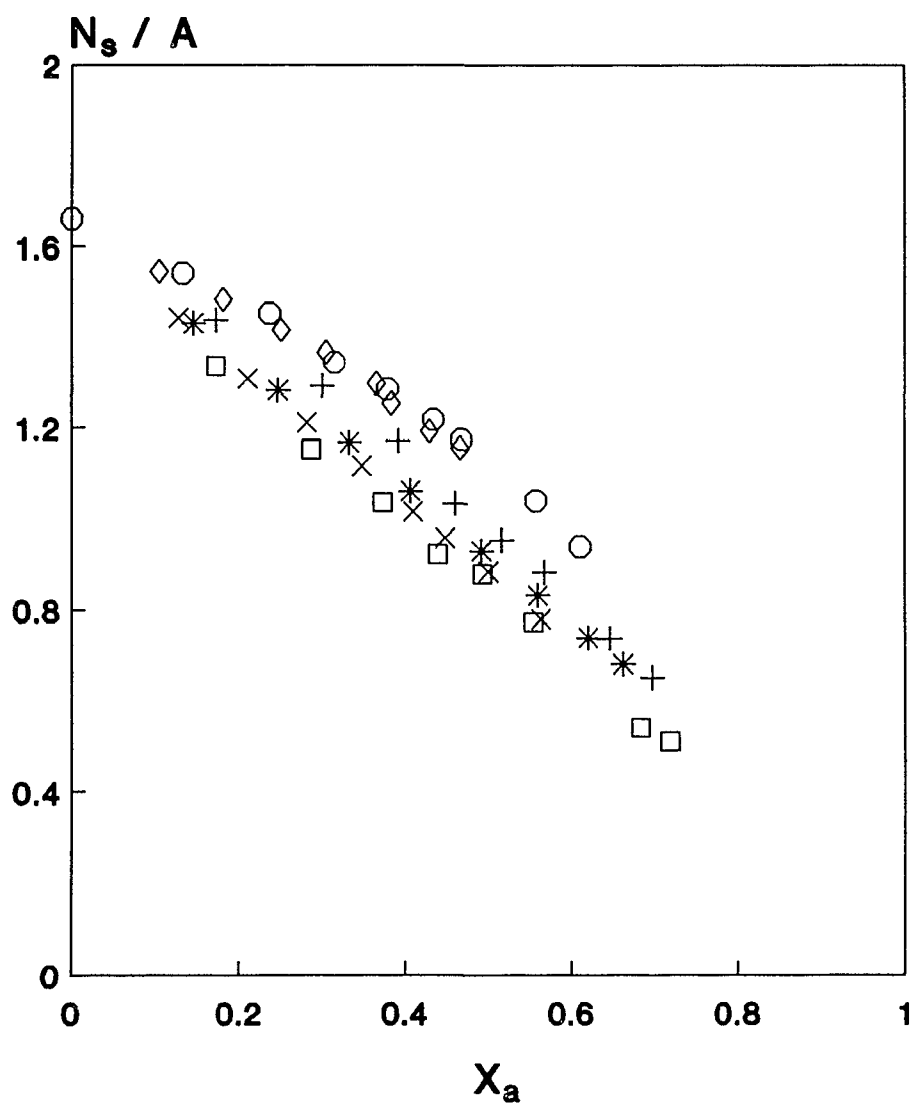


Figure 6.7. Plot of N_s/A vs. X_a for SDS/alkoxyethanol mixed micelles. \circ C_4E_0 ; $+$ C_4E_1 ; $*$ C_4E_2 ; \square C_4E_3 ; \diamond C_6E_0 ; \times C_6E_2 .

fraction of alcohol in the mixed micelle, combining data for all the added alcohols. It can be clearly seen from Fig. 6.7 that a single line can be drawn through all the calculated points, indicating that the micelle size seems to be, at least in part, determined by the surface charge density of the aggregate. Similar behaviour was observed previously by Almgren and Swarup for mixed micelles composed of SDS and a number of polar additives.¹⁷⁶ According to these authors, the surfactant aggregation number and, hence, the micelle size, are determined primarily from the volume contributions of the surfactant and additive, and are independent of the nature of the headgroup. This appears to be the case for mixed micelles composed of SDS and alkoxyethanols as well.

The effect of additives on the surface charge density can also be deduced from an examination of the variation of the degree of counterion binding with alcohol concentration. In Figure 6.8, the β values for SDS/alkoxyethanol mixed micelles are plotted against the molality of alcohol in the micellar phase, i.e., pC_1 . As was the case for the calculated values of the surface charge density in Figure 6.7, the data are well represented by a single curve, indicating that the β values, which are proportional to the surface charge densities, are affected by the number of moles of alcohol in the micellar phase.

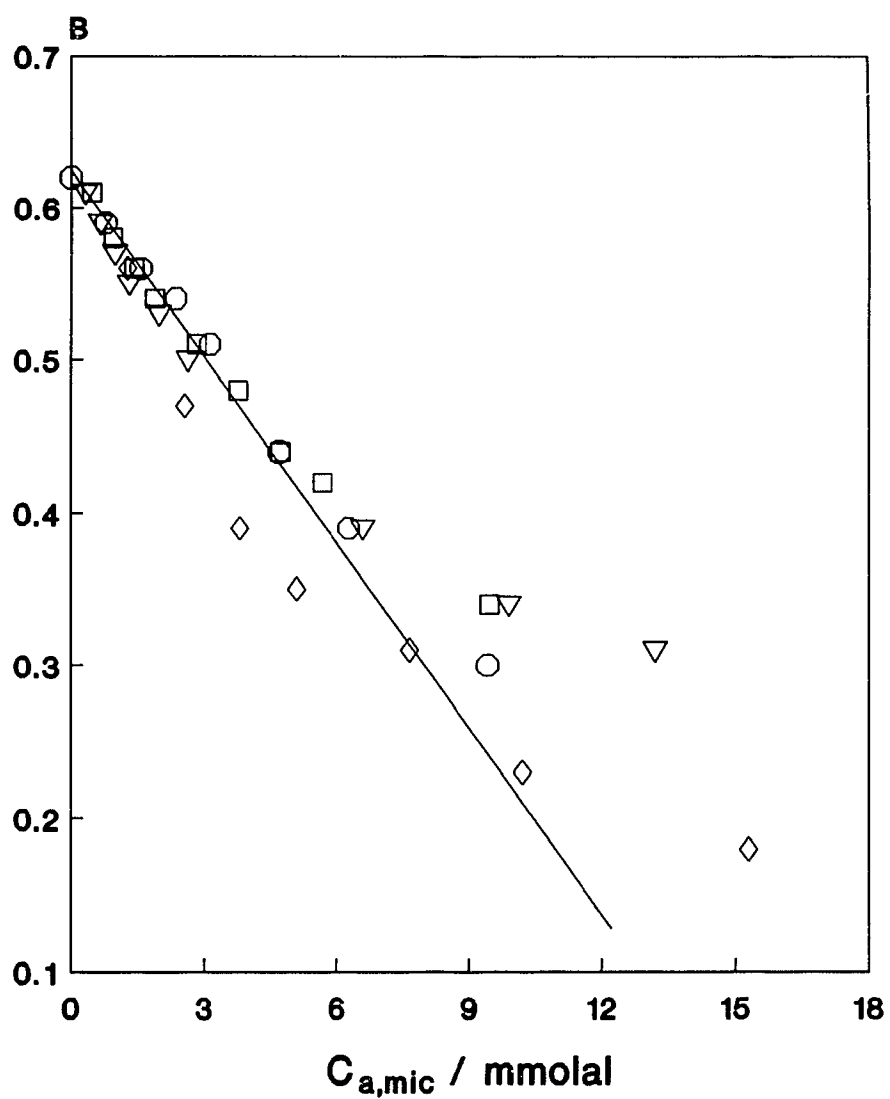


Figure 6.8. Plot of β vs. $c_{a,m}$ for SDS/alkoxyethanol mixed micelles. ○ C_4E_0 ; ◇ C_4E_1 ; □ C_4E_2 ; ▽ C_4E_3 .

(b) Cationic Surfactant/Alcohol Mixed Micelles

The aggregation numbers of the surfactant, alcohol, and the total aggregation number for mixed micelles composed of the cationic surfactant DTAB with a number of alkoxyethanols and alcohols are presented in Tables 6.4 - 6.5, and plotted in Figs. 6.9 - 6.10. Also presented in Tables 6.5 - 6.7 are the I_1/I_3 ratios of the micellar solubilized pyrene probe. The errors in the aggregation numbers were calculated in the same manner as for the aggregation numbers in SDS/alcohol mixed micelles presented earlier. The aggregation number for 0.0750 molal DTAB is in good agreement with the results of some pyrene excimer time-resolved experiments.¹⁷³

The differences between the interactions of ethoxylated alcohols with anionic and cationic surfactants have been explored in the previous chapters of this thesis. These differences are also evident upon examination of the aggregation numbers of DTAB/alkoxyethanol mixed micelles. As expected, N_s decreases with an increase in the concentration of alcohol for all the alkoxyethanols studied in the present thesis. It is of particular interest to observe that, similar to the *CMC*'s reported in chapter 4, changing the alcohol from C_4E_0 to C_4E_1 has a small effect on the aggregation numbers determined from the static quenching experiment. Changing the cosurfactant from C_4E_1 to C_4E_2 or C_4E_3 has a negligible effect on the determined aggregation numbers. A similar comparison can be made for the systems DTAB/ C_6E_0 and C_6E_2 . Additional information can be obtained from the I_1/I_3 ratios of the pyrene probe in these mixed micellar systems. The pyrene I_1/I_3 ratio is higher in DTAB micelles than in SDS micelles, which can be attributed to the well-known specific interaction between aromatic solubilizates and the

Table 6.4. Aggregation Numbers of Surfactant and Alcohol¹ for 0.0750 molal DTAB/Alkoxyethanol Mixed Micelles as a Function of the Concentration of Alcohol

C ₂ /molal	C ₄ E ₀			C ₄ E ₁			C ₄ E ₂			C ₄ E ₃		
	N _s	N _a	I ₁ /I ₃	N _s	N _a	I ₁ /I ₃	N _s	N _a	I ₁ /I ₃	N _s	N _a	I ₁ /I ₃
0.000	52	0	1.40	52	0	1.40	52	0	1.40	52	0	1.40
0.100	47	14	1.39	40	14	1.39	45	13	1.39	44	11	1.41
0.200	40	23	1.39	35	22	1.36	35	19	1.36	34	17	1.39
0.300	38	31	1.38	31	28	1.36	31	22	1.36	28	20	1.39
0.400	34	34	---	28	31	1.31	32	26	1.35	26	24	1.37
0.500	32	45	1.30	28	39	1.30	26	23	1.34	20	22	1.36

1. $N_s \pm 2, N_a \pm 5$

Table 6.5. Aggregation Numbers of Surfactant and Alcohol¹ for 0.0750 molal DTAB/C₆E₀ and DTAB/C₆E₂ Mixed Micelles as a Function of the Alcohol Concentration.

C _a /molal	C ₆ E ₀			C ₆ E ₂		
	N _s	N _a	I ₁ /I ₃	N _s	N _a	I ₁ /I ₃
0.000	52	0	1.47	52	0	1.47
0.010	47	7	1.45	46	4	1.44
0.020	48	13	1.45	42	7	1.44
0.030	47	19	1.44	41	10	1.43
0.040	46	24	1.43	41	13	1.42
0.050	46	28	1.41	38	15	1.41
0.060	43	31	1.40	36	18	1.39
0.070	42	36	1.38	34	18	1.38

1. N_s ± 2, N_a ± 5

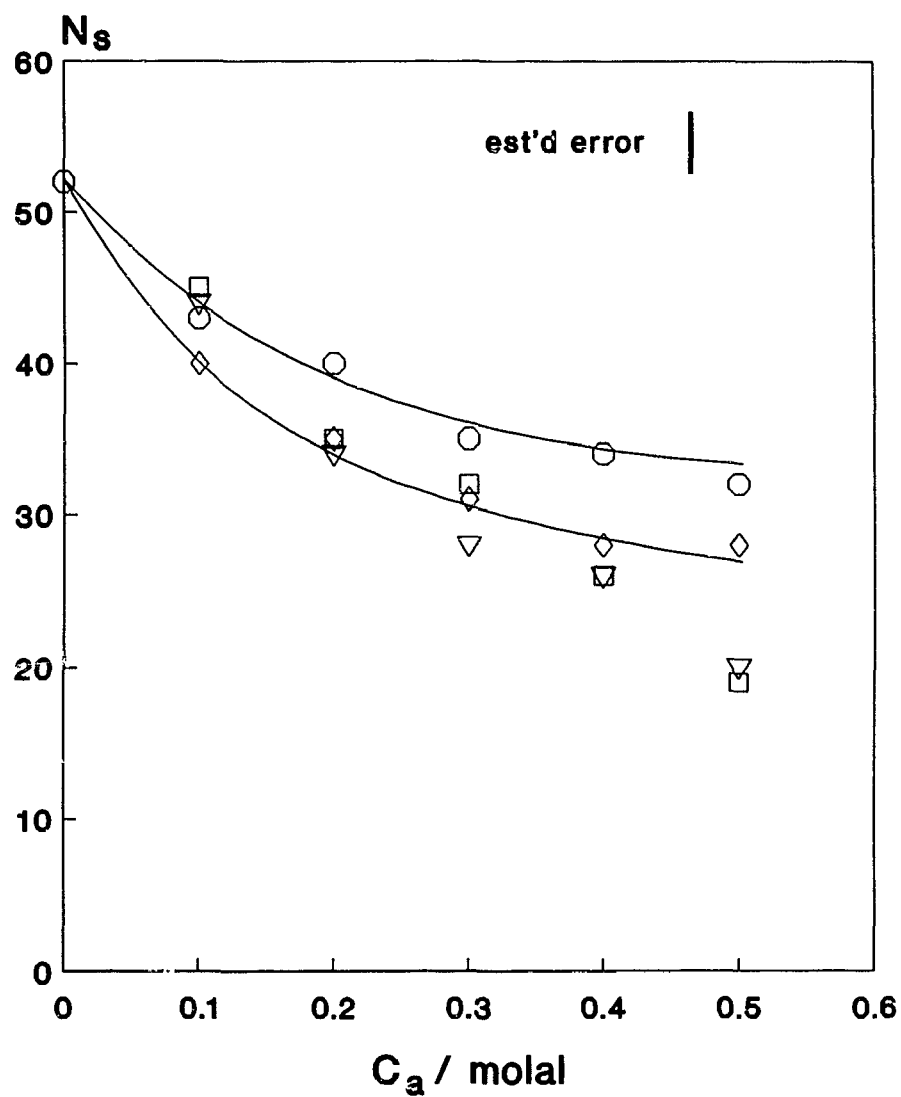


Figure 6.9. Surfactant aggregation numbers, N_s , for DTAB/alkoxyethanol mixed micelles as a function of c_a . \circ C_4E_0 ; \diamond C_4E_1 ; \square C_4E_2 ; ∇ C_4E_3 .

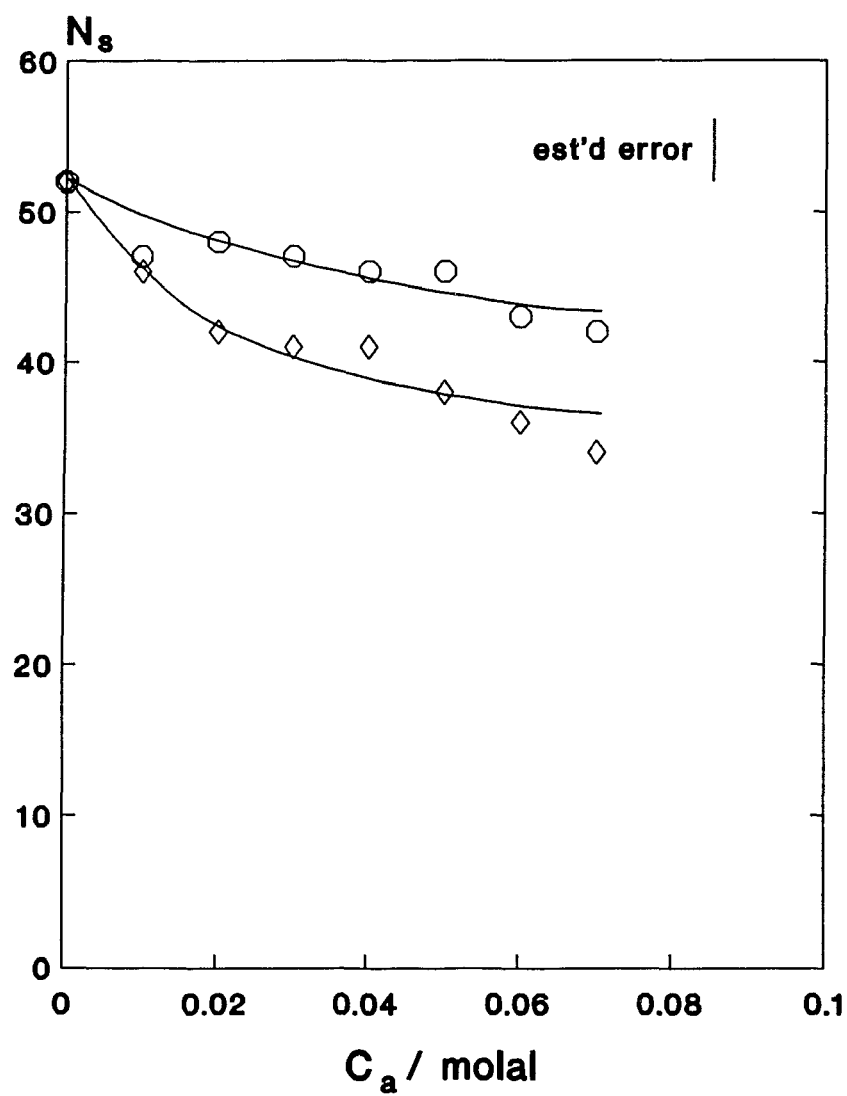


Figure 6.10. Surfactant aggregation numbers, N_s , for DTAB/alkoxyethanol mixed micelles as a function of c_a . \circ C_6E_0 ; \diamond C_6E_2 .

head group region of cationic micelles.^{42,179,200} In DTAB micelles, the average location of the pyrene is near the palisade layer, hence, the higher micropolarity sensed by the probe. With the addition of alcohols to DTAB micelles, the I_1/I_3 ratios decrease as noted above. However, there is not a significant difference between the I_1/I_3 ratios for mixed micelles in the series DTAB/C₄E₀ → C₄E₃ and DTAB/C₆E₀ and C₆E₂. This insensitivity of the pyrene I_1/I_3 ratio to the number of EO groups in the cosurfactant is similar to the trends observed for the distribution constants (p 's) of ethoxylated alcohols in cationic DTAB and DPC micelles, and the decrease of the CMC 's of DTAB/alkoxyethanol mixed micelles as a function of the alcohol concentration, reported previously in this thesis and in the literature.^{227,228}

The values of N_s/A for DTAB/alkoxyethanol mixed micelles were calculated as described above for SDS/alkoxyethanol mixed micelles. In this case, the contribution of the added EO groups to the micellar volume was neglected. A plot of N_s/A against the mole fraction of the alkoxyethanol is given in Fig. 6.11. The plot again appears to be best described by a single straight line, indicating that, as was discussed above for the SDS/alkoxyethanol mixed micelles, the micelle size appears to be influenced by the surface charge density, independent of the nature of the solubilize. The slope of the plot in Fig. 6.12 is lower than that for the SDS/alkoxyethanol data, reflected in the smaller decrease in the aggregation number for DTAB vs. SDS micelles at the same alcohol concentration.

The effect of the micellar bound alkoxyethanols on the surface charge density has also been examined by plotting the β values, determined from conductance vs. $c_{surf,t}$

measurements, against pc_a (Figure 6.12). As was the case above for the data for SDS/alkoxyethanol mixed micelles (Figure 6.8), the data for DTAB/C₄E₁ → C₄E₃ are well represented by a single curve, while the DTAB/C₄E₀ data appear to deviate somewhat. This could indicate that the EO groups, although probably not penetrating into the micellar interior, still have an effect on the surface charge density of the mixed micelles, due to their probable location in the palisade region. It should be noted that the trend observed here is consistent with the *CMC* values and the N_s values, i.e., the first EO group has a small effect on the micellar properties, while subsequent addition of EO groups has little or no effect. Indeed, the effect of adding the first EO group may be electrostatic in the case of cationic surfactant/alkoxyethanol mixed micelles. In the anionic surfactant/alkoxyethanol mixed micelles, however, the effect of adding EO groups to the cosurfactant on the properties of the mixed micelles appears to be hydrophobic in nature.

It appears that the difference in the interaction of alcohols containing EO groups can best be explained by the contribution of the EO group to the hydrophobic interactions. In anionic surfactant/ethoxylated alcohol mixed micelles, interactions between the EO groups and the surfactant CH₂ groups result in an overall lowering of the free energy of transfer of these alcohols from water to the interior of anionic micelles. These interactions appear to be negligible in the transfer of alkoxyethanols from water (or D₂O) to the interior of cationic micelles. These observations are supported by the results of Chapters 4 and 5. It is well known that the degree of water penetration, and the degree of headgroup hydration, is different for anionic and cationic micelles.¹⁷⁹ The difference

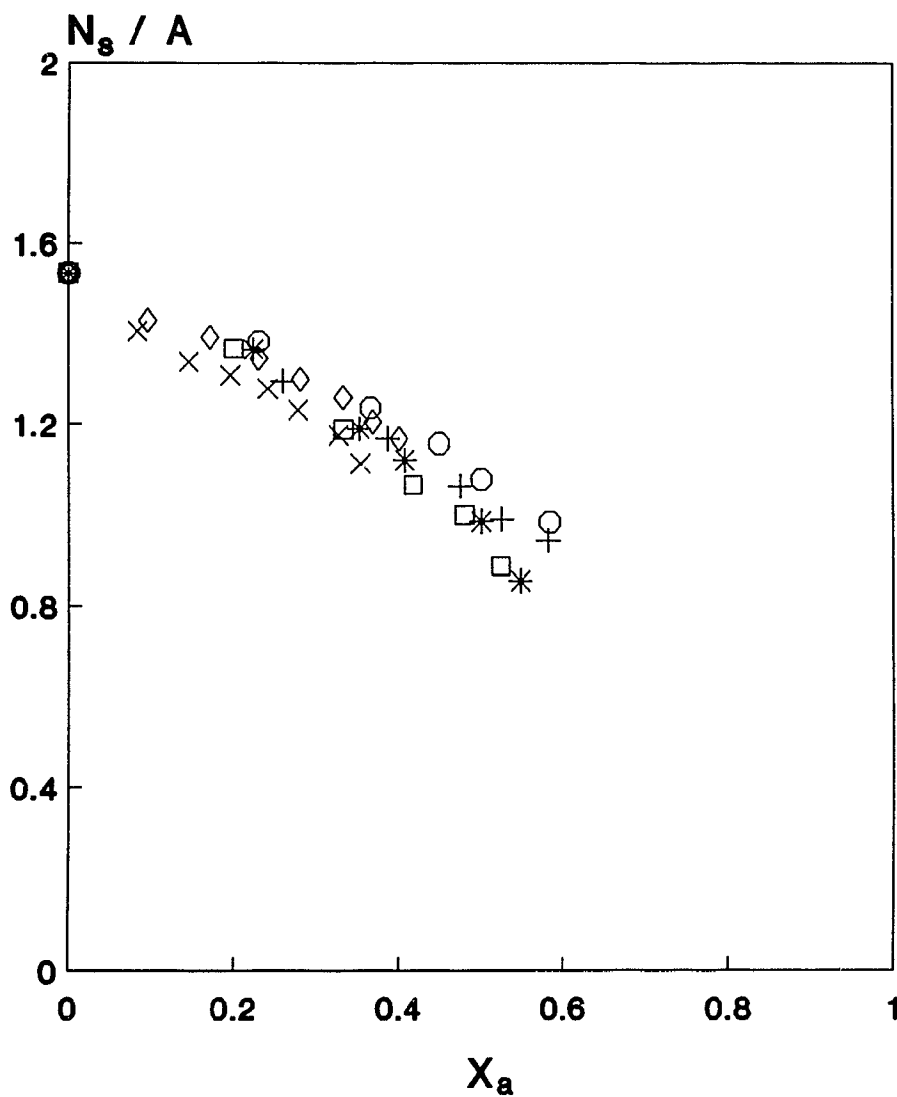


Figure 6.11. Plot of N_s/A vs. X_a for DTAB/alkoxyethanol mixed micelles. \circ C_4E_0 ; $+$ C_4E_1 ; $*$ C_4E_2 ; \square C_4E_3 ; \diamond C_6E_0 ; \times C_6E_2 .

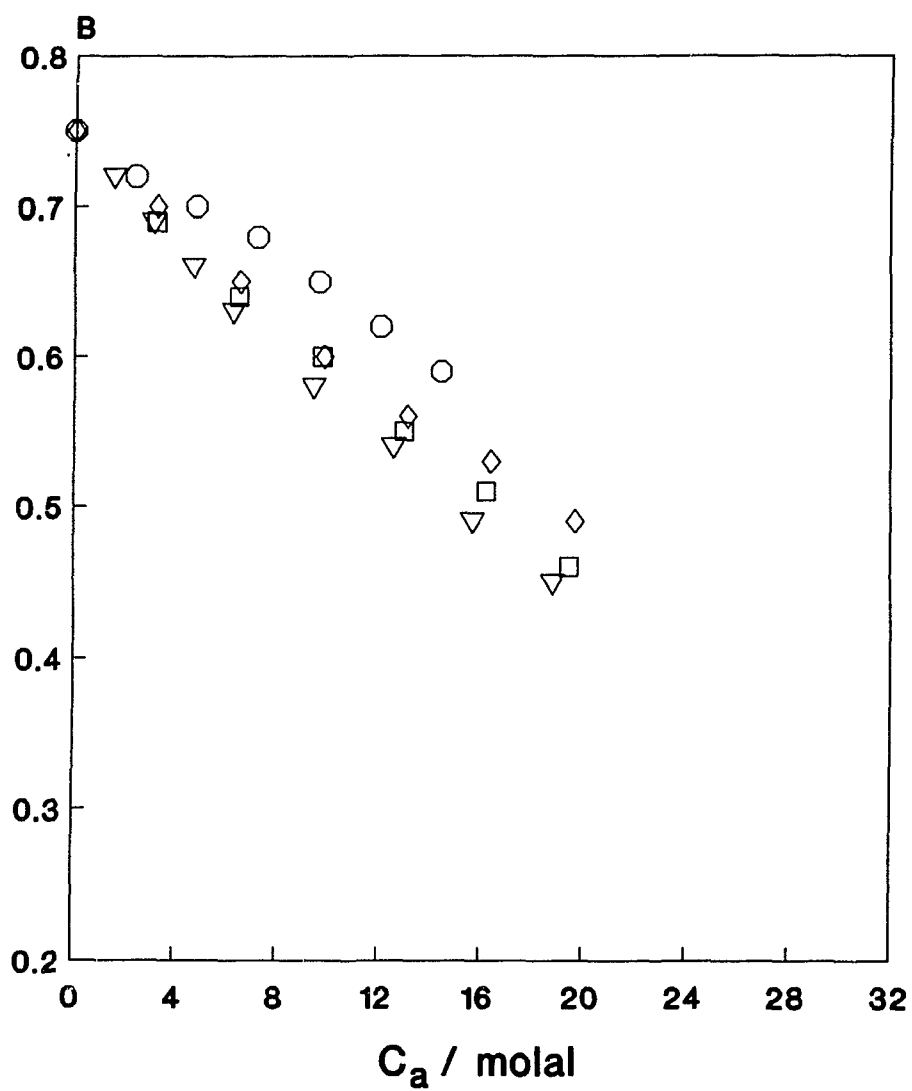


Figure 6.12. Plot of β vs. $c_{a,m}$ for DTAB/alkoxyethanol mixed micelles. \circ C_4E_0 ; \diamond C_4E_1 ; \square C_4E_2 ; ∇ C_4E_3 .

in the degree of penetration by water is usually attributed to a looser micelle structure for anionic surfactant micelles. It is possible that these differences between anionic and cationic micelles, in the degree of hydration of the α -CH₂ groups and the hydration of the micellar surfaces, has some role in the transfer of the EO's from water to the micelles. A detailed theoretical treatment is, however, beyond the scope of this work.

*c) Ionic Surfactant/Tetraethylene Glycol,
Tetraethylene Glycol Dimethyl Ether Mixed Micelles.*

Tetraethylene glycol dimethyl ether (TGD) is an ethoxylated alcohol similar to tetraethylene glycol (TEG), but with the OH groups replaced by the more hydrophobic methoxy group, OCH₃. In Chapter 5, the interaction of TGD and TEG with anionic SDS and cationic DTAB micelles was investigated through a determination of the distribution constants (p values) from the NMR paramagnetic relaxation experiment. In this chapter, the idea was advanced that for TEG (a low molecular weight PEO) the interaction of the EO groups in the alcohol with the surfactant methylene chains for SDS was dominated by the interaction of the OH group with water, with the overall effect being that TEG resides exclusively in the aqueous phase. However, when the OH groups are replaced with OCH₃ groups, as in the case of TGD, a large decrease in ΔG_i° is observed. This appears to be the case for the aggregation numbers as well. In Table 6.6, the aggregation numbers for 0.0500 m SDS/TEG mixed micelles are compared with the aggregation numbers for 0.0500 m SDS/TGD mixed micelles. It can be seen from Table 6.6 and the plotted values of the aggregation numbers (Figure 6.13) that the N_i values

Table 6.6. Aggregation Numbers of Surfactant and Alcohol¹ for 0.0500 molal SDS/TEG and SDS/TGD Mixed Micelles as a Function of the Concentration of Alcohol

C_a /molal	TGD			TEG		
	N_s	N_a	I_1/I_3	N_s	N_a	I_1/I_3
0.000	66	0	1.26	66	0	1.26
0.025	59	4	1.23	--	--	----
0.050	53	8	1.25	59	0	1.26
0.075	49	11	1.26	--	--	----
0.100	46	14	1.27	61	0	1.25
0.150	43	19	1.28	55	0	1.26
0.200	40	26	1.28	52	0	1.24
0.250	43	30	1.29	53	0	1.25
0.300	40	37	1.29	47	0	1.24

1. $N_s \pm 3, N_a \pm 5$

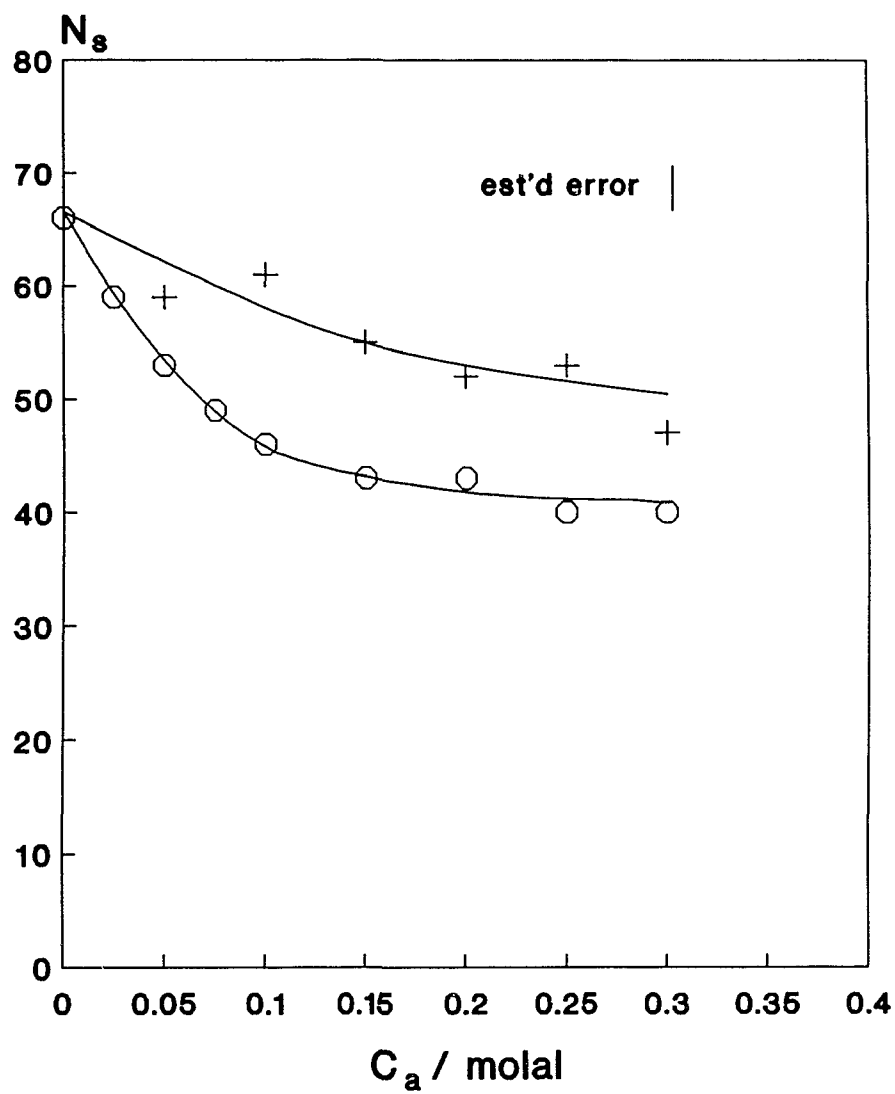


Figure 6.13. Surfactant aggregation numbers for SDS/TEG (+) and SDS/TGD (O) mixed micelles.

of 0.0500 m SDS/TEG mixed micelles decrease very slowly, indicating, again, a negligible interaction of TEG with SDS micelles. However, for 0.0500 m SDS/TGD mixed micelles, the aggregation number decreases rapidly with an increase in the concentration of TGD. In fact, the rate of the decrease in the aggregation number for the SDS/TGD mixed micelles as a function of the concentration of TGD, is identical with the rate of decrease for SDS/C₄E₀ mixed micelles, two alcohols with similar distribution constants. This is a strong indication that the EO groups are penetrating the micellar palisade layer and mixing with the surfactant CH₂ groups.

Another peculiar feature of the SDS/TGD mixed micellar system can be seen from the trend in the I_1/I_3 ratios of solubilized pyrene. The I_1/I_3 ratios *increase* indicating, again, the penetration of the EO groups into the micellar interior. All these results are consistent with a recent light scattering study²²⁹ indicating a greater degree of self-association (i.e., hydrophobicity) in aqueous solution for TGD over TEG, due to the presence of the more hydrophobic OCH₃ group. The results of this thesis indicate a greater degree of interaction of TGD than TEG with anionic micelles, reflecting a difference in the hydrophobic interactions for these two alcohols in the formation of mixed SDS/TGD and SDS/TEG mixed micelles.

The aggregation numbers for 0.075 m DTAB/TEG and DTAB/TGD mixed micelles are presented in Table 6.7, and are plotted in Figure 6.14. Unlike what was observed for 0.0500 m SDS/TGD mixed micelles, there is no large decrease in the N_p values as the concentration of either TEG or TGD is increased. As well, the I_1/I_3 ratios remain constant with increasing alcohol concentration. This information, coupled with the low

Table 6.7. Aggregation Numbers of Surfactant and Alcohol¹ for 0.0750 molal DTAB/TGD and DTAB/TEG Mixed Micelles as a Function of the Alcohol Concentration.

C_a /molal	TGD			TEG		
	N_s	N_a	I_1/I_3	N_s	N_a	I_1/I_3
0.000	52	0	1.47	50	0	1.46
0.050	49	1	1.46	50	0	1.46
0.100	49	2	1.46	51	0	1.46
0.150	48	2	1.47	45	0	1.46
0.200	45	3	1.46	51	0	1.45
0.250	44	4	1.47	--	--	----
0.300	45	4	1.46	--	--	----

1. $N_s \pm 3, N_a \pm 5$

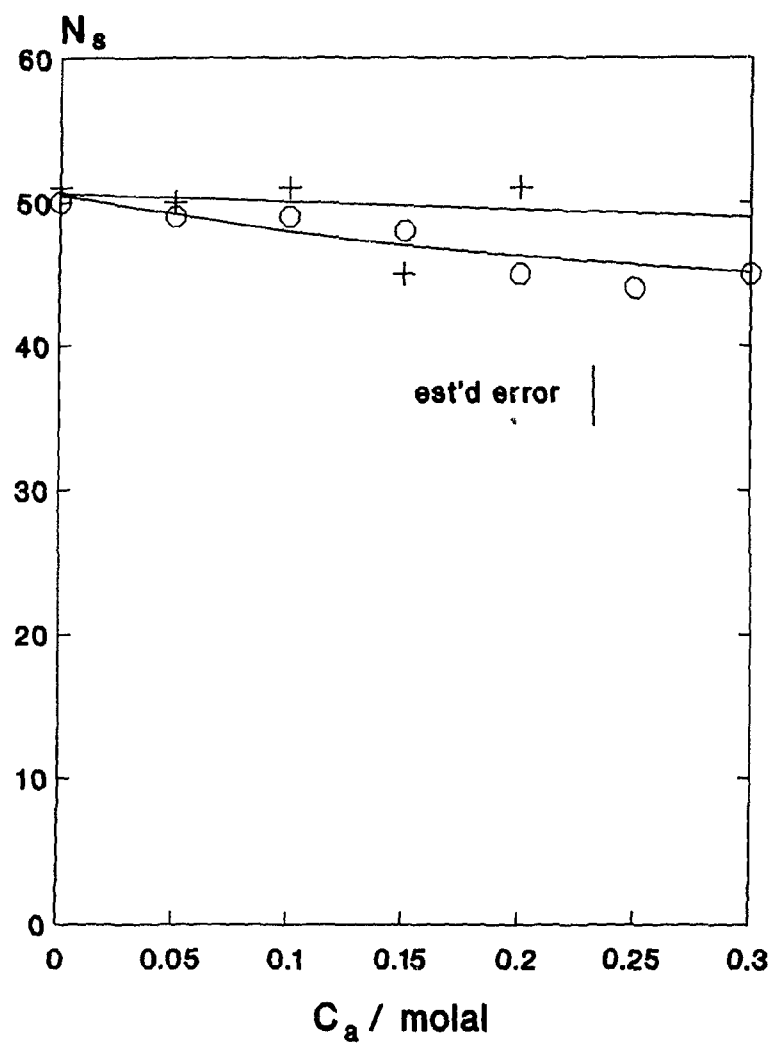


Figure 6.14. Surfactant aggregation numbers for DTAB/TEG (+) and DTAB/TGD (O) mixed micelles.

distribution constant of TGD and TEG in DTAB micelles (Chapter 5), indicates a very low penetration of the EO groups into the DTAB micellar interior. This is consistent with the observations of Chapters 4 and 5, where the $d\ CMC/d\ c_a$ values for DTAB/alkoxyethanol mixed micelles, and the distribution constants of alkoxyethanols in DTAB and DPC micelles (the p -values), were independent of the number of EO groups in the alcohol.

6.4 Conclusions

The aggregation numbers of both the surfactant and the alcohol, N_s and N_a , have been obtained for a large number of alcohol surfactant mixed micellar systems, using the static quenching fluorescence method and the distribution constants (p -values) previously determined in Chapter 5. As expected, the addition of alcohols to ionic micellar solutions decreases N_s while N_a increases, with the overall effect being the micellar radius remains essentially constant. In 0.0500 m SDS/alkoxyethanol mixed micelles at the same concentration of alcohol, N_s , N_a , and the pyrene I_1/I_3 ratios were found to be dependent on the number of EO groups in the alkoxyethanol, while for cationic DTAB/alkoxyethanol mixed micelles, N_s , N_a , and I_1/I_3 were found to be unchanged as the number of EO groups in the cosurfactant was increased. This has been interpreted in terms of the contribution of the EO group to the hydrophobic interactions.

A comparison of the N_s and N_a values for SDS/TGD and SDS/TEG mixed micelles illustrates the importance of the end groups in determining the degree and type of solubilization of low molecular weight neutral polymers. For SDS/TEG mixed micelles,

changing the end group from OH to OCH₃ greatly increases the interaction of the alcohol with the host surfactant micelle, as indicated by the large differences in the N_s and N_a values, the pyrene I_1/I_3 ratios, and the p -values from Chapter 5.

Chapter 7**Summary**

A number of physico-chemical investigations have been carried out in order to examine the interaction of ethoxylated alcohols with anionic and cationic micelles. In Chapter 3, the utility of the recently developed NMR paramagnetic relaxation experiment for determining the free energy gain when a solubilize is transferred from the aqueous to the micellar phase was examined. From the p -value, K_x , the distribution coefficients and the transfer free energy, ΔG_i° , of an alcohol from D_2O to the micellar interior were obtained. The results of Chapter 3 indicated that the NMR paramagnetic relaxation technique can be used to study the solubilization equilibria of alcohols in anionic and cationic micellar systems. The degrees of solubilization of alcohols determined in anionic and cationic micellar solutions do not depend on the paramagnetic ion concentration, but the error in p decreases with increasing paramagnetic ion concentration. For SDS micellar solutions, the degree of solubilization obtained using 3-carboxylate-proxyl was observed to be slightly lower than the value obtained using $Mn(EDTA)^{2-}$ as the paramagnetic relaxation reagent.

The free energies of transfer of n -alcohols from the aqueous phase to the SDS, SD, DTAB, and DPC micellar phase relate linearly to the total number of carbons in the alcohols. From the slopes of these plots, the free energy of transfer of an alcohol methylene group from the aqueous phase to the micellar phase was determined to be -2.67 ± 0.23 kJ/mol and -2.57 ± 0.27 kJ/mol in DTAB and DPC micelles, respectively, -2.57 ± 0.53 kJ/mol in SDS, and -2.33 ± 0.47 kJ/mol in SD micelles. This estimate

of the transfer free energy of the CH₂ micelles is in excellent agreement with the results of Stilbs,^{84,85} based on the p values determined with the NMR PGSE self-diffusion method.

In Chapter 4, the *CMC* values and degrees of counterion binding (β) of a number of ionic surfactant/alkoxyethanol mixed micelles were determined via conductance measurements (SDS/alkoxyethanol and DTAB/alkoxyethanol mixed micelles) and ion-selective electrode measurements (SDecS/alkoxyethanol and DTAB/alkoxyethanol mixed micelles). In SDS and SDecS/alkoxyethanol mixed micelles, the *CMC* values and β 's were found to be dependent on the both the alcohol concentration, and, more importantly, on the EO chain length of the alkoxyethanol. These results were contrasted with the *CMC* values determined in DTAB/alkoxyethanol mixed micelles. The *CMC* values and β 's of the mixed micelles were found to be independent of the number of EO chains in the cosurfactant; at a constant concentration of alcohol, the measured *CMC* values differed only slightly as the EO chain length was increased. These results were interpreted in terms of either a hydrophobic interaction or an electrostatic interaction, due to the presence of the alcohol EO groups. At this point in the thesis, however, the information necessary in order to make a distinction was not yet reported.

In Chapter 5, the distribution constants (p -values) of alkoxyethanols in anionic and cationic micellar systems were determined. In anionic SDS and SD micellar solutions, the distribution of alkoxyethanols was found to be dependent on the number of EO groups in the alcohol; this indicated that the EO group imparts some hydrophobic character to the cosurfactant. The contribution of the EO group in the alcohol to the

hydrophobic interactions was estimated from the transfer free energies of alkoxyethanols from D₂O to the micellar phase of anionic surfactants ($\approx -1.1 \pm 0.3$ kJ/mol), in very good agreement with the free energy of transfer calculated from the decrease in the *CMC*'s as a function of alcohol concentration in Chapter 4. It is this increase in the hydrophobicity of the cosurfactant that dominates the trends in the *CMC* values and β 's reported in Chapter 4. In cationic DTAB and DPC micelles, the *p*-values of ethoxylated alcohols were found to be independent of the number of the alcohol EO groups. These results indicated a negligible contribution from the alcohol EO group to the formation of cationic surfactant/alkoxyethanol mixed micelles. The insensitivity of the thermodynamic parameters (the transfer free energies of the alcohols) indicated that the small interaction observed after the addition of the first EO group was electrostatic in nature. These observations parallel the interaction of PEO and other neutral polymers with anionic and cationic micelles.

The results from the measurement of the degree of solubilization of TEG and TGD in anionic and cationic micelles (Chapter 5), indicate the importance of the end groups in the interaction of small, water soluble, nonionic polymers with micelles. TEG was observed to interact very little with either SDS or DTAB, while TGD, by virtue of the hydrophobic effect of the OCH₃ group and the favourable transfer free energy of the EO groups to the interior of anionic micelles, interacts very strongly with SDS; TGD interacts weakly with DTAB, due mainly to the negligible interaction of the EO group with DTAB.

In Chapter 6, the aggregation numbers of both the surfactant and the alcohol, N_s and

N_a , were obtained for a number of alcohol surfactant mixed micellar systems, using the static quenching fluorescence method and the distribution constants (p -values) previously determined in Chapter 5. As expected, the addition of alcohols to ionic micellar solutions decreased N_s while N_a increased; the overall effect being that the total micellar aggregation number, and, hence, the micellar radius, remained essentially constant. In 0.0500 M SDS/alkoxyethanol mixed micelles at the same concentration of alcohol, N_s , N_a , and the pyrene I_1/I_3 ratios were found to be dependent on the number of EO groups in the alkoxyethanol, while for cationic DTAB/alkoxyethanol mixed micelles, N_s , N_a , and I_1/I_3 were found to be unchanged as the number of EO groups in the cosurfactant was increased. This has also been interpreted in terms of the contribution of the EO group to the hydrophobic interactions.

A comparison of the N_s and N_a values for SDS/TGD and SDS/TEG mixed micelles again illustrated the importance of end group interactions in determining the degree and type of solubilization of low molecular weight neutral polymers. For SDS/TEG mixed micelles, changing the end group from OH to OCH₃ greatly increased the interaction of the alcohol with the host surfactant micelle, as indicated by the large differences in the N_s and N_a values, the pyrene I_1/I_3 ratios, and the p -values from Chapter 5. For DTAB/TEG and DTAB/TGD mixed micelles, the consistency in the surfactant aggregation numbers with an increase in the cosurfactant concentration, indicated a negligible interaction of these alcohols with cationic micelles. Although changing the end group from OH to the more hydrophobic OCH₃ may have resulted in an increase in the interaction of the TGD with DTAB over TEG, the interaction of these molecules is

dominated by the lack of affinity of the EO group for cationic micelles.

In conclusion, the most important contribution of this thesis is the investigation of the differences in the interaction of alkoxyethanols with anionic and cationic micelles. In the literature, most investigations of mixed micelle formation tend to concentrate on a specific property of the mixed micelles (e.g., *CMC* values, N_s values). However, for the mixed micellar systems of interest here, a complete description of the equilibrium properties of the mixed micelles now exists. The research in this thesis clearly demonstrates the need for fully characterizing simple model systems. Extending this type of work to vesicle systems would be extremely interesting, while computer simulations of the interactions of alkoxyethanols with anionic and cationic micelles might prove fruitful. It is hoped that this work will be extended to include microemulsion systems, where alkoxyethanols have proven to be effective cosurfactants.

References

1. Israelachvili, J. N; Mitchell, D. J.; Ninham, B. W. *J. Chem. Soc., Faraday Trans. II* **1976**, *72*, 1525.; Israelachvili, J. N.; Wennerström, H. *Langmuir* **1990**, *6*, 873.
2. Franks, F, in *Water - A Comprehensive Treatise*; Franks, F; Ed., Plenum: New York, 1975; Vol. 4, pp. 1-93.
3. Lindman, B.; Wennerstrom, H. *Top. Current Chem.* **1980**, *87*, 1.
4. Ben-Naim, A. Y. *Hydrophobic Interactions*; Plenum: New York, 1980.
5. Hartley, G. S. *Aqueous Solutions of Parrifin Chain Salts*; Hermann and Cie: Paris (1936).
6. Tanford, C. *The Hydrophobic Effect: The Formation of Micelles and Biological Membranes*; 2nd. Ed.; John Wiley: New York, 1980.
7. *Industrial Applications of Surfactants*; Karsa, D. R. Ed., The Royal Society of Chemistry, Whitestable Litho. Ltd.: Kent, Great Britian, 1987.
8. *Surfactants Based Separation Processes*; Harwell, J. H; Scamehorn, J. F.; Eds., Surf. Sci. Ser. No. 33; Marcel Dekker: New York, 1989.
9. *Surfactants in Emerging Technologies*; Rosen, M. J, Ed.; Surf. Sci. Ser., No. 26; Marcel Dekker: New York, 1986.
10. Fendler, J. H.; Fendler, E. H. *Catalysis in Micellar and Macromolecular Systems*; Academic Press: New York (1975).
11. Mukerjee, P.; Banerjee, K. *J. Phys. Chem.* **1964**, *69*, 45.

12. Stigter, D.; Mysels, K. J. *J. Phys. Chem.* 1955, 59, 45.
13. *Micellization, Solubilization, and Microemulsions*; Mittal, K. L.; Ed., Plenum: New York, 1977.
14. *Solution Chemistry of Surfactants*, Mittal, K. L., Ed.; Plenum: New York, 1979.
15. *Solution Behaviour of Surfactants*; Mittal, K. L.; Fendler, E. J.; Eds., Plenum: New York, 1982.
16. *Surfactants in Solution*; Lindman, B.; Mittal, K. L.; Eds., Plenum: New York, 1984.
17. *Surfactants in Solution*; Mittal, K. L.; Bothorel, P., Eds.; Plenum: New York, 1987.
18. *Surfactants*; Tadros, T. F., Ed.; Plenum: New York, 1984.
19. Myers, D. *Surfactant Science and Technology*; VCH Publishers, Inc.: New York, 1988.
20. *Anionic Surfactants*; Lucassen-Reynders, E. H., Ed.; Surf. Sci. Ser., No. 11; Marcel Dekker: New York, 1981.
21. *Nonionic Surfactants: Physical Chemistry*; Schick, M. J., Ed.; Surf. Sci. Ser., No. 23; Marcel Dekker: New York, 1987.
22. *Cationic Surfactants*; Jungermann, E., Ed.; Surf. Sci. Ser., No. 4, Marcel Dekker: New York, 1970.
23. *Surfactants in Chemical Processes and Engineering*; Wasan, D.T.; Ginn, M. E.; Shah, D. O., Eds.; Surf. Sci. Ser., No. 28; Marcel Dekker: New York, 1989.

24. Mukerjee, P; Mysels, K. J. *Critical Micelle Concentrations of Aqueous Surfactant Systems*; NSRDS-NBS 36; U. S. Government Printing Office: Washington, 1971.
25. Treiner, C.; Nguyen, D. *J. Phys. Chem.* **1990**, *94*, 2021.
26. Goddard, E. D.; Benson, G. C. *Can. J. Chem.* **1957**, *35*, 1936.
27. Van Os, N. M.; Daane, G. J.; Bolsman, T. A. B. M. *J. Colloid Interface Sci.* **1987**, *115*, 402.
28. Van Os, N. M.; Daane, G. J.; Bolsman, T. A. B. M. *J. Colloid Interface Sci.* **1988**, *123*, 267.
29. Brun, T. S.; Hoiland, H; Vikingstad, E; *J. Colloid Interface Sci.* **1978**, *63*, 89.
30. Kaneshina, S.; Tanaka, M.; Tomida, T.; Maturra, R. *J. Colloid Interface Sci.* **1974**, *48*, 450.
31. Corti, M; Degiorgio, V. *J. Phys. Chem.* **1981**, *85*, 711.
32. Hayashi, S; Ikeda, S. *J. Phys. Chem.* **1980**, *84*, 744.
33. Emerson, M. F.; Holtzer, A. *J. Phys. Chem.* **1967**, *71*, 1898.
34. Stigter, D.; Mysels, K. J. *J. Phys. Chem.* **1955**, *59*, 45.
35. Matijevic, E.; Pethica, B. V. *Trans. Faraday Soc.* **1958**, *54*, 587.
36. Singh, H. N.; Swarup, S. *Bull. Chem. Soc. Jpn.* **1978**, *51*, 1534.
37. Abu-Hamidiyyah, M.; Kumari, K. *J. Phys. Chem.* **1990**, *94*, 6445.
38. Bostrom, S.; Backlund, S.; Blokhuis, A. M.; Hoiland, H. *J. Colloid Interface Sci.* **1989**, *128*, 169.
39. Malliaris, A.; LeMoigne, J.; Sturm, J.; Zana, R. *J. Phys. Chem.* **1985**, *89*, 2709.

40. Cronen, Y.; Géladé, E.; Van Der Zegal, M.; Van Der Auweraer, M.; Vanderdriessche, H.; De Schryver, F.; Almgren, M. *J. Phys. Chem.* **1983**, *87*, 1426.
41. Lianos, P.; Viriot, M.-L.; Zana, R. *J. Phys. Chem.* **1984**, *88*, 1098.
42. Zana, R., in *Surfactant Solutions: New Methods of Investigation*; Zana, R., Ed.; Surf. Sci. Ser., No. 22; Marcel Dekker: New York, 1987.
43. Israelachvili, J., in *Physics of Amphiphiles, Micelles, Vesicles, and Microemulsions*; DeGiorgio, V; Corti, M., Eds.; Italian Physical Society; Elsevier: Amsterdam, 1985.
44. Nusselder, J. J.; Engberts, J. B. F. N. *J. Am. Chem. Soc.*, **1989**, *93*, 5000.
45. Ruckenstein, E.; Buenen, J. A. *Langmuir*, **1988**, *4*, 77.
46. Gunnarsson, G.; Jönsson, B.; Wennerström, H. *J. Phys. Chem.* **1980**, *84*, 3114.
47. Vikingstad, E.; Hoiland, H. *J. Colloid Interface Sci.* **1978**, *64*, 126.
48. Gustavsson, H.; Lindman, B.; *J. Am. Chem. Soc.* **1978**, *100*, 4647.
49. Li, P.; Jansson, M.; Stilbs, P. *J. Phys. Chem.* **1987**, *91*, 113.
50. Shedlovsky, L.; Jakob, C. W.; Epstein, M. B. *J. Phys. Chem.* **1984**, *87*, 1983.
51. Rathman, J. F.; Scamehorn, J. F. *J. Phys. Chem.* **1984**, *88*, 5807.
52. Tokiwa, F.; Tsujii, K. *J. Colloid Interface Sci.* **1972**, *41*, 343.
53. Hall, D. G.; Prince, T. J. *J. Chem. Soc. Faraday Trans. 1* **1984**, *80*, 1193.
54. Corkill, J. M.; Goodman, J. F.; Tak, J. R. *Trans. Faraday Soc.* **1984**, *60*, 986.
55. Abuin, E.; Lissi, E. *J. Colloid Interface Sci.* **1991**, *143*, 97.
56. Sepulveda, L.; Cabrera, W. J. *J. Colloid Interface Sci.* **1989**, *129*, 536.

57. Abuin, E.; Lissi, E.; Nunez, R.; Olea, A. *Langmuir* **1989**, *5*, 753.
58. Manabe, M.; Kawamura, H.; Kondo, S.; Kojima, M.; Tokunaga, S. *Langmuir* **1990**, *6*, 1596.
59. Zana, R. *J. Colloid Interface Sci.* **1980**, *78*, 330.
60. Vikingstad, E.; Skuage, A.; Hoiland, H. *J. Colloid Interface Sci.* **1978**, *66*, 510.
61. Evans, D. F.; Evans, J. B.; Sen, R.; Warr, G. C. *J. Phys. Chem.* **1988**, *92*, 784.
62. Moiri, Y. *J. Colloid Interface Sci.* **1988**, *122*, 308.
63. Mukerjee, P.; Mysels, K. J.; Kapauan, P. *J. Phys. Chem.* **1967**, *71*, 4166.
64. Evans, D. F.; Mitchell, D. J.; Ninham, B. W. *J. Phys. Chem.* **1984**, *88*, 6344.
65. Chang, N. J.; Kaler, E. W. *J. Phys. Chem.* **1985**, *89*, 2996.
66. Yasunaga, T.; Oguri, H.; Miura, M. *J. Colloid Interface Sci.* **1967**, *23*, 352.
67. Malliaris, A.; Binana-Limbale, W. *J. Colloid Interface Sci.* **1984**, *102*, 305.
68. Singh, H. N.; Singh, S.; Mahalwar, D. S. *J. Colloid Interface Sci.* **1977**, *59*, 386.
69. Manabe, M.; Kawamura, H.; Yamashita, A.; Tokunaga, S. *J. Colloid Interface Sci.* **1987**, *115*, 147.
70. Manabe, M.; Koda, M.; Shirahama, K. *J. Colloid Interface Sci.* **1980**, *77*, 189.
71. *Phenomena in Mixed Surfactant Systems*; Scamehorn, J. F., Ed.; A. C. S. Symposium Series, No. 311, American Chemical Society, Washington D. C., 1986.
72. Tanford, C. *Science* **1978**, *200*, 1012.
73. Zana, R.; Yiv, S.; Straizelle, C.; Lianos, P. *J. Colloid Interface Sci.*, **1981**, *80*, 208.

74. Singh, H.; Swarup, S. *Bull. Chem. Soc. Jpn.* **1978**, *51*, 1534.
75. Lawrence, A. S. C.; Pearson, J. T. *Trans. Faraday Soc.*, **1967**, *63*, 495.
76. *Proc. 3rd Intl. Congr. Surface Activity*; Hyde, A. J.; Lawrence, A. S. C., Eds.; Univ. Press: Mainz, Germany, 1960.
77. Shinoda, K. *Bull. Chem. Soc. Japan* **1953**, *26*, 101.
78. Shinoda, K. *J. Phys. Chem.* **1954**, *58*, 1136.
79. Larsen, J. W.; Tepley, L. B. *J. Colloid Interface Sci.* **1974**, *49*, 113.
80. Singh, H. N.; Singh, S.; Mahalwar, D. L. *J. Colloid Interface Sci.* **1974**, *49*, 113.
81. Nishikido, N.; Moiri, Y.; Uehara, H.; Maturra, R. *Bull. Chem. Soc. Jpn.* **1974**, *47*, 2634.
82. Manabe, M.; Shirahama, K.; Koda, M. *Bull. Chem. Soc. Jpn.* **1976**, *49*, 2904.
83. Hayase, K.; Hayano, S. *Bull. Chem. Soc. Jpn.* **1977**, *50*, 83.
84. Stilbs, P. *J. Colloid Interface Sci.* **1982**, *87*, 385.
85. Stilbs, P. *J. Colloid Interface Sci.* **1982**, *89*, 547.
86. Carlfors, J.; Stilbs, P. *J. Colloid Interface Sci.* **1985**, *104*, 489.
87. Yamashita, F.; Perron, G.; Desnoyers, J. E.; Kwak, J. C. T. *ACS Symp. Ser.*, **1986**, *311*, 79.
88. Yamashita, F.; Perron, G.; Desnoyers, J. E.; Kwak, J. C. T. *J. Colloid Interface Sci.* **1986**, *114*, 548.
89. Yamashita, F.; Perron, G.; Desnoyers, J. E.; Kwak, J. C. T.; unpublished results.
90. Vikingstad, E.; Kvammen, O. *J. Colloid Interface Sci.* **1980**, *74*, 16.

91. Lianos, P.; Zana, R. *J. Colloid Interface Sci.* **1984**, *101*, 587.
92. Abuin, E.; Lissi, E. *J. Colloid Interface Sci.* **1983**, *95*, 198.
93. Zana, R.; Candeau, S. *J. Colloid Interface Sci.* **1985**, *84*, 206.
94. Lianos, P.; Zana, R. *J. Colloid Interface Sci.* **1984**, *84*, 100.
95. Kibblewhite, J.; Drummond, C. J.; Greiser, F.; Healy, T. W. *J. Phys. Chem.* **1987**, *91*, 4658.
96. Stilbs, P. *J. Colloid Interface Sci.* **1988**, *122*, 593.
97. Nguyen, C. M.; Scamehorn, J. F.; Christian, S. D. *Colloids and Surfaces* **1988**, *30*, 335.
98. Christian, S. D.; Tucker, E. E.; Lane, E. H. *J. Colloid Interface Sci.* **1981**, *84*, 423.
99. Thomas, D. C.; Christian, S. D. *J. Colloid Interface Sci.* **1982**, *82*, 430.
100. Ekwall, P.; Stenius, P. *Acta Chem. Scan.* **1967**, *21*, 1643.
101. Ekwall, P.; Mandell, L.; Fontell, K. *J. Colloid Interface Sci.* **1969**, *29*, 542.
102. Ekwall, P.; Mandell, L.; Fontell, K. *Mol. Cryst. Liq. Cryst.* **1969**, *8*, 157.
103. Blokhus, A. M.; Hoiland, H.; Backlund, S. *J. Colloid Interface Sci.* **1986**, *114*, 9.
104. Backlund, S.; Bakken, J.; Blokhus, A. M.; Hoiland, H.; Vikholm, I. *Acta Chem. Scan.* **1986**, *A40*, 241.
105. Hoiland, H.; Ljosland, E.; Backlund, S. *J. Colloid Interface Sci.* **1984**, *101*, 467.
106. Hoiland, H.; Blokhus, A. M.; Kvammen, O.; Backlund, S. *J. Colloid Interface Sci.* **1985**, *107*, 576.

107. Perrson, B. D.; Drakenberg, T.; Lindman, B. *J. Phys. Chem.* **1979**, *83*, 3011.
108. Backlund, S.; Rundt, K. *Acta Chem. Scan.* **1980**, *A34*, 433.
109. Lissi, E.; Abuin, E.; Rocha, A. M. *J. Phys. Chem.* **1980**, *84*, 2406.
110. Blatt, E.; Sawyer, W. H.; *Biophys. Biochim. Acta* **1985**, *822*, 43.
111. Almgren, M.; Greiser, F.; Powell, J. R.; Thomas, J. K. *L. Chem. Eng. Data* **1979**, *24*, 285.
112. Encinas, M. V.; Lissi, E. A.; *Chem. Phys. Lett.* **1982**, *91*, 55.
113. Harris, R. K. *Nuclear Magnetic Resonance Spectroscopy: A Physico-Chemical View*; Longman Press: Essex, U. K., 1986.
114. Shaw, D. *Fourier Transform NMR Spectroscopy*; 2nd. Ed.; Elsevier: Amsterdam, 1984.
115. Slichter, C. P. *Principles of Magnetic Resonance*; Harper and Row/John Weatherhill: New York/Tokyo, 1963.
116. Becker, E. E. *High Resolution NMR*; Academic Press: New York, 1980.
117. Farrar, T. C. *An Introduction to Pulse NMR*; Farragut Press: Chicago, 1987.
118. Wasylshen, R. E. in *NMR Spectroscopy Techniques*; Lichter, R. L.; Dybowski, C., Eds.; Marcel Dekker: New York, 1986; pp. 45-91.
119. Freeman, R. *A Handbook of Nuclear Magnetic Resonance*; Longman: New York, 1987.
120. Jardetzky, O.; Roberts, G. C. K. *NMR in Molecular Biology*; Academic: New York, 1987.
121. Solomon, I; Blömbergen, N. *J. Chem. Phys.* **1956**, *25*, 261.

122. Blömbergen, N; Morgan, L. O. *J. Chem. Phys.* **1961**, *34*, 842.
123. Hwang, L.-P.; Freed, J. H. *J. Chem. Phys.* **1975**, *63*, 4017.
124. Ayant, Y.; Belorizky, E.; Alizon, J.; Gallice, J. *J. Phys. (Paris)* **1975**, *36*, 991.
125. Freed, J. H. *J. Chem. Phys.* **1978**, *68*, 3034.
126. Sholl, C. A. *J. Phys. C: Solid State Phys.* **1981**, *14*, 447.
127. Garnesh, K. N.; Mitra, D.; Balasubramanian, D. *J. Phys. Chem.* **1982**, *86*, 4291.
128. Chevalier, Y.; Chachaty, C. *Colloid Polymer Sci.* **1984**, *262*, 489.
129. Kilpatrick, P. K.; Wilmer, W. G. *J. Phys. Chem.* **1984**, *88*, 1649.
130. Robb, I. D.; Smith, J. *J. Chem. Soc. Faraday Trans. 1* **1984**, *70*, 287.
131. Gustavsson, H.; Lindman, B. *J. Am. Chem. Soc.* **1975**, *97*, 3923.
132. Stilbs, P.; Lindman, B. *J. Colloid Interface Sci.* **1984**, *99*, 290.
133. Carifors, J.; Stilbs, P. *J. Colloid Interface Sci.* **1985**, *103*, 332.
134. Stilbs, P. *J. Colloid Interface Sci.* **1983**, *94*, 463.
135. Lindman, B.; Shinoda, K.; Jonströmer, M.; Shinohara, A. *J. Phys. Chem.* **1988**, *92*, 4702.
136. Jansson, M.; Linse, P.; Rymden, R. *J. Phys. Chem.* **1988**, *92*, 6689.
137. Cabane, B. *J. Phys. Chem.* **1981**, *47*, 847.
138. Chachaty, C. *Progress NMR Spectros.* **1987**, *19*, 183.
139. Gao, Z.; Wasylshen, R. E.; Kwak, J. C. T. *J. Phys. Chem.* **1989**, *93*, 2190.
140. Söderman, O.; Carlström, G.; Monduzzi, M.; Olsson, U. *Langmuir* **1988**, *4*, 1039.
141. Chachaty, C.; Ahlnas, T.; Lindstrom, B.; Nery, H.; Tistchenko, A. M. *J. Colloid*

- Interface Sci.* **1988**, *122*, 122.
142. Chachaty, C.; Caniparoli, J.; Faure, A.; Tistchenko, A. M. *J. Phys. Chem.* **1988**, *92*, 6330.
143. Söderman, O.; Monduzzi, M.; Ceglie, A.; Lindman, B. *J. Colloid Interface Sci.* **1990**, *136*, 113.
144. Ceglie, A.; Monduzzi, M.; Söderman, O. *J. Colloid Interface Sci.* **1991**, *142*, 129.
145. Söderman, O.; Hansson, E.; Monduzzi, M. *J. Colloid Interface Sci.* **1990**, *141*, 512.
146. Brown W.; Rymden, R. *J. Phys. Chem.* **1987**, *91*, 3565.
147. Faucompré, B.; Lindman, B. *J. Phys. Chem.* **1987**, *91*, 383.
148. Jansson, M.; Rymden, R. *J. Colloid Interface Sci.* **1987**, *119*, 185.
149. Jansson, M.; Li, P.; Stilbs, P. *J. Phys. Chem.* **1987**, *91*, 5279.
150. Stilbs, P.; *Progress NMR Spectros.* **1987**, *19*, 1.
151. Lindman, B. *Z. Phys. Chemie (N. F.)* **1987**, *Bd. 153*, 499.
152. Lindman, B.; Brun, B. *J. Colloid Interface Sci.* **1973**, *42*, 388.
153. Gao, Z.; Kwak, J. C. T.; Labonté, R.; Marangoni, D. G.; Wasylshen, R. E. *Colloids and Surfaces* **1990**, *45*, 269.
154. Shinoda, K.; Lindman, B. *Langmuir* **1987**, *3*, 135.
155. Lindman, B.; Stilbs, P.; Moseley, M. E. *J. Colloid Interface Sci.* **1981**, *83*, 569.
156. Warnheim, T.; Sjöblom, E.; Henriksson, U.; Stilbs, P. *J. Phys. Chem.* **1984**, *88*, 5420.

157. Stilbs, P.; Rapacki, P.; Lindman, B. *J. Colloid Interface Sci.* **1983**, *95*, 583.
158. Gao, Z.; Kwak, J. C. T.; Wasylshen, R. E.; unpublished results.
159. Herzfeld, S. H.; Corrin, M. L.; Harkins, W. D. *J. Phys. Chem.* **1950**, *54*, 271.
160. Blatt, E.; Chatelier, R. C.; Sawyer, W. H. *Photochemistry and Photobiology* **1984**, *39*, 477.
161. Roelants, E.; De Schryver, F. *Langmuir* **1987**, *3*, 209.
162. Lang, J. *J. Phys. Chem.* **1990**, *94*, 3734.
163. Roelants, E.; Geladé, E.; Van Der Auweraer, M.; Croonen, Y.; De Schryver, F. C. *J. Colloid Interface Sci.* **1983**, *96*, 288.
164. Almgren, M.; Löfroth, J.-E. *J. Colloid Interface Sci.* **1981**, *81*, 486.
165. Atik, S. S.; Singer, L. A. *Chem. Phys. Lett.* **1978**, *59*, 519.
166. Turro, N. J.; Lee, P. C. C. *J. Phys. Chem.* **1982**, *86*, 3367.
167. Dederen, J. C.; Van Der Auweraer, M.; De Schryver, F. C. *J. Phys. Chem.* **1981**, *85*, 1198.
168. Wikander, G.; Johansson, L. B.-Å. *Langmuir* **1989**, *5*, 728.
169. Yekta, A.; Aikawa, M.; Turro, N. J. *Chem. Phys. Lett.* **1979**, *63*, 243.
170. Turro, N. J.; Yekta, A. *J. Am. Chem. Soc.* **1978**, *100*, 5951.
171. Roelants, E.; Geladé, E.; Smid, J.; De Schryver, F. C. *J. Colloid Interface Sci.* **1985**, *107*, 337.
172. Infelta, P. P. *Chem. Phys. Lett.* **1979**, *61*, 1978.
173. Lianos, P.; Zana, R.; Lang, J. *J. Colloid Interface Sci.* **1983**, *91*, 279.
174. Infelta, P. P.; Grätzel, M. *J. Chem. Phys.* **1983**, *78*, 5280.

175. Mulo, E. C. C.; Costa, S. M. B.; Macanita, A. L.; Santos, H. *J. Colloid Interface Sci.* **1991**, *141*, 439.
176. Almgren, M.; Swarup, S. *J. Colloid Interface Sci.* **1983**, *91*, 256.
177. Lianos, P.; Zana, R. *Chem. Phys. Lett.* **1980**, *72*, 171.
178. Georges, J. *Spectrochimica Acta Rev.* **1990**, *13*, 27.
179. Thomas, J. K. *The Chemistry of Excitation at Interfaces*; American Chemical Society: Washington, 1984.
180. Turro, N. J. *Modern Molecular Photochemistry*; Benjamin/Cummings: Menlo Park, CA, 1978.
181. Thomas, J. K. *Chemical Reviews* **1980**, *80*, 283.
182. Ueno, M.; Kimoto, Y.; Ikeda, Y.; Momose, H.; Zana, R. *J. Colloid Interface Sci.* **1987**, *117*, 179.
183. Thomas, J. K.; Almgren, A.; Greiser, F. *J. Am. Chem. Soc.* **1980**, *102*, 3188.
184. Oakenfull, D. *J. Chem. Soc. Faraday Trans. 1* **1980**, *76*, 1875.
185. Moroi, Y.; Humphrey-Baker, R.; Grätzel, M. *J. Colloid Interface Sci.* **1987**, *119*, 588.
186. Tachiya, M. *Chem. Phys. Lett.* **1975**, *33*, 289.
187. Tachiya, M. *J. Chem. Phys.* **1983**, *78*, 5282.
188. Tachiya, M. *J. Phys. Chem.* **1982**, *76*, 340.
189. Maistri, M.; Infelta, P. P.; Grätzel, M. *J. Chem. Phys.* **1978**, *69*, 1522.
190. Lianos, P.; Zana, R. *J. Colloid Interface Sci.* **1981**, *84*, 100.
191. Hashimoto, S.; Thomas, J. K. *J. Colloid Interface Sci.* **1984**, *102*, 152.

192. Hoffman, H.; Nagel, R.; Platz, G.; Ulbricht, W. *Colloid Polymer Sci.* **1976**, *254*, 812.
193. Malliaris, A. *Adv. Colloid Interface Sci.* **1987**, *27*, 153.
194. Velazquez, M. M.; De Costa, S. M. B. *J. Chem. Soc., Faraday Trans.* **1990**, *86*, 4043.
195. Malliaris, A.; Lang, J.; Zana, R. *J. Chem. Soc., Faraday Trans. 1* **1986**, *82*, 109.; *J. Colloid Interface Sci.* **1986**, *110*, 237.
196. Brackman, J. *Langmuir* **1991**, *7*, 236.
197. Candau, S. in *Surfactant Solutions: New Methods of Investigation*; Zana, R., Ed.; Surf. Sci. Ser., No. 22; Marcel Dekker: New York, 1987, pp. 147-207.
198. Cabane, B. in *Surfactant Solutions: New Methods of Investigation*; Zana, R., Ed.; Surf. Sci. Ser., No. 22; Marcel Dekker: New York, 1987, pp. 57-145.
199. Binana-Limbalé, W.; Zana, R.; Platone, E. *J. Colloid Interface Sci.* **1988**, *124*, 647.
200. Zana, R.; Yiv, S.; Straizelle, C.; Lianos, P. *J. Colloid Interface Sci.* **1981**, *80*, 208.
201. Lianos, P.; Zana, R. *Chem. Phys. Lett.* **1980**, *76*, 62.
202. Almgren, M.; Swarup, S. *J. Phys. Chem.* **1982**, *86*, 4212.
203. Almgren, M.; Swarup, S. *J. Phys. Chem.* **1983**, *87*, 876.
204. Manabe, M.; Koda, M. *Bull. Chem. Soc. Jpn.* **1978**, *51*, 1599.
205. Quirion, F.; Drifford, M. *Langmuir* **1990**, *6*, 786.
206. Caron, G.; Hetu, D.; Désnoyers, J. E. *Colloids and Surfaces* **1989**, *35*, 169.

207. Quirion, F.; Désnoyers, J. E. *J. Colloid Interface Sci.* **1987**, *115*, 176.
208. Goddard, E. D. *Colloids and Surfaces* **1986**, *19*, 255.
209. Hayakawa, K.; Kwak, J. C. T. in *Cationic Surfactants*; Holland, P.; Rubingh, D., Eds.; Marcel Dekker, New York, 1991.
210. Vikingstad, E. *J. Colloid Interface Sci.* **1979**, *72*, 68.
211. Vikingstad, E. *J. Colloid Interface Sci.* **1980**, *73*, 260.
212. Lange, H. *Proc. 3rd Intl. Congress Surface Active Agents*; Cologne, 1960; Vol. I.
213. Rosen, M. J.; Cohen, A. W.; Dahanayke, M.; Hua, X. Y. *J. Phys. Chem.* **1982**, *86*, 541.
214. Tanford, C.; Nozaki, Y.; Rhode, M. F. *J. Phys. Chem.* **1977**, *81*, 1555.
215. Schwuger, M. J. *A. C. S. Symp. Ser.* **1984**, *253*, 3.
216. Weil, J. K.; Bristline, R. G.; Stirton, A. J. *J. Phys. Chem.* **1963**, *67*, 1796.
216. Lange, H.; Schwuger, M. J. *Colloid Polymer Sci.* **1980**, *258*, 1264.
217. Tokiwa, F.; Ohki, H. *J. Phys. Chem.* **1967**, *71*, 1343.
218. Tokiwa, F. *J. Phys. Chem.* **1968**, *72*, 1214.
219. Lin, I. J.; Marszall, L. *J. Colloid Interface Sci.* **1976**, *57*, 85.
220. Roux, G.; Perron, G.; Desnoyers, J. E. *J. Solution Chem.* **1978**, *7*, 619.
221. Söderman, O.; Geuring, P. *Colloid Polym. Sci.* **1987**, *265*, 76.
222. Malliaris, A.; Lang, J.; Zana, R. *J. Phys. Chem.* **1986**, *90*, 655.
223. Luo, H.; Boens, N.; Van der Auweraer, M.; De Schryver, F. C.; Malliaris, A. *J. Phys. Chem.* **1989**, *93*, 3244.

224. Anderson, A. M.; Kwak, J. C. T., unpublished results.
225. Wasylishen, R. E.; Kwak, J. C. T.; Gao, Z.; Verpoorte, E.; MacDonald, J. B.; Dickson, R. M. *Can. J. Chem.* **1991**, *69*, 822.
226. Harada, S.; Nakagawa, T. *J. Solution Chem.* **1979**, *8*, 267.
227. Kwak, J. C. T.; Marangoni, D. G. *Langmuir*, accepted for publication.
228. Marangoni, D. G.; Rodenhiser, A. P.; Thomas, J. M.; Kwak, J. C. T. *A. C. S. Symp. Ser.*, Submitted for publication.
229. Bender, T. M.; Pecora, B. *J. Colloid Interface Sci.* **1988**, *126*, 638.